

7-12-2014

DEVELOPMENT AND KINETIC MODELING OF MULTIPLEX MICROSPHERE ASSAYS FOR HIGH- THROUGHPUT DISCOVERY OF PROTEASE ACTIVE SMALL MOLECULE COMPOUNDS

Jingsh Zhu

Follow this and additional works at: https://digitalrepository.unm.edu/nsms_etds

Recommended Citation

Zhu, Jingsh. "DEVELOPMENT AND KINETIC MODELING OF MULTIPLEX MICROSPHERE ASSAYS FOR HIGH-THROUGHPUT DISCOVERY OF PROTEASE ACTIVE SMALL MOLECULE COMPOUNDS." (2014).
https://digitalrepository.unm.edu/nsms_etds/10

This Dissertation is brought to you for free and open access by the Engineering ETDs at UNM Digital Repository. It has been accepted for inclusion in Nanoscience and Microsystems ETDs by an authorized administrator of UNM Digital Repository. For more information, please contact disc@unm.edu.

Jingshu Zhu

Candidate

Nanoscience & Microsystems Engineering

Department

This dissertation is approved, and it is acceptable in quality and form for publication:

Approved by the Dissertation Committee:

Steven W. Graves , Chairperson

Bruce S. Edwards

Larry A. Sklar

Andrew P. Shreve

David G. Whitten

**DEVELOPMENT AND KINETIC MODELING OF MULTIPLEX
MICROSPHERE ASSAYS FOR HIGH-THROUGHPUT DISCOVERY OF
PROTEASE ACTIVE SMALL MOLECULE COMPOUNDS**

BY

JINGSHU ZHU

B.E. Marine Fishery Science and Technology, Jimei University, China P.R. 2006

M.S. Chemistry, Nanjing University, China P.R. 2009

DISSERTATION

Submitted in Partial Fullfillment of the
Requirtments for the Degree of

Doctor of Philosophy

Nanoscience & Microsystems Engineering

The University of New Mexico

Albuquerque, New Mexico

May, 2014

ACKNOWLEDGMENTS

I am very grateful to my research advisors, Prof. Graves and Prof. Edwards, for their guidance and assistance in my research project, and I am extremely fortunate to have had their help and support for the completion of my project work. I would also like to express my deepest gratitude to my advisors for their caring, for their patience, and for providing me with an excellent atmosphere for doing research.

I would like to thank Prof. Sklar for his recommendations and guidance on my project. In addition, I would like to express my appreciation to my committee members, Prof. Shreve and Prof. Whitten. Thank you very much for serving as my committee.

I would like to thank the Cancer Nanotechnology Training Center Student Fellowship for supporting my research work.

I would like to acknowledge my colleagues at the Center for Biomedical Engineering and the Center for Molecular Discovery: Travis Woods, Carl Brown, Mark Carter and Yang Wu, for their valuable help and contributions to my research.

Finally, I would like to thank my husband, Ying Wang, my parents, and my friends for their support and encouragement during this time.

DEVELOPMENT AND KINETIC MODELING OF MULTIPLEX MICROSPHERE ASSAYS FOR HIGH-THROUGHPUT DISCOVERY OF PROTEASE ACTIVE SMALL MOLECULE COMPOUNDS

BY

JINGSHU ZHU

B.E. Marine Fishery Science and Technology, Jimei University, China P.R. 2006

M.S. Chemistry, Nanjing University, China P.R. 2009

**Ph.D. Nanoscience & Microsystems Engineering, The University of New Mexico,
USA, 2014**

ABSTRACT

In this dissertation, we have designed a series of recombinant fluorescent full-length protease substrates containing the cleavage sites separated by a biotinylation tag and a GFP domain, which can be associated with streptavidin-coated microspheres/nanospheres. We have developed microsphere-based platforms to detect the cleavage activities of several proteases simultaneously. In addition, we have performed high-throughput screening (HTS) to identify potential inhibitors for the *Bacillus anthracis* lethal factor protease (LF) and the Botulinum neurotoxin type A & F light chain proteases (BoNT/A & F LC). In order to select the efficient inhibitors, a chemical library of 350,000 compounds was screened with the HyperCyt[®] high-throughput flow cytometry system, which can screen thousands of compounds per day for drug discovery. In order to understand the kinetic mechanisms of these proteases as well as the inhibitory mechanisms of some inhibitor candidates, we have carried out surface-based analysis to characterize the enzymatic reaction in terms of the key kinetic parameters of BoNT/A LC

(K_m , k_{cat} etc.) for surface-bound substrates by flow cytometry. In my work, we have also created a FRET full-length substrate solution assay to determine the kinetic constants of the proteases and inhibitory mechanisms of some known inhibitors. However, despite the advantages of the microsphere-based assay, the surface area to volume ratio of microspheres limits us to sub-saturating concentrations of substrate (in the low nM range). Therefore, we developed a nanosphere-based protease assay platform to increase substrate concentrations. To demonstrate this approach, we have implemented our nanosphere-based protease assay using the toxin protease models to prove the concept. The surface-based system is a promising method for the use of multiple protease assays to evaluate the kinetic mechanisms and to select inhibitors for several different proteases simultaneously. This provides the advantages of robustness, sensitivity, low substrate cost and reproducibility.

Table of Contents

Chapter 1 Introduction.....	1
1.1 Bacterial Zinc Dependent Metalloproteases.....	2
1.2 Botulinum Neurotoxins.....	3
1.2.1 BoNT/A Cleaves SNAP-25.....	7
1.2.2 BoNT/F Cleaves VAMP-2.....	9
1.3 Anthrax Lethal Factor.....	12
1.4 Protease Inhibitors.....	14
1.4.1 Botulinum Neurotoxin Inhibitors.....	15
1.4.1.1 Botulinum Neurotoxin Type A Inhibitors.....	16
1.4.1.2 Botulinum Neurotoxin Type F Inhibitors.....	17
1.4.2 Anthrax Lethal Factor Inhibitors.....	19
1.5 Surface-based Protease Assays.....	20
1.6 High-throughput Flow Cytometry for Drug Discovery.....	21
Chapter 2 Goal and Overview of This Work.....	23
Chapter 3 Parallel Protease Assays Using Suspension Microsphere Arrays.....	27
3.1 Introduction.....	27
3.2 Materials and Methods.....	30
3.2.1 Materials.....	30
3.2.2 Preparation of Biotinylated Substrate Plasmids.....	31
3.2.3 Expression and Purification of Biotinylated Protease Substrates.....	32
3.2.4 Prestwick Library Screening.....	33
3.2.5 Screen of 350,000 Compounds.....	35
3.2.6 Dose Response Measurement on Microspheres.....	35
3.2.7 FRET Solution Dose Response.....	36
3.3 Results and Discussion.....	37
3.3.1 Development of Multiplexed Protease Assay.....	37
3.3.2 Primary Screening of Chemical Libraries.....	41
3.3.3 Riboflavin Can Inhibit Lethal Factor Activity.....	45
3.3.4 Tests of Structure-activity Related Compounds.....	50
3.3.5 Evaluation of Lead Compounds Against BoNT/A LC in Solution Assay.....	55

3.4 Conclusion.....	60
Chapter 4 Kinetic Analysis of Botulinum Neurotoxin Type A Light Chain Using FRET Full-length Substrate.....	63
4.1 Introduction.....	63
4.2 Materials and Methods.....	64
4.2.1 Materials.....	64
4.2.2 GFP Quenching by Cy3-streptavidin.....	64
4.2.3 FRET Solution Kinetic Assay.....	65
4.3 Results and Discussion.....	66
4.3.1 GFP Quenching by Cy3-streptavidin.....	66
4.3.2 BoNT/A LC Cleavage of A Full-length SNAP-25 Substrate in Solution.....	68
4.3.3 Determination of The Cleavage Rate of A Small FRET Peptide.....	70
4.3.4 Inhibition Mechanism Determination of Specific Compounds Using Full-length Substrate in Solution.....	73
4.4 Conclusion.....	75
Chapter 5 Kinetic Study of Botulinum Neurotoxin Type A Light Chain on Microspheres by Flow Cytometry.....	76
5.1 Introduction.....	76
5.2 Materials and Methods.....	78
5.2.1 Materials.....	78
5.2.2 Expression and Purification of SNAP-25 GFP.....	78
5.2.3 Microsphere Based Protease Assays.....	79
5.2.4 Dead Time Measurement of Accuri C6 Flow Cytometer.....	80
5.3 Results and Discussion.....	80
5.3.1 Titration of Binding of SNAP-25 GFP to The Surface of Microspheres.....	81
5.3.2 BoNT/A LC Cleavage of Full-length SNAP-25 Fusion Proteins from A Microsphere Surface.....	83
5.3.3 Kinetics of BoNT/A LC Cleavage from The Microsphere Surface.....	85
5.3.4 Dead Time Measurement of Accuri.....	90
5.3.5 Protease Cleavage Measurement Using Accuri at Fast Flow Rate.....	92

Chapter 6 Nanosphere-based Kinetic Analysis of Botulinum Neurotoxin Type A	
Light Chain.....	95
6.1 Introduction.....	95
6.2 Materials and Methods.....	97
6.2.1 Materials.....	97
6.2.2 Prepare Fluorescent Fusion Protease Substrates.....	98
6.2.3 Determine Events Rate by BD FORTESSA Flow Cytometry.....	98
6.2.4 Titration of Protease Substrate on Nanospheres.....	98
6.2.5 Nanosphere-based Protease Cleavage Assay.....	99
6.2.6 Size Measurement of Nanospheres.....	100
6.3 Results and Discussion.....	100
6.3.1 Predicted and Measured Event Rates.....	100
6.3.2 Titration of SNAP-25 GFP on 380 nm Nanospheres.....	102
6.3.3 Protease Cleavage Assay on Nanospheres.....	104
6.3.4 Size Measurement of Nanospheres.....	107
6.4 Conclusion.....	109
Chapter 7 Conclusions and Future Directions.....	110
7.1 Conclusions.....	110
7.1.1 Parallel Protease Assay Using Suspension Microsphere Arrays for High-throughput Screening.....	110
7.1.2 FRET Solution Assays for Protease Kinetic Analysis.....	111
7.2 Future Directions.....	112
7.2.1 Nanosphere-based Protease Assay.....	112
7.2.2 Future Drug Targets: Matrix Metalloproteases.....	113
7.2.3 High-throughput Screening and Kinetic Studies of MMPs.....	114
List of Appendices.....	115
Appendix 1. DNA Sequence of VMAP-2 with Restriction Sites (<i>SacI</i> and <i>BamHI</i>)...	115
Appendix 2. Identified inhibitors for Botulinum Neurotoxin type A light chain in microsphere-based high-throughput screening.....	115
Appendix 3. Identified inhibitors for Botulinum Neurotoxin type F light chain in microsphere-based high-throughput screening.....	120

Appendix 4. Identified inhibitors for <i>Bacillus anthracis</i> Lethal Factor in microsphere-based high-throughput screening.....	123
References.....	128

List of Figures

Chapter 1 Introduction

Figure 1.1 Botulinum Neurotoxin Mechanism.....	5
Figure 1.2 BoNT/A Cleaves SNAP-25 at A Specific Site.....	8
Figure 1.3 BoNT/F Cleaves VAMP-2 with Two Binding Sites V1 and V2.....	11
Figure 1.4 Lethal Toxin Mechanism.....	13

Chapter 3 Parallel Protease Assays Using Suspension Microsphere Arrays

Figure 3.1 Four-plex Substrate System Schematic.....	38
Figure 3.2 Four-plex Protease Cleavage Assay.....	40
Figure 3.3 384-well Plate High-throughput Screening.....	42
Figure 3.4 Dose Response Curves of Riboflavin.....	47
Figure 3.5 Riboflavin Against BoNT/A LC.....	49
Figure 3.6 Dose Response Curves of 11 Compounds.....	51
Figure 3.7 Dose Response Curves of Compounds 2865835 and 2827281.....	52
Figure 3.8 Dose Response Curves in FRET Peptide Assay.....	56
Figure 3.9 Dose Response Curves of Three Specific Compounds in FRET Full- length Assay.....	59

Chapter 4 Kinetic Analysis of Botulinum Neurotoxin Type A Light Chain Using FRET Full-length Substrate

Figure 4.1 GFP Quenching by Cy3-streptavidin.....	67
Figure 4.2 FRET Full-length Kinetic Assay.....	69
Figure 4.3 FRET Peptide Kinetic Assay.....	72
Figure 4.4 Inhibition Determination of Specific Compounds.....	74

Chapter 5 Kinetic Study of Botulinum Neurotoxin Type A Light Chain on Microspheres by Flow Cytometry

Figure 5.1 Equilibrium Binding of SNAP-25 GFP on Microspheres.....	82
Figure 5.2 The Fluorescence Measurement of Cleavage from Microspheres vs. Time.....	84
Figure 5.3 Kinetic Analysis of BoNT/A LC Based on Microsphere.....	89
Figure 5.4 Dead Time Measurement of Accuri.....	91
Figure 5.5 Protease Cleavage Assay at Fast Flow Rate of Accuri.....	93

Chapter 6 Nanosphere-based Kinetic Analysis of Botulinum Neurotoxin Type A Light Chain

Figure 6.1 Predicted and Observed Event Rates of Nanospheres.....	101
Figure 6.2 Titration of SNAP-25 GFP on Nanospheres.....	103
Figure 6.3 Protease Cleavage of SNAP-25 on Nanospheres.....	106
Figure 6.4 DLS Measurement of Nanospheres.....	108

List of Tables

Chapter 1 Introduction

Table 1.1 Cleavages Sites of Botulinum Neurotoxin on SNARE Proteins.....	6
---	----------

Chapter 3 Parallel Protease Assays Using Suspension Microsphere Arrays

Table 3.1 Primary and Confirmatory Screening Results.....	44
Table 3.2 Summary of 11 Compounds into Four Scaffolds.....	54
Table 3.3 IC₅₀ Values of 11 Compounds in Both Microsphere and FRET Peptide Assays.....	57
Table 3.4 Specific Compounds Against BoNT/A LC.....	60

Chapter 1

Introduction

1.1 Bacterial Zinc Dependent Metalloproteases

Proteases are of great interest as possible drug targets, because they regulate many physiological processes including infection, cell growth and death, fertilization, inflammation, allergic reactions, bone remodeling, tumor growth and blood clotting.¹ Bacterial proteases are critical to the toxicity of many pathogens as they commonly target host pathways that lead to the death of the host organism.² Therefore, the development of novel drugs and antibiotics that target bacterial protease is of great importance.³ At present, there are five catalytic types of bacterial proteases that have been recognized. Four are based on the type of amino acid found at the active site (serine, threonine, cysteine, or aspartate), while the fifth type coordinates a metal ion in its active site.² These metalloproteases (MPRs) are specific proteases use coordinated metal ions to attack the peptide bond to cleave proteins. The metal ion is usually zinc, cobalt, or manganese.² Generally, MPRs are divided into two groups depending on how many metal ions are required in the catalytic mechanism. So far, most MPRs are one-metal-ion-dependent proteases, with the exception of some exopeptidases that require two catalytic metal ions for efficient cleavage.^{2,4} MPRs are widely used by bacteria and play various pathogenic roles in infection.^{5,6} For example, some bacteria use MPRs to process enterotoxin (*e.g.* cholera toxin) to their active state. Other bacteria use proteases as part of their toxins, which is the case for the Botulinum neurotoxins (BoNT) and Tetanus

neurotoxins (TeNT) that use MPRs to directly cleave target host proteins.^{7,8} For these reasons, MPRs are important targets for therapeutic compounds.

Most MPRs are zinc-dependent proteases and are integral to virtually all aspects of metabolism.⁹ The consensus binding motif for zinc-containing metalloproteases is HEXXH, in which two histidine residues coordinate zinc divalent cationic binding.¹⁰ This zinc-binding motif has been found in the light chain of *Clostridium Botulinum* neurotoxins¹¹, *Bacteroides fragilis* enterotoxin¹², and *Bacillus anthracis* lethal factor¹³. These light chain proteases require the presence of zinc for activity.¹⁰ Of specific interest to this work, Botulinum neurotoxin (BoNT) light chains cleave one of three soluble N-ethylmaleimide-sensitive factor-attachment protein receptor (SNARE) proteins that are components of the neuroexocytosis machinery. Cleavage of these proteins leads to the blockade of neurotransmitter release and consequent paralysis.¹⁴ The light chain of *Bacillus anthracis* lethal toxin, known as lethal factor (LF) cleaves the mitogen-activated protein kinase-kinases (MAPKKs) at their amino-terminus.¹⁴ Though the toxicity of many bacterial toxins are due to the Zn metalloproteases activity, the Zn coordinating active site is highly conserved across many families of zinc metalloproteases. This makes it difficult to target the active site of toxin MPRs, as the numerous cellular Zn metalloproteases, such as matrix metalloprotease (MMPs) and metalloproteases with a disintegrin domain (ADAM) are critical for cell processes. Therefore, understanding the structure-activity relationships of these enzymes would be beneficial for the development of potential inhibitors. In addition, a further understanding of the mechanism of these enzymes will offer great opportunity to screen for or create new and useful protease compounds that specifically target toxin MPRs.

1.2 Botulinum Neurotoxins

Botulinum neurotoxins (BoNTs) are the most toxic substance known.^{15,16} They are produced by *Clostridium botulinum*.^{17,18,19} Each BoNT serotype is a two-chain holotoxin made up of two polypeptides with a molecular weight of 150 kDa, which is modified post-translationally by bacterial or host protease. This precursor protein is composed of a subunit of one 100 kDa heavy chain (HC) subunit linked to a 50 kDa light chain (LC) subunit by an essential interchain disulfide bridge and a poorly structured protein segment, called the belt, which extends from the HC to LC.^{7,20} The HC is a binding domain containing two unique subdomains, the NH₂-terminal half (H_C-N) and the C-terminal half (H_C-C), with few protein-protein contacts between one and another. H_C-N is composed of a jelly-roll motif arranged with two seven-stranded β -strands while H_C-C embraces a modified β -trefoil folding motif for recognition and binding functions.⁷ The LC at the N-terminal is a zinc-dependent metalloprotease that cleaves the protein substrates.²¹ The LC itself is nontoxic and inhibits exocytosis while direct microinjection of the LC into the cytosol causes blockage of membrane exocytosis.^{22,23}

BoNTs exist as seven serologically distinct isoforms (denoted A to G). All BoNTs (A-G) inhibit signaling at nerve terminals leading to the symptoms of botulism.⁷ The release of acetylcholine at the neuromuscular junction, is mediated by the soluble N-ethylmaleimide-sensitive factor-attachment protein receptor (SNARE) proteins that allow the membrane of the synaptic vesicle containing acetylcholine to fuse with the neuronal cell membrane. The two-part botulinum neurotoxin binds to the neuronal cell membrane via its heavy chain and enters the neuron by endocytosis. Once inside the cell, the light chain cleaves at specific sites on the SNARE proteins, preventing complete

assembly of the synaptic fusion complex and thereby blocking acetylcholine release (Figure 1.1).²⁴ BoNTs cleave the SNARE proteins that include synaptobrevin (or vesicle associated membrane protein; VAMP), the 25 kDa synaptosomal-associated protein (SNAP-25), and syntaxin.⁷ Specifically, BoNT/A, BoNT/C and BoNT/E cleave SNAP-25 at different peptide bonds; BoNT/B, BoNT/D, BoNT/F and BoNT/G cleave VAMP; and, BoNT/C cleaves syntaxin (Figure 1.1).⁷ The specific cleavage sites of each BoNT serotype are shown in Table 1.1. Several clinical types of human botulism have been identified that are caused by BoNT/A, BoNT/B, BoNT/E, and occasionally BoNT/F.²⁴

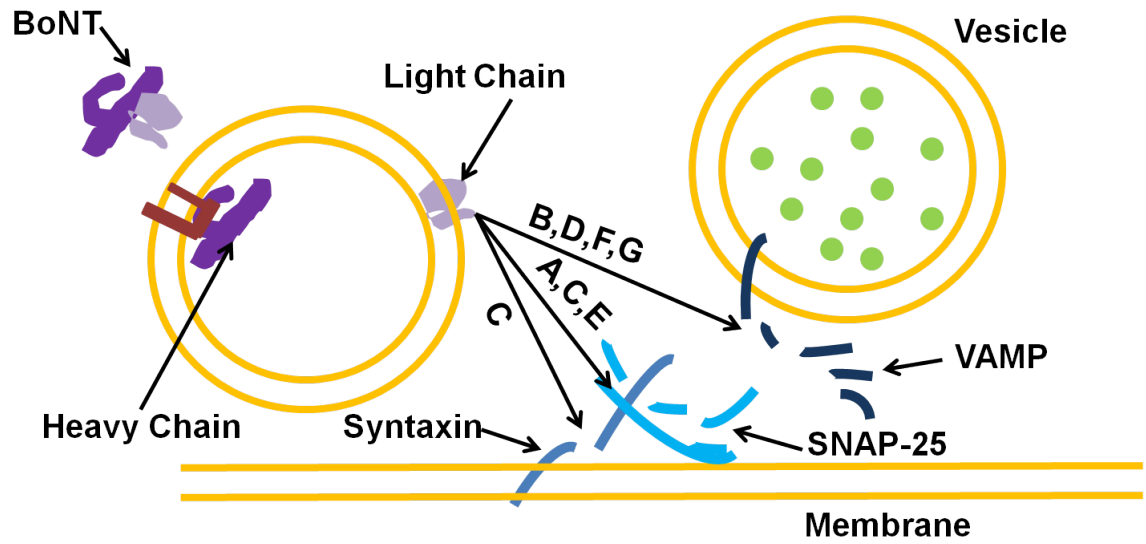


Figure 1.1 Mechanism of action of BoNTs. BoNT heavy chain binds to the neuronal cell at the nerve terminus and transfers the light chain to cleave SNARE proteins so that the SNARE complex does not form and the membranes do not fuse. This figure is modified from reference 24.

Table 1.1 The cleavage sites of each BoNT serotype on SNARE proteins.

BoNT Serotype	SNARE Substrate	Cleavage Site
A	SNAP-25	Gln197-Arg198
B	VAMP-2	Gln76-Phe77
C	SNAP-25	Arg198-Ala199
C	Syntaxin	Lys253-Ala254 and Lys260-Ala261
D	VAMP-2	Lys59-Leu60
E	SNAP-25	Arg180-Ile181
F	VAMP-2	Gln58-Lys59
G	VAMP-2	Ala81-Ala82

1.2.1 BoNT/A Cleaves SNAP-25

Botulinum neurotoxin type A (BoNT/A), which cleaves SNAP-25, is the most frequent cause of human botulism.²⁴ SNAP-25 regulates vesicle exocytosis and belongs to the SNARE superfamily of small membrane proteins, which anchor to the cytosolic surface of membranes through palmitoyl side chains, located in the central domain of the molecule. SNAP-25 is composed of two α -helices that form the exocytotic fusion complex with syntaxin-1 and synaptobrevin, all of which are required for vesicle fusion.^{25,26} In addition, SNAP-25 provides an essential mechanism for triggering Ca^{2+} -dependent membrane fusion and controlling fusion pore dynamics during the final steps of exocytosis by interacting with the synaptic vesicle protein synaptotagmin I.^{27,28} Therefore, SNAP-25 has been considered as a multifunctional protein that controls neurotransmitter secretion via several interactions.

To cleave SNAP-25, BoNT/A inserts into the vesicle and undergoes a pH-dependent conformational change that causes the dissociation of the heavy and light chains and an increase of the toxin's hydrophobicity.²⁹ BoNT/A recognizes the highly conserved SNARE motif that is found four times (S1-S4) within the SNAP-25 molecule.³⁰ BoNT/A requires the presence of the C-terminal region of SNAP-25 including the S4 site, while the three N-terminal sites (S1-S3) are not required (Figure 1.2).³¹ BoNT/A recognizes its substrate via both a structural motif and the sites containing the peptide bond to be cleaved.³² The activity of BoNT/A LC is strongly influenced by distal substitutions and deletions.^{33,34}

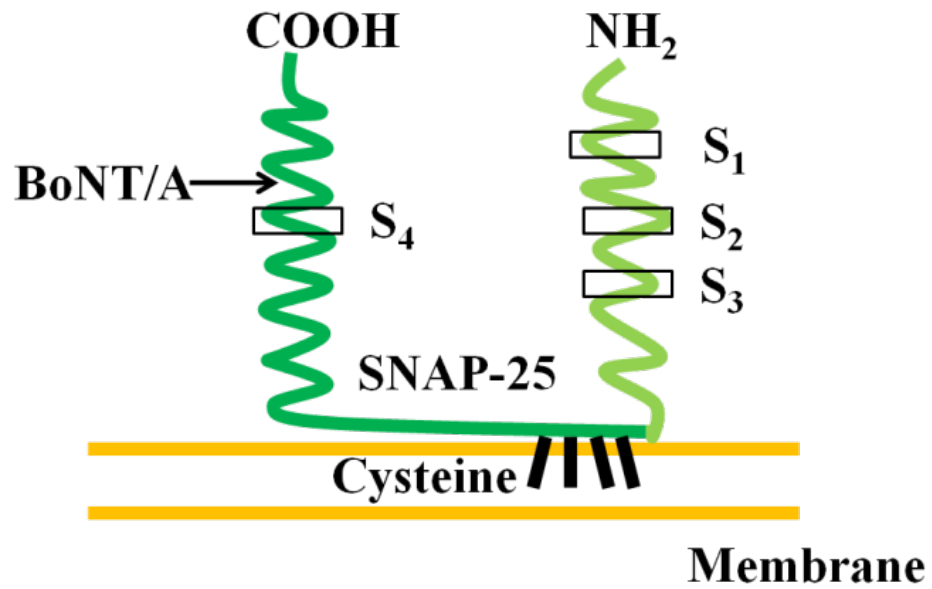


Figure 1.2 BoNT/A cleaves SNAP-25 at a specific site as shown by the arrow. The binding motifs are denoted by boxes at C-terminal (S4) and N-terminal (S1-S3) regions.

The exosites are distant from the cleavage sites and play crucial roles in efficient substrate recognition and cleavage of light chain.³² The concept that a distant binding site is necessary for efficient cleavage of SNAP-25 was supported by co-crystal structures of a truncated SNAP-25 bound to BoNT/A. This showed that there was a distant binding site required for BoNT/A binding.³⁵ This site overlaps the S4 site and likely represents the same interaction point noted in both studies.^{31,35} The significant structural changes near the toxin's catalytic pocket upon substrate binding may serve to render the protease competent for catalysis.³⁵ Understanding the binding mechanism of BoNT/A and SNAP-25 at the distal site may provide insight into a modification of BoNT/A that would optimize therapeutic potential as well as develop serotype-specific inhibitors against botulism.³⁶ Importantly, inhibitors that target the distal site are likely to be very specific to a BoNT serotype and less likely to target host MPRs, which could be expected to reduce compound toxicity.

1.2.2 BoNT/F Cleaves VAMP-2

Botulinum neurotoxin type F is a zinc-endopeptidase with a unique specificity for VAMP/synaptobrevin, which is an essential component of SNARE proteins for the exocytosis apparatus.³⁷ VAMP is a tail-anchored membrane protein of exocytotic vesicles³⁸ and is composed of different isoforms.³⁹ Neurotoxin-insensitive isoforms are present in many non-neuronal tissues.^{40,41} *Clostridial* neurotoxins lack activity on non-neuronal cells because they do not bind to these cells that lack cell surface neurotoxin receptors.³⁷ Three isoforms have been identified containing VAMP-1 and VAMP-2

present in the neural and neuroendocrine tissues,⁴² and a third, cellubrevin, which is present in non-neuronal cells.⁴³ BoNT/F can cleave both VAMP-1 and VAMP-2. VAMP-1 is preferentially expressed in the motor system, whereas VAMP-2 is predominantly present in nuclei associated with sensory and integrative functions.^{42,44} BoNT/F cleaves VAMP-2 within a conserved region containing the cleavage sites, and the recognition sites (V1 and V2).³² BoNT/F cleaves the peptide bond Gln58-Lys59, which is located between V1 and V2 (Figure 1.3). Mutation studies verify that both V1 and V2 play major roles in BoNT/F activity.³⁷ So far, only a few mechanistic studies of BoNT/F have been published, but very few inhibitors of BoNT/F have been reported. It is of great importance to research and identify inhibitors for BoNT/F in order to treat human botulism. Because BoNT/F LC is nontoxic, it has been the main target for in vitro assays to identify potential inhibitors. In addition, the mechanistic study of full-length substrate containing distal sites will provide a great platform to design potential inhibitors and modify the protease analogues for clinical therapy. Again, targeting the distal sites (V1 and V2) may offer a path to the development of highly specific inhibitors that have reduced cellular toxicity.

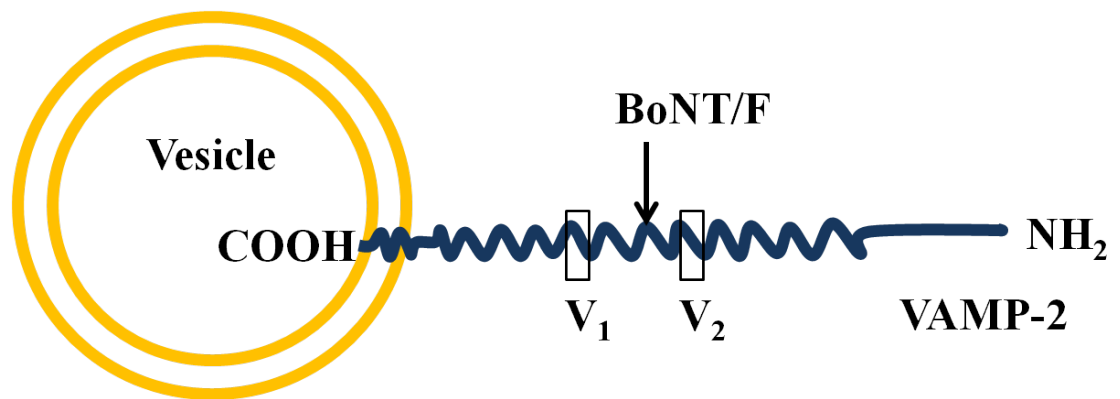


Figure 1.3 BoNT/F cleaves VAMP-2 with two binding sites V1 and V2.

1.3 Anthrax Lethal Factor

Bacillus anthracis is a gram-positive, aerobic, spore-forming, rod-shaped bacterium, which causes Anthrax.⁴⁵ This disease is initiated by the entry of spores into the body of the host causing three types of infections. They are cutaneous, gastrointestinal and inhalational, which can occur via a minor abrasion, an insect bite, or by eating contaminated meat or inhaling airborne spores.⁴⁶ *B. anthracis* has long been of concern as a potential agent of biological warfare.⁴⁷ *B. anthracis* is composed of two virulence factors that are the gamma-linked, the poly-D-glutamic acid capsule and the secreted anthrax toxin.⁴⁸ Anthrax toxin is composed of three proteins that are termed protective antigen (PA), lethal factor (LF) and edema factor (EF).⁴⁹ Each of the three components is individually non-toxic.⁴⁷ The combination of PA and LF produces lethal toxin (LT) whereas the combination of PA and EF produces edema toxin (ET). Both toxins are sufficient to produce many of the symptoms of anthrax infection.^{50,51} LT is a binary toxin consisting of a binding moiety (PA) and an enzymatic moiety (LF). PA binds to toxin receptors on the surface of the host cell and is subsequently processed by the host enzyme furin.^{52,53} Then a seven-member ring oligomer is formed which can bind up to three molecules of LF. The resulting toxin complex is endocytosed and trafficked to an acidic compartment where the low pH triggers a conformational change in PA that promotes membrane insertion and translocation of LF into the cytosol (Figure 1.4).⁵⁴

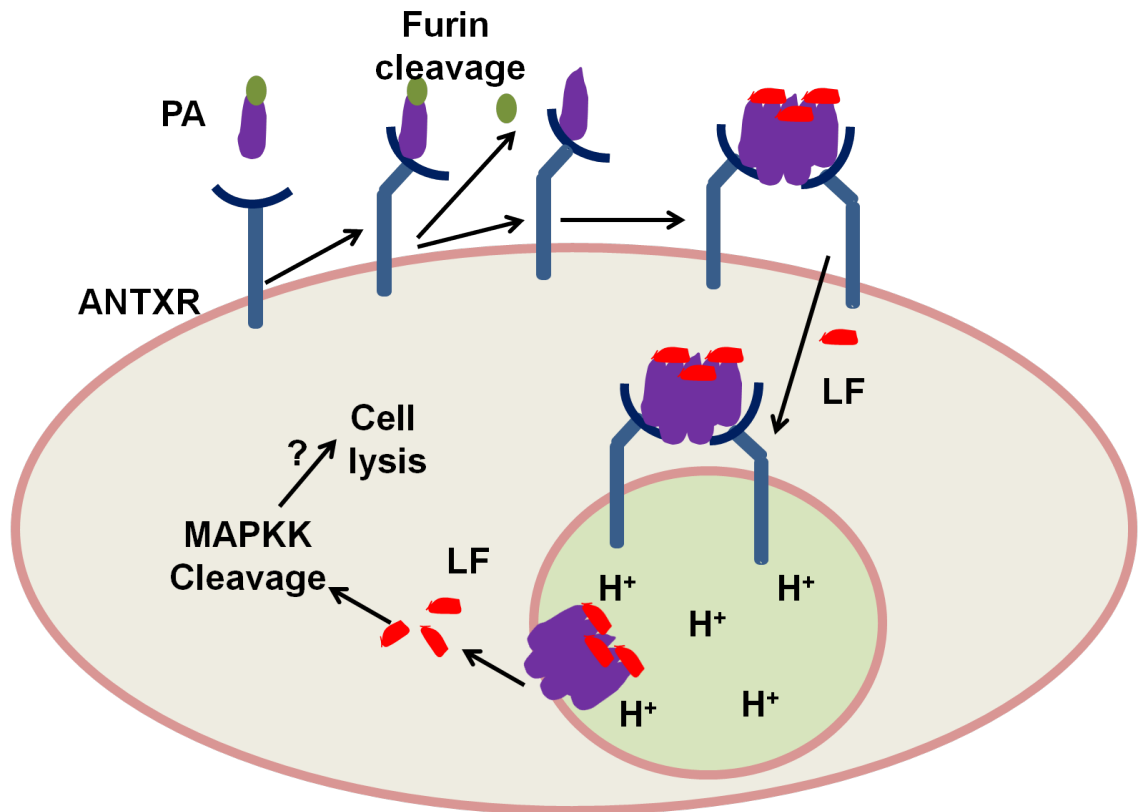


Figure 1.4 Entry and action of anthrax lethal toxin (LT). PA binds to its receptor (ANTXR) and is cleaved by furin to form a seven-member ring oligomer, which binds up to three LF molecules. The resulting toxin complex is endocytosed and trafficked to an acidic compartment, low pH triggers a conformational change in PA that promotes membrane insertion and translocation of LF into the cytosol for cleavage of MAPKK proteins. This figure is modified from reference 54.

LF is a 90 kDa zinc-dependent metalloprotease that cleaves mitogen-activated protein kinase kinase (MAPKK) isotypes 1-4 and 6-7.^{55,56} LF is an elongated protein (>10 nm) comprised of four partially related domains containing: 1) a N-terminal PA-binding domain of EF, 2) a domain involved in binding to residues in MAPKK substrates distant from the cleavage site, 3) an inserted helical domain involved in binding to substrates, and 4) a catalytic domain related to *Clostridial* neurotoxins.⁵⁷ LF cleaves the peptide bond within the N-terminal proline-rich region that precedes the kinase domain of the substrates by disrupting the protein interaction involved in assembling signaling complexes, thus preventing MAPKK activation, leading to the death of the host via a poorly defined sequence of events.⁵⁸ Therefore, treatment with LT-caused disease is of great importance, because the MAPKK pathway is a key regulatory signal transduction pathway that sends signals from the cell surface to intracellular effectors through a cascade of phosphorylation events.⁵⁹

Anthrax is a complex toxin and fully effective treatment may require complementary approaches. It would be of great interest to design therapeutics targeting the clinical effects of the toxins because the consequences of LF activity and downstream of proteolytic cleavage of MAPKKs may lead to the death of the host.⁴⁶

1.4 Protease Inhibitors

Potential protease inhibitors are emerging with promising therapeutic uses in the treatment of diseases including cancer,⁶⁰ infections,^{61,62} as well as inflammatory, immunological, respiratory, and neurodegenerative disorders.^{63,64,65} A potential inhibitor

must be not only highly selective in binding to a particular protease, but must also have appropriate pharmacokinetic and pharmacodynamic properties. Protease inhibitors have been widely developed by screening natural products to identify lead compounds. Varied methods have been developed for subsequent optimization of these lead compounds or the substrates,⁶⁶ which include truncating polypeptide substrates to short peptides, replacing the cleavable amide bond by a noncleavable isostere, and optimizing inhibitor potency via structural modifications.⁶⁷

Typically, all known metalloproteases are zinc-dependent proteases that use a zinc atom to affect amide bond hydrolysis. The zinc ion is generally tetrahedral-coordinated to three donor groups from the enzyme and a water molecule.⁶⁷ Therefore, the inhibitors blocking this coordination have been widely designed and synthesized as metalloprotease inhibitors. Since many metalloproteases from the same protein families share a common active site architecture, compounds designed to inhibit one protease could be used as inhibitors of the other proteases by virtue of their complementary specificity.⁶⁸ Unfortunately, the cross reactivity of many inhibitors also leads to a great deal of off target toxicity for metalloprotease inhibitors.⁶⁹ Thus, there is a great need for screening approaches that result in specific inhibitors that do not target the highly conserved active site.

1.4.1 Botulinum Neurotoxin Inhibitors

Many current research efforts seek to identify BoNT protease inhibitors, as metalloprotease activity is critical to the function of the toxin.⁷⁰ Many approaches have

been envisioned for inhibitor development including mimicking peptide sequences based upon the native SNARE protein substrate or identifying small molecules that bind to the toxin and inactivate it.⁷⁰ Several effective inhibitors have been reported based upon peptide scaffolds.^{71,72,73} Given the presence of zinc ion in the LC active site, the hydroxamate zinc-binding functionality when coupled to a suitable scaffold to impart specificity, would seem to provide a promising platform for potent BoNT inhibitors. However, directly targeting the highly conserved active site may lead to cross reactivity to other MPRs, which may lead to compound side effects. Nonetheless, the use of heavy-metal chelators has been considered for potential therapeutic applications.⁷⁰ We and others have suggested that targeting the distal site interaction of BoNT inhibitors may lead to inhibitors with reduced toxicity.^{35,74} Regardless of the approach, the development of potent but low toxicity BoNT LC protease inhibitors could be a critical step in rescuing nerve activity after toxin internalization.

1.4.1.1 Botulinum Neurotoxin Type A Inhibitors

So far, BoNT/A has been the main focuses for many researchers owing to their potent toxicity. The studies for screening natural products to identify small molecule inhibitors have reported a series of 4-aminoquinolines that were originally distinguished to prolong the time required for BoNT/A to block neuromuscular transmission.⁷⁵ A high-throughput FRET-based assay for the screening of compounds libraries has reported that arginine hydroxamic acid could modestly inhibit BoNT/A with a K_i value of 60 μM .⁷⁶ On the basis of screening a library of hydroxamic acids, 4-chlorocinnamic hydroxamate with an IC_{50}

value of 15 μM has been considered as a promising lead compound for further development. Furthermore, a 2,4-dichloro-substituted compound displayed competitive inhibition against BoNT/A with a K_i value of $0.3 \pm 0.01 \mu\text{M}$.⁷⁷ The use of recombinant fluorescent substrate in high-throughput screening of natural product extracts resulted in identification of both an aqueous extract from the green star coral *Pachyclavularia tosana* and three extracts from the African deciduous tree *Terminalia brownii* as inhibitors against BoNT/A.⁷⁸ In addition, a pseudopeptide inhibitor mimic of the 7-residue sequences (QRATKML) of 206-residue SNAP-25 has been reported as a specific BoNT/A inhibitor, which is the most potent non-zinc-chelating, non-hydroxamate-based antagonist with a K_i value of 41 nM.⁷⁹ Furthermore, the microsphere-based high-throughput screening of an off-patent chemical library has reported ebselen as an in vitro inhibitor for BoNT/A LC by using full-length substrate.⁷⁴ In summary, varied inhibitors have been found including natural products, synthesized organic compounds with structure-activity relationships, and peptide analogues based on different in vitro assay methods. These studies have provided a strong framework to discover new BoNT/A inhibitors as therapeutic agents. However, effective inhibitors that specifically target the distal site interaction have not been discovered as of yet.

1.4.1.2 Botulinum Neurotoxin Type F Inhibitors

Among zinc metalloproteases, BoNT/F is unique with respect to its requirement of inhibitor-binding groups on the N-terminal side of the substrate. The substrate analogues introducing zinc-binding moiety (the sulfhydryl group), which is near the scissile bond in

peptide 37-75, would inhibit BoNT/F protease activity.^{80,81,98} A series of peptide analogues with a C-terminal Q58_D-C mutations show effective inhibition against BoNT/F with K_i values in nanomolar range.⁸² For instance, the substrate-based inhibitors inh1 and inh2 consisted of VAMP residues 22-58 and 27-58 with Q58 replaced by _D-cysteine showed K_i values of 1.0 nM and 1.9 nM, respectively.⁸² In addition, several naturally lectins containing sialic acid have been reported as effective inhibitors with a K_i value around 100 nM in preventing BoNT/F from binding to the presynaptic terminal.⁸³

However, very few BoNT/F inhibitors have been reported. Even though zinc chelators are common inhibitors against BoNT/F, they are relatively inefficient in blocking the activities of BoNT/F. As well, small molecule zinc chelators could have undesirable side effects since they might inhibit other zinc-dependent proteases, with similar zinc binding sites.⁸⁴ At present, the development of substrate analogues with mutations of residues has been the main focus of inhibitor studies. High-throughput screening of a library of chemical compounds has also been used to identify potential inhibitors for BoNT/F, but few compounds were identified as specific inhibitors. To discover small molecule inhibitors for BoNT/F, the more compounds would be referred and screened based on different high-throughput methods and chemical libraries. Again, inhibitors that target the interaction between the VAMP distal sites and BoNT/F LC would potentially reduce inhibitor toxicity.

1.4.2 Anthrax Lethal Factor Inhibitors

Since the protease activity of lethal factor leads to the anthrax toxicity, inhibitors of LF are currently being sought as effective therapeutics for the treatment of anthrax. Many peptide substrate analogues and small molecule compounds have been reported as LF inhibitors. The hydroxylamine derivative of peptide substrate, In-2-LF, has been found with a K_i value of 1 nM, which is the most potent inhibitor identified to date.⁸⁵ A series of compounds containing *N*-oleoyldopamine and their analogues have been demonstrated to be uncompetitive inhibitors of LF, owing to the presence of the oleic acid moiety and double bond.⁸⁶ Recently, Karginov *et al* have reported that some derivatives of β -cyclodextrin inhibit LF action by blocking the transmembrane pore formed by PA subunit.⁸⁷ A systematically generated series of hydrazones with IC_{50} values in the micromolar range have been reported against LF activity based on different *in vitro* assays.⁸⁸ Additionally, a series of mono-, di-, and tri-guanidinylated derivatives of neamine have been synthesized representing a novel scaffold for LF inhibitors.⁸⁹

Currently, many other small molecule inhibitors have been identified via high-throughput screening methods. For instance, a fluorescence polarization (FP)-based high-throughput screening of a collection of 2,835 small molecules and natural product extracts using a full-length MAPKK substrate was used to identify inhibitors targeting protease distal sites as well as active sites.⁹⁰ A yeast-hybrid-based high-throughput assay has been reported depending on a site-specific cleavage of the chimeric yeast containing an LF-substrate to screen about 6,500 represented scaffolds to identify specific inhibitors.⁹¹ A high-throughput fluorescence-based assay has also been performed to screen a library of 14,000 compounds leading to the identification of new scaffolds that

inhibit LF activity in the low micromolar range.⁹² In addition, a chemical library of 10,000 small molecule compounds has been evaluated by matrix-assisted laser-desorption ionization (MALDI) time-of-flight (TOF) MS combined with self-assembled monolayers (SAMs) for parallel screening experiments to identify a LF inhibitor with a K_i of 1.1 μM .⁹³ The discovery of small molecule compounds may facilitate the development of novel, safe and effective anthrax pharmaceutical agents. The identification of LF inhibitory peptides would allow us to synthesize more peptide analogues that potentially have increased potency.

1.5 Surface-based Protease Assays

The development of a method to study proteases and identify their inhibitors with high sensitivity in a multiplexed manner is of great importance in diagnosis of protease-relevant diseases.^{94,95,96,97} Over the past decade, many attempts have relied on affinity-based methods to assay proteases including liquid chromatography,⁹⁸ gel electrophoresis,⁹⁹ or immunoassay.^{100,101} But many of them have a limitation for a multiplexed assay or high-throughput screening. Afterwards, Forster (or fluorescence) resonance energy transfer (FRET) has been employed for protease assays where two fluorophores (energy donor and acceptor) are typically attached to the ends of the substrates with a distance of less than 10 nm.^{102,103,104,105} Even though the FRET technique has been widely used in solution assays, they are difficult to perform as multiplexed assays for more than one protease simultaneously. More recently, quantum dots (QDs) have been more attractive for use in protease assays, because they have more

desirable photophysical properties than organic dyes including high quantum yield, less photobleaching, and size-tunable photoluminescence with broad excitation and narrow emission bandwidth.^{106,107} Due to these properties, QDs can serve as excellent probes for a multiplexed and high-throughput protease assay with high sensitivity. Usually, the QD-based FRET assays use peptide substrates, which are smaller than full-length substrates and don't contain distant sites for protease binding that are present in full-length substrates. What is needed is a multiplexable assay that can use full-length substrates. This enables the use of multiple substrates that also include the necessary distal binding elements.

The ability to study multiple proteases in a single assay format has many advantages over single-target systems, that contains high-throughput screening, low consumption of reagents and samples, protease selectivity and specificity. The need to measure the activities of multiple proteases simultaneously using full-length substrates has resulted in the invention of the multiplexed microsphere/nanosphere based protease assays.^{74,108} The streptavidin-biotin system has been widely used to immobilize the substrate on surfaces due to the strong non-covalent interaction between each other. In my research, I have used this system to immobilize the protease substrates on microspheres or nanospheres for protease activity measurement.

1.6 High-throughput Flow Cytometry for Drug Discovery

High-throughput screening is a critical step in the drug discovery process for the pharmaceutical industry. Flow cytometry can perform homogeneous analysis of

molecular assemblies or ligand binding by resolving the free vs. surface-bound fluorescence molecules, when the single particle passes through a laser beam.¹⁰⁹ This property makes it simple to measure time-dependent fluorescence loss by determine the original fluorescence intensity on the microspheres and the remaining fluorescence on microspheres after protease cleavage without requirement of a wash step to remove cleaved fluorophore.⁷⁴ In addition, flow cytometry enables the simultaneous quantitative analysis of a multiplex bead-based suspension array as the beads are color coded with varying intensities of fluorescence to produce a series of bead sets.¹¹⁰ The microsphere based high-throughput flow cytometry assay is a promising approach with several advantages including: low substrate costs, small reaction volumes, homogenous assay format, and use of full-length substrates to detect all pertinent interactions; however, it has limitations in collection of traditional kinetic data. In my dissertation, I have developed 1536-well plate-based high-throughput screening approach for evaluating a library of about 350,000 compounds against three proteases simultaneously. Several compounds have been identified to be potential inhibitors for specific proteases with K_i values in the low micromolar or nanomolar range.

Chapter 2

Goals and Overview of This Study

The goal of this work is to develop a surface-based protease assay that enables the use of full-length protease substrates, multiplexed assays, and most importantly, is high-throughput. These technical advances have also provided new insights into protease kinetics and drug discovery.

In Chapter 3, we describe development of a four-plex microsphere based protease assay. In this assay, three of the microsphere populations bear a unique fluorescent protease substrate that is specific for a toxin protease and the fourth bears a negative control substrate. Specific protease cleavage is reported via the loss of fluorescence from a specific microsphere set. The fluorescent substrates containing the cleavage sites are designed with a biotinylation tag at N-terminal and a GFP domain at C-terminal for three proteases (LF, BoNT/A&F LCs) that can associate with streptavidin-coated microspheres. When used in combination with high throughput flow cytometry, I demonstrated its use to simultaneously screen the 1280 compound Prestwick library for inhibitory compounds. This screen discovered a new inhibitory compound (riboflavin) that is specific for Lethal Factor. Microsphere and FRET peptide-based dose response assays indicated that the IC₅₀ values of riboflavin against Lethal factor were 15 μ M and 17.4 μ M, respectively. It also confirmed the discovery of ebselen, which is a BoNT/A inhibitor that was previously discovered using a BoNT/A specific screen.⁷⁴

In order to identify additional efficient inhibitors, we then performed high-throughput screening for a chemical library of 350,000 compounds using 1536-well plates and

implemented on the HyperCyt[®] flow cytometry system, that could screen thousands of compounds per day for protease inhibition. The hits were further characterized by measuring IC₅₀ values via microsphere-based, FRET peptide and FRET full-length solution based protease assays. This screening led to the identification of 13 compounds that inhibited the activities of LF, BoNT/A & F in the low micromolar range. To understand the structure-activity relationships of these compounds, about 60 chemical compounds with structure-activity relationships were tested in dose response reactions. Then 11 compounds were distinguished with low IC₅₀ values (< 20 μM) against three proteases. These compounds were grouped in four scaffold types. Comparing the results of full-length and peptide assays, three compounds with inhibition against BoNT/A LC were shown to be potentially active at distal sites of SNAP-25 substrate. The relatively low IC₅₀ values, bioavailability, and potential distal interactions of these compounds suggest that they may have great potential for medical applications and demonstrate the value of simultaneous screening of multiple proteases using multiplex microsphere assays.

In Chapter 4, we built the FRET full-length substrate solution assay to determine the kinetic constants of BoNT/A LC and inhibition mechanisms of some known inhibitors. In this case, we used a biotinylation-tag and GFP-labeled protein substrates connected to streptavidin-Cy3 conjugate as the cleavage targets for proteases in solution. Based on the FRET (GFP to Cy3), the fluorescence intensity change was recorded on a fluorimeter or a plate reader. Here, in addition to obtaining the key kinetic constants including k_{cat} , K_{m} and $k_{\text{cat}}/K_{\text{m}}$ of BoNT/A LC, the inhibition mechanisms of three specific compounds against BoNT/A LC were determined.

In Chapter 5, we would seek to understand the kinetic mechanism of these proteases and further inhibition mechanisms of some inhibitor candidates based on surfaces. We used the microsphere-based system to characterize the enzymatic reaction in terms of three key kinetic parameters of BoNT/A LC (K_m , k_{cat} and k_{cat}/K_m) for surface-bound substrate by flow cytometry. Due to the dead time limitation of typical flow cytometers, we were limited in the ability to obtain the true protease cleavage rates. To understand surface-based enzymatic reaction, it will be helpful to study the inhibition mechanisms and determine the inhibition constants of some potential inhibitors. However, despite the many advantages of microsphere-based assays used for screening, the surface area to volume ratio of the microspheres limited us to sub-saturating concentrations of substrate (the low nM).

Therefore, we developed a nanosphere-based protease assay platform using 380 nm streptavidin-coated nanospheres. To demonstrate this approach, we implemented the nanosphere-based protease assay using the toxin protease models to first demonstrate the concept in Chapter 6. By triggering flow cytometric analysis on the fluorescence on the nanospheres, the substrate concentration was increased to the micromolar range and it also confirmed the protease cleavage measurement for BoNT/A LC. The success of nanosphere-based protease assay would provide a great platform to do both high-throughput screening for potential inhibitors and the kinetic study of these proteases.

Our future work discussed in Chapter 7 will focus on development of a nanosphere-based, multiplexed protease assay for proteases such as matrix metalloproteases (MMPs) that have reduced specificity and affinity for their substrates, which necessitates the use of higher substrate concentrations to measure protease activities. Once developed, we

will optimize the assay for use in high throughput flow cytometry screening and demonstrate its effectiveness by screening the Prestwick library of chemical compounds for potential MMP inhibitors. Additionally, we will study the enzyme kinetics of each MMP to explore how MMPs recognize their substrates. The ability to screen several proteases simultaneously will dramatically reduce screening labor and cost, immediately provide information on specificity and mechanism of inhibition, and demonstrate an approach to screening many members from a family of related proteases simultaneously.

Chapter 3

Parallel Protease Assays Using Suspension Microsphere Arrays

3.1 Introduction

Anthrax lethal toxin (LT) and Botulinum neurotoxins (BoNTs) are critical to the lethality of their host organisms, *Bacillus anthracis* and *Clostridium botulinum*, respectively.^{58, 111} LT and BoNT are two-part toxins that have large protein subunit that bonds to cells and an smaller subunit, which is an active protease component that cleaves intracellular proteins to exert a toxic effect.¹¹² As LT is a critical component of Anthrax, a significant biothreat agent, and BoNT is a widespread pharmaceutical that is also most toxic compound known, which makes it also a biothreat agent of grave concern, the development of effective inhibitors for these toxins is of great interest.^{62,113}

To this end, we are specifically interested in the protease subunits, which are lethal factor (LF) of LT and the light chain (LC) of BoNT. Both of these proteases are zinc-dependent metalloproteases that target specific host proteins and are required for the toxicity of the host organism or toxin, which makes them attractive targets for inhibitor discovery.^{54,114} LF cleaves mitogen-activated protein kinase kinases (MAPKK) within the N-terminal proline-rich region to disrupt protein interaction site for assembling signaling complexes, leading to the death of host.⁵⁸ Botulinum neurotoxins (BoNTs) family consists of seven antigenically different botulinum neurotoxins (abbreviated BoNT/X LC where the X is the type) serotypes, A-G, with serotype A, B, E and F responsible for most natural human intoxications.¹¹⁵ Each of BoNT LC serotype is also a zinc-dependent metalloprotease that cleaves a protein element of the SNARE (soluble N-ethylmaleimide-

sensitive fusion attachment protein receptor) complex found within the neurotransmitter pathway, which leads to paralysis and death.^{116,117} Specifically, BoNT/A, C, & E LCs cleave the synaptosomal-associated protein of 25 kDa (SNAP-25), while BoNT/B, D, F & G LCs cleave vesicle-associated membrane protein (VAMP-2 also called synaptobrevin), and BoNT/C LC also cleaves syntaxin.^{118,119}

The detailed knowledge of these proteolytic pathways has led to many efforts, including both rational inhibitor design and high throughput screening approaches, to identify or synthesize potent and effective inhibitors for these critical proteases. These efforts have developed few effective inhibitors leads and there are no effective pharmaceuticals currently available for either the treatment of the late stage Anthrax infection or BoNT intoxication.¹²⁰

Rational design efforts have resulted in the development of peptide based inhibitors of LF that include In-2-LF with a K_i of 1 nM,⁸⁵ which is a peptide hydroxamate designed on the basis of the N-terminal sequence of its MAPKK substrates. Many researchers have designed small molecule inhibitors of LF that are weak hydroxmates (IC_{50} s > 100 μ M) and chelating agents such as EDTA and *ortho*-phenanthroline.¹²¹ Additionally, a series of competitive inhibitors against BoNT type A protease activity were reported recently, which were synthesized by basing the inhibitor on the peptide structure from the cleavage site within SNAP-25, with the K_i values higher than 300 nM.⁷¹ On the other hand, substrate-analogue inhibitors of BoNT type F exhibited strong inhibition with K_i values of nanomolar range.⁸² Hydroxamate inhibitors of proteases mimic the substrate in its bound form or in the transition state form,¹²² this theory provides a structural basis for the rational design of LF and BoNTs inhibitors with improved activities.

There has also been extensive work towards the development of high-throughput protease assays.^{92,123} These include FRET assays¹²⁴, enzyme-linked immunosorbent assay (ELISA)¹²⁵, and solid-phase assay.¹²⁶ Of particular interest here are the microsphere-based assays that use immobilized protease substrates on surfaces.⁶⁹ An advantage of surface based assays is the ability to use full-length substrates that include all elements required for tight interactions between the protease and its substrate. This is of particular importance for the development of assays for all strains of BoNT LC and LF, as these proteases have extensive interactions at substrate sites distant from the cleavage site that are required for optimal activity. Therefore, it is highly desirable to use full-length substrates for BoNT LC and LF protease assays. Moreover, such assays may offer a method to discover inhibitory compounds that do not target the highly conserved zinc metalloprotease active site, which may lead to compounds with limited cross-reactivity with cellular proteases such as matrix metalloproteases.⁷⁴ Such an approach may lead to metalloprotease inhibitors with much reduced toxicity, which has been problematic for such compounds in the past.⁹²

Due to the emergence of high-throughput flow cytometry, microsphere-based protease assays have become effective methods to screen for protease inhibitory compounds.¹⁰⁸ This approach has been used to screen individual proteases against relatively small libraries of about 1000 compounds or less.^{74,127}

Here, we have extended the strategy used to screen BoNT/A LC against the Prestwick library of 1280 off-patent compounds using 384-well plates analyzed on the HyperCyt[®] high-throughput flow cytometer.⁷⁴ This approach uses a fusion protein that has a full-length protease substrate between a biotinylation domain and a GFP domain. The

biotinylation domain enable specific attachment of the protein to the surface of a streptavidin coated microsphere. Proteolytic cleavage results in loss of GFP derived fluorescence on the microspheres, which is monitored via flow cytometry.

In this study, we created a multiplex microsphere assays that can assay three proteases simultaneously and demonstrated that we can use this assay to screen both the Prestwick library and a large chemical library of 350,000 compounds. This work was implemented using a cluster high-throughput flow cytometry system that can screen a 1536-well plate in 12 minutes.¹²⁸ These screens identified several lead compounds. We performed secondary screening using FRET peptide assays and a newly developed FRET protein assay. Both microsphere-based and FRET assays were implemented for dose response measurement of compounds against LF, BoNT/A & F LCs, respectively. We also use comparison of inhibitor activity on full-length substrate vs. peptide substrates to evaluate for compounds that may specifically disrupt protease activity at sites distant from the active site of the protease. This study has developed a method to screen three proteases simultaneously against large chemical libraries, demonstrated that full-length substrates can be used to discover distal site inhibitors, has discovered several new inhibitors for BoNT/A & F LC and LF proteases.

3.2 Materials and Methods

3.2.1 Materials

DNA oligonucleotide primers were synthesized by IDT (Coralville, IA) and Operon (Huntsville, AL). Terrific broth (TB) was purchased from Fisher scientific (Pittsburg,

PA). SoftLinkTM avidin resin was obtained from Promega Corporation (Madison, WI). Streptavidin-coated microspheres were obtained from Spherotech Corporation (Lake Forest, IL). BoNT/A & F LCs and MAPKKide, SNAPtide FRET peptide were obtained from List Biological Laboratories (Campbell, CA). Dithiothreitol (DDT), Isopropyl- β -D-thiogalactopyranoside (IPTG), Tris base, Tween 20, Bovine serum albumin (BSA), Hepes hemisodium salt, Sodium chloride, Phosphate-buffered saline (PBS), Carbenicillin, Chloramphenicol, Biotin, were purchased from Sigma-Aldrich corporation (St. Louis, MO). The 384 and 1536-well plates were obtained from ISC BioExpress (Kaysville, UT).

3.2.2 Preparation of Biotinylated Substrate Plasmids

With enhanced green fluorescent protein (EGFP) cloned at the C terminus of the open reading frame as described previously,⁶⁹ protease substrate plasmids were designed based on the Promega (Madison, WI) Pinpoint biotinylation tag vectors.⁶⁹ The plasmids LF-15 GFP and SNAP-25 GFP were created as described previously.⁷⁴ The VAMP-2 green fluorescent protein (GFP) plasmid was created by first restricting the Factor Xa substrate plasmid, also known as PinPiont GFP originally available from Promega (Madison, WI) with (*SacI* and *BamHI*)⁶⁹ and ligation of a VAMP-2 polymerase chain reaction (PCR) product. To create the VAMP-2 substrate, we obtained the VAMP-2 sequence (msataatvpp aapageggpp apppnltsnr rlqqtqaqvd evvdimrvnv dkvlerdqkl selddradal qagasqfets aaklkrkyww knlkmmiilg vicaiiliii ivyfss) synthesized by Integrated DNA Technologies (Coralville, IA). To move the synthetic construct into an expression plasmid we use PCR to amplify the VAMP-2 from amino acid 1-96. The VAMP-2 PCR

primers were 5'-ATCTATGAGCTCATGTCTGCTACCGCT-3' and 5'-ATCCTAGGATCCTAGAAGTGCTGAAGTAAA-3'. The VAMP-2 DNA sequence was denatured at 96 °C for 5 min, then the PCR procedure using AccuPrime™ Pfx DNA polymerase that was performed with 39 amplification cycles as follows: 1) 96 °C for 30 s, 2) 60 °C for 30 s, 3) 72 °C for 45 s, then the product was extended at 72 °C for 10 min. Finally, the reaction was maintained at 4 °C and the product was stored at -20 °C until use. Then the PCR product was digested with *SacI* and *BamHI*, and cloned into the PinPoint GFP plasmid between the same two sites.⁶⁹ This effectively removed the Factor Xa specific cleavage sequence and replaced it with VAMP-2 (1-96) sequence. This VAMP-2 sequence was between the amino terminal biotinylation tag and the carboxy terminal EGFP domain. This VAMP-2 (1-96) plasmid ligations were transformed into calcium competent SCS1 *Escherichia Coli*.¹²⁹ Minipreps were done with a Qiagen (Valencia, CA) QIAprep miniprep kit (25) and were sequenced to confirm that the VAMP-2 sequence was correct. For expression, the plasmids of interest were transformed into calcium competent BL21 (DE3) pLysS competent *E. coli* cells from Novagen (Madison, WI).

3.2.3 Expression and Purification of Biotinylated Protease Substrates

The expression and purification of all four biotinylated protease substrates were performed essentially as described in our previous work.⁶⁹ Briefly, a single colony containing the respective plasmid for one of the four protease substrates was picked from a LB plate and grown overnight in 3 mL of TB media containing 50 µg/mL carbenicillin and 34 µg/mL chloramphenicol. Then the transformed cells were transferred to 250 mL

of TB media with 50 µg/mL carbenicillin, 34 µg/mL chloramphenicol, 40 µM biotin and grown at 37°C until OD₆₀₀ reached 0.6-0.8. Then, cultures were induced by 100 µM IPTG and grow overnight at 30°C. The cultured cells were harvested by centrifugation at 3500 rpm on a Beckman Avanti J-301 centrifuge for 30 min at 4°C and washed by water twice to remove the biotin. The bacteria were resuspended in 40 mL of lysis buffer (PBS+1mM DTT) followed by sonication. The suspended cells were sonicated in an ice bath for 15 min and centrifuged at 14,800 rpm on a Beckman Coulter Allegra™ 64R centrifuge using rotor FO685 for another 30 min at 4°C. The clear supernatant was loaded onto a 5 mL SoftLink™ soft release avidin resin from Promega (Madison, WI) at a flow rate of 1 mL/min at 4°C. The PBS buffer with 5 mM biotin was used for eluting the protein from the column. Following, the eluted sample was dialyzed with protease buffer (50 mM HEPES, 100 mM NaCl, pH 7.4) for three times at 4°C to remove the free biotin. The purified protein was confirmed with sodium dodecyl sulfate polyacrylamide gel electrophoresis (SDS-PAGE) with 80% purity after a single step. The concentration was determined by using A₂₈₀ spectroscopic measurement and the calculated extinction coefficients.¹³⁰

3.2.4 Prestwick Library Screening

Each of the four different GFP containing protease substrates were attached to a specific population of Spherotech (Lake Forest, IL) streptavidin-coated pink particle kit (SVFA-2558-6K) microspheres with different fluorescence intensities. The Factor Xa substrate pinpoint GFP was incubated with the P.05 microspheres and used as a negative

control. VAMP-2 GFP was bound to P.01 microspheres. SNAP-25 GFP and LF-15 GFP were bound to P.09 and P.11 microspheres, respectively. To achieve binding, all the microspheres were incubated with 100 nM of a specific protease substrate in a rotator for an hour at room temperature. Then the bound microspheres were washed for three times with protease buffer (50 mM HEPES, 100 mM NaCl, 1mg/mL BSA, 0.025% Tween-20, pH 7.4) and centrifuged for one minute to remove the residual unbound protein. The multiplex protease assay was carried out and measured by flow cytometry. All the bound microspheres were mixed together in protease buffer (50 mM HEPES, 100 mM NaCl, 1mg/mL BSA, 0.025% Tween-20, pH 7.4). Then, four 384-well plates were used to set up the reaction of 1280 compounds from the Prestwick chemical library. Wells 1 and 24 with only substrates from each row were used as positive controls. Wells 2 and 23 with substrates and proteases from each row were used as negative controls. Other wells on the plate were the samples with compounds and protease mixture. The assay plates were incubated at room temperature for 2 hours on a plate rotator to keep beads in suspension. All the plates were set up and sampled twice on the HyperCyt[®] high-throughput screening system so as to get reliable assay results. Data were analyzed using HyperView software.¹³¹ When analyzing the data, the Z' factor was calculated for each microsphere set by using the average mean and standard deviation values for wells containing no protease as a positive control and wells without test compound as a negative control as described in our previous work.⁷⁴ Percent inhibition for each compound was calculated by the following formula, $100\% \times [(\text{averaged median well fluorescence} - \text{negative control average median fluorescence}) / (\text{positive control average median fluorescence} - \text{negative control average median fluorescence})]$.

3.2.5 Screen of 350,000 Compounds

In order to identify more efficient inhibitors against the proteases (LF, BoNT/A & F LCs), the 1536-well plates were used to set up the reactions for screening of 350,000 compounds from NIH chemical library. Wells 45 and 46 from each row were used as positive controls with substrates only and negative controls containing substrate and proteases, respectively. Wells 1, 2, 3 and 4 from each row were added with protease buffer alone to wash the probes. Other wells on the plate were the samples containing mixtures of compounds and protease. The assay plates were incubated at room temperature overnight on a plate rotator to keep beads in suspension. In this way, the time points would supply the maximum protease cleavage of substrates and the ability to screen plates sequentially. All the plates were set up and sampled on the HyperCyt[®] high-throughput screening system so as to get the reliable assay results. Data were analyzed as described previously for Prestwick library.

3.2.6 Dose Response Measurement on Microspheres

The compounds with high inhibition efficiency (>30%) in HTS were advanced to the confirmation testing with the same compound concentration used in HTS. The concentration range of the compounds was from 10 nM to 50 μ M. Percent inhibition was calculated by the formula: $100\% \times [(test\ sample\ fluorescence\ value - negative\ control\ fluorescence\ value) / (positive\ control\ fluorescence\ value - negative\ control\ fluorescence\ value)]$. To test the inhibition of riboflavin against BoNT/A LC, a duplex protease assay

was set up and measured by an Accuri C6 flow cytometer. The samples were tested every 30 min within two hours.

3.2.7 FRET Solution Dose Response

The FRET peptides including MAPKKide for LF and SNAPtide for BoNT/A LC from List Biological Laboratories were used as substrates to test the inhibition ability of the potential inhibitors by a fluorimeter (QuantaMaster™ 50 spectrofluorometer, Photon Technology International) with an excitation wavelength of 490 nm and emission wavelength of 523 nm. The concentrations of the compounds were varied from 10 nM to 50 µM. The positive control sample was prepared with FRET substrate with mixing with the proteases, whereas the negative control sample was the substrates only. The test sample was the mixture of substrates, proteases and selected compounds. Percent inhibition was calculated by the formula: $100\% \times [(\text{slope of test sample} - \text{slope of negative control sample}) / (\text{slope of positive control sample} - \text{slope of negative control sample})]$.

The FRET full-length substrate for BoNT/A LC was used to test the inhibition ability of the potential inhibitors by a fluorimeter (QuantaMaster™ 50 spectrofluorometer, Photon Technology International) with an excitation wavelength of 450 nm and emission wavelength of 507 nm. The concentrations of the compounds were varied from 10 nM to 50 µM. The positive control sample was prepared with FRET substrate and proteases, whereas the negative control sample was the substrates only. The test sample was the mixture of the substrates, proteases and test compounds. Percent inhibition was

calculated by the formula: $100\% \times [(\text{slope of test sample} - \text{slope of negative control sample}) / (\text{slope of positive control sample} - \text{slope of negative control sample})]$.

3.3 Results and discussion

3.3.1 Development of Multiplexed Protease Assay

A multiplex microsphere-based assay can allow parallel evaluation of multiplex proteases and identification of specific inhibitors against the corresponding proteases. Here, we designed a few protease substrates that are fusion proteins containing a biotinylation tag and GFP domain separated by the full-length protease substrates. We used the streptavidin-coated fluorescent suspension microsphere arrays (SAM) where a unique protease substrate was borne by each microsphere population. We developed a multiplex substrate set containing four substrates (a SNAP-25 fusion protein, a VAMP-2 fusion protein, a fusion protein bearing a LF cleavage site, and a negative control substrate) that have been engineered for use with three proteases, *Clostridium botulinum* neurotoxin type A & F light chains and *Bacillus anthracis* lethal factor (BoNT/A & F LCs and LF), simultaneously in HTS assays for discovery of small molecule inhibitors (Figure 3.1A). Each protease substrate was attached to a set of fluorescent streptavidin-coated microspheres via its biotinylation tag. The protease assay was incubated overnight in order to obtain maximal protease cleavage. The protease activity is measured by detecting the fluorescence loss from microspheres as shown in Figure 3.1B.

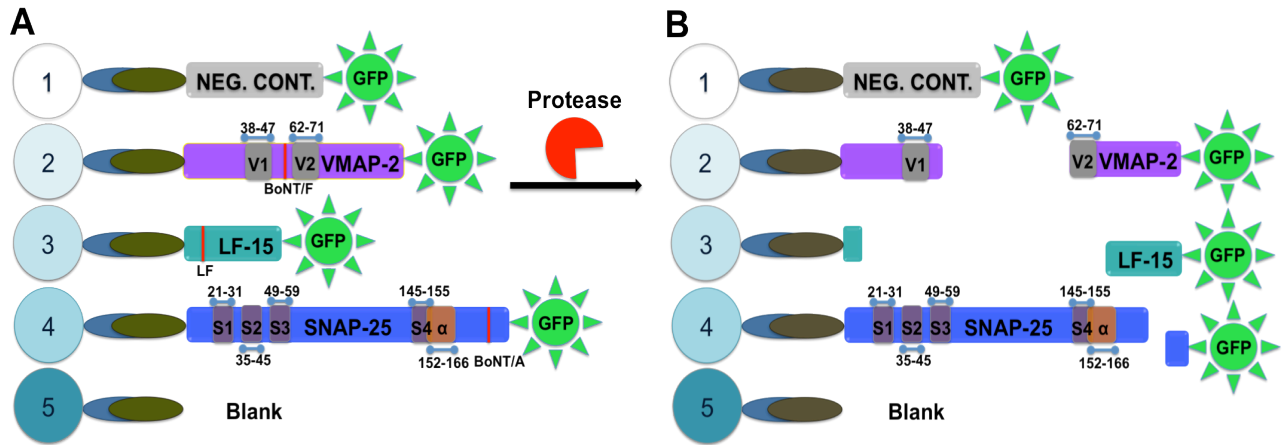


Figure 3.1 A. 4-plex multiple protease assay. VAMP-2 (BoNT/ F substrate), SNAP-25 (BoNT/A substrate), LF-15 (LF substrate) attached to microspheres and control Pinpoint GFP (Factor Xa substrate). The colored circle stands for different microspheres, the blue crescent for streptavidin, the brown oval for biotinylation tag, the colored cylinders for different protease substrates. Cleavage sites are red, distal sites are brown & orange. B. Protease cleavage activities were measured by loss of fluorescence from microspheres via flow cytometry after adding three proteases simultaneously.

The microsphere population was analyzed via flow cytometry and gated based side scatter vs. forward scatter (Figure 3.2A). The different microsphere populations were distinguished by gating on differences in fluorescence intensities as shown in a bivariate dot plot of side scatter vs. red fluorescence (Figure 3.2B). The multiplex protease assay was executed by adding three proteases (1 nM BoNT/A LC, 75 nM BoNT/F LC and 300 nM LF) as a single mixture simultaneously. The results indicated that all the proteases could recognize and cleave their specific substrates (Figure 3.2C). In comparison with anthrax lethal factor, BoNT/A & F LCs exhibited higher proteolytic cleavage activity. This may be due to the presence of exosites on the VAMP-2 and SNAP-25 substrates, which are lacking from the LF-15 substrate as it is simply a 15 amino acid sequence derived from a consensus cleavage site.^{35,132} Regardless, this method demonstrated feasibility of measuring the activity of several different proteases in the same sample.

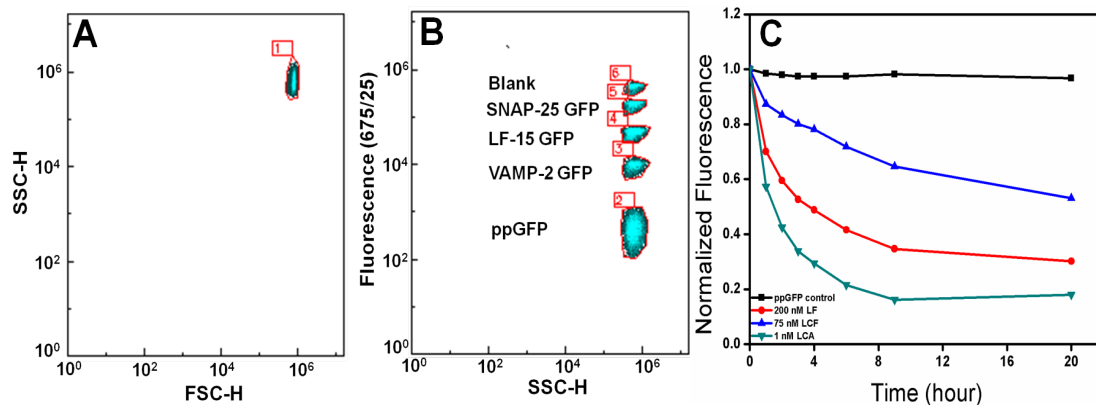


Figure 3.2 A. Bead populations were gated in the dot plot. B. Each bead population was separated by FL4 (Red) channel, One type of beads are used as blank. Each other type bears different GFP substrate. C. The time-course cleavage results of three multiple protease assay. Substrate types are as follows: control ppGFP, VAMP-2 GFP, LF-15 GFP and SNAP-25 GFP.

3.3.2 Primary Screening of Chemical Libraries

In the Prestwick library, about 1280 off-patent drugs and bioavailable compounds were screened in four 384-well plates twice. The activities of proteases led to the loss of fluorescence of substrate proteins resulting about 80% reduction of fluorescent signal. All Z' values were calculated for each substrate based on the time endpoint fluorescence intensity of positive and negative control wells, respectively. When the Z' value was lower than 0.4 or the event number was lower than 50, the data would not be analyzed or used. The average Z' value for each substrate was as following: 0.81 for SNAP-25 GFP, 0.86 for VAMP-2 GFP and 0.7 for LF-15 GFP, respectively (Figure 3.3). In the primary screen, two compounds were discovered to inhibit cleavage by more than 30% inhibition. Riboflavin showed about 80% inhibition against LF and 40% inhibition against BoNT/A LC respectively. Tolazamide showed about 35% inhibition against LF.

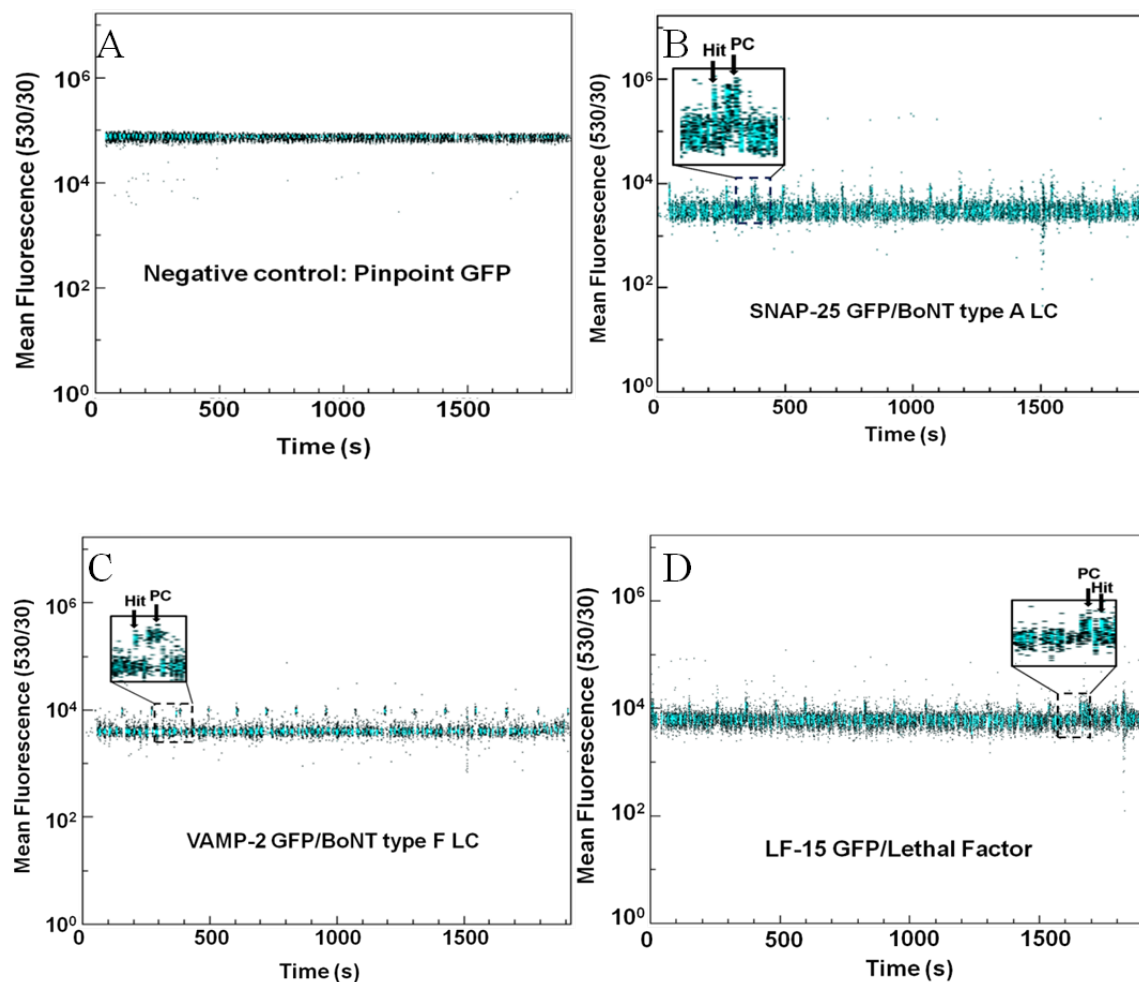


Figure 3.3 High-throughput screening for small molecule inhibitors against proteases. (A) Plot of high-throughput screening data of positive control substrate Pinpoint GFP. All the data were collected in the FL1-A green fluorescence channel. (B) Plot of high-throughput screening data of BoNT/A LC. Arrow denotes the positive control well (PC) and the inhibitor well Hit). (C) High-throughput screening data of BoNT/F LC. Arrow denotes the positive control well (PC) and the inhibitor well (Hit). (D) High-throughput screening data of LF. Arrow denotes the positive control well (PC) and the inhibitor well (Hit). All the reactions were performed in protease buffer (pH=7.4) and at room temperature. Each panel represents fluorescence intensity data from all wells of a 384-well plate that were gated on the bead set bearing the indicated protease substrate.

In addition, about 350,000 chemical compounds were screened in around two hundred 1536-well plates. All Z' values were calculated for each substrate based on the time endpoint fluorescence intensity of positive and negative control wells, respectively. The average Z' values for each substrate were above 0.7 showing excellent HTS quality. Hundreds of compounds with inhibition >50% were advanced into confirmatory screening. There were 610 compounds for BoNT/A LC, 780 compounds for BoNT/F LC and 423 compounds for LF, respectively. In the confirmatory screening, all these compounds were tested in triplicate for their effect against three proteases. Confirmed results were reviewed, 19 compounds that inhibited the activity of BoNT/A LC, 11 compounds that inhibited the activity of BoNT/F LC, and 10 compounds that inhibited activity of LF. These compounds were selected into follow-up dose response assays to determine the IC_{50} values.

From the dose response reactions above, 13 compounds were selected with great IC_{50} values (< 20 μ M) as showing in Table 3.1. In these compounds, some of them displayed specific inhibition against BoNT/A LC including CID 4464849, CID 4293343 and CID 256073. CID 3626685 and CID 3095057 inhibited the activity of BoNT/F LC. Four compounds showing inhibition against LF are CID 3335282, CID 4472168, CID 51360688 and CID 51361178. Meanwhile, CID 392789 inhibited the activities of BoNT/A & F LCs. Only CID 12006136 inhibited the activities of BoNT/A & F LCs and LF. This HTS assay exhibited robust, rapid and reproductive advantages, which also demonstrated significant selectivity of the compounds.

Table 3.1 IC₅₀ values of each inhibitor for microsphere-based assay.

CID	Inhibition (approximate IC ₅₀ , μ M)		
	BoNT/A LC	BoNT/F LC	LF
4464849	4.2	>20	>20
4293343	1.0	>20	>20
256073	8.6	>20	>20
3626685	>20	2.9	>20
3095057	>20	2.7	>20
3335282	>20	>20	19.5
4472168	>20	>20	11.5
51360688	>20	>20	10.6
51361178	>20	>20	17.9
392789	5.1	9.4	>20
45281164	1.6	>20	0.6
4129168	4.9	>20	1.4
1200613	17.8	8.0	16.7

3.3.3 Riboflavin Can Inhibit Lethal Factor Activity

Because of the excellent inhibition activity of riboflavin (Figure 3.4A) found in HTS of the Prestwick library, a detailed dose response assessment was carried out afterwards. The results showed that riboflavin inhibited the activity of lethal factor at the concentration of 20 μM (Figure 3.4B), and the IC_{50} value of riboflavin against LF was about 15 μM . However, tolazamide could not inhibit lethal factor at even higher concentrations (data not shown). In order to confirm the inhibitory activity of riboflavin, MAPKKide peptide was used in the FRET solution assay. The peptide substrate was synthesized with a fluorophore FITC (energy donor) linked at the C-terminal end and another fluorophore DABCYL (energy acceptor) attached to the N-terminal end. When the peptide bond of the substrate was cleaved, the FRET was interrupted and the fluorescence signal from FITC was increased. It is a sensible strategy to test the inhibition ability of riboflavin against LF by measuring the cleavage rate of LF. The fitting results demonstrated that riboflavin inhibited the activity of LF at the IC_{50} value of 17.4 μM (Figure 3.4C), which was very close to that obtained with the microsphere-base method (15 μM).

Based on these results, it is reasonable to infer that the inhibition mediated by riboflavin represents a complex mechanism. Because riboflavin is an amphipathic molecule that allows a large variety of different interactions with the enzyme itself and the substrate,¹³³ Riboflavin may interfere with the interaction of LF-substrate complex. It is necessary to note that riboflavin is essential for many important enzymatic reactions *in vivo*. Furthermore, riboflavin has been used in several clinical and therapeutic situations because of its importance in the maintenance of many human tissues. In this assay, we

found that riboflavin inhibited the activity of lethal factor, so it may have utility in the development of lead compounds that may result in therapeutics for late stage Anthrax infections.

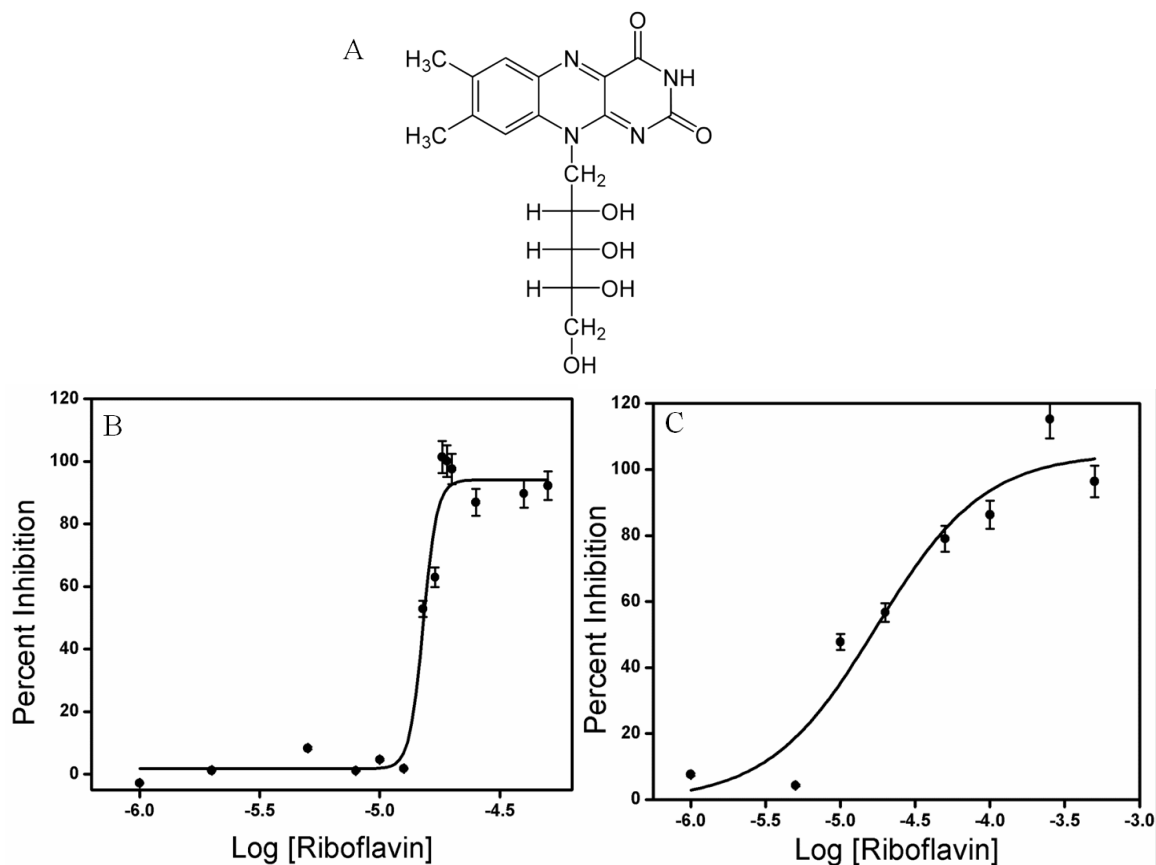


Figure 3.4 Dose-response inhibition curves for the compound riboflavin against 400 nM lethal factor. All the reactions were performed in protease buffer (pH=7.4) and at room temperature. All the data were fitted according to the equation: % inhibition = Bottom + (Top - Bottom)/(1+ 10^{((Log(IC₅₀)-X) × (Hill coefficient))}). (A) Structure of riboflavin. (B) Microsphere-based assay using biotinylated tag lethal factor substrate green fluorescence protein. The fit resulted in an estimate of the IC_{50} to be 15 μ M and the fit gave an R^2 of 0.962. (C) Inhibition of riboflavin against lethal factor was tested by MAPKKide peptide substrate. The data were collected and calculated for 10 min after protease addition. The result showed the IC_{50} to be 17.4 μ M and R^2 of 0.893.

The HTS results showed that riboflavin inhibited BoNT/A LC activity around 40%. The detailed dose response assay was also applied for riboflavin against BoNT/A LC using the microsphere-based method. After one-hour incubation, the percent inhibition mediated by riboflavin was about 40% at a concentration 25 μ M. Even at higher concentrations (100 μ M, 500 μ M), no greater inhibition was detected (Figure 3.5). This result was consistent with HyperCyt[®] screening results. Over two-hour incubation, the fluorescence intensity was measured for each sample every 30 minutes. Maximum inhibition of BoNT/A LC cleavage of about 40% was observed at 30 min at riboflavin concentrations of 25 μ M and 100 μ M, with no additional inhibition at long time (Figure 3.5). Here, we also used ebselen as a contrast, which has been identified as an inhibitor against BoNT/A LC with the IC₅₀ value of 5 μ M.⁷⁴ In this assay, 10 μ M ebselen was added for incubation of two hours, the results showed that ebselen inhibited the activity of BoNT/A LC with about 100% consistent the previous report.

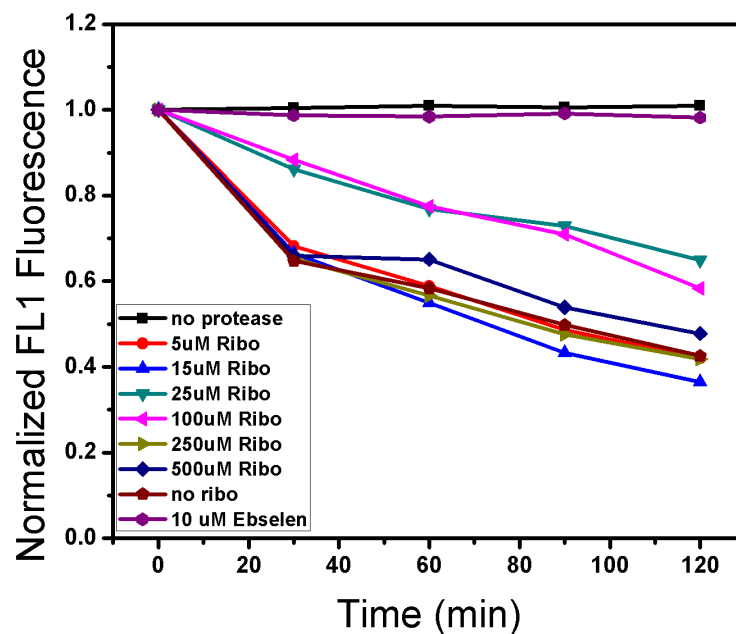


Figure 3.5 Microsphere-based assay of riboflavin against the BoNT/A LC substrate SNAP-25 GFP by measuring loss of green fluorescence. 5 nM of BoNT/A LC was added into the microspheres containing a green fluorescent protein labeled substrate. The fluorescence intensity was measured every 30 min by flow cytometry. All the reactions were performed in protease buffer (pH=7.4) and at room temperature.

3.3.4 Tests of Structure-activity Related Compounds

To find more potent compounds, we tested about 60 structurally related compounds that were synthesized based on the structures of the lead compounds. This synthesis occurred at Vanderbilt University. Using the microsphere-based assay, 11 compounds were identified with inhibition against the three proteases. The dose response curve of each compound was diagramed to determine the IC_{50} value (Figure 3.6). Of these dose response curves, all were well behaved with the exception of compounds 2865835 and 2827281. These curves were clearly affected by spurious values at high concentration of compound, which is believed to have occurred due to the fluorescence for these compounds. When the spurious values were removed for compounds 2865835 and 2827281, the fits provided improved estimates of IC_{50} values (Figure 3.7).

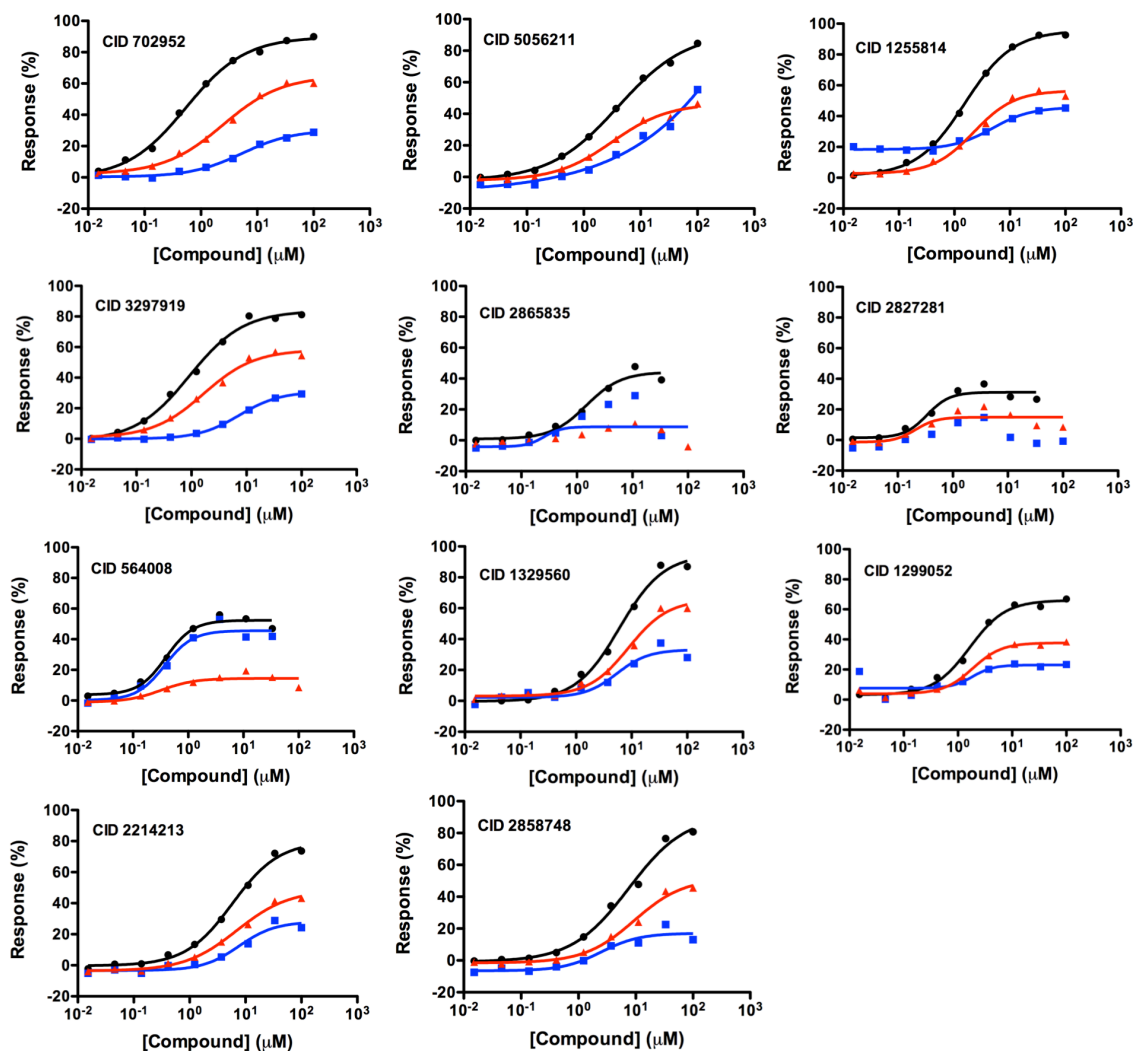


Figure 3.6 Dose response curves of 11 compounds with structure-activity relationships. The concentration range of compounds was from 10 nM to 100 μ M. Black circle is for BoNT/A LC. Blue square is for BoNT/F LC. Red triangle is for LF.

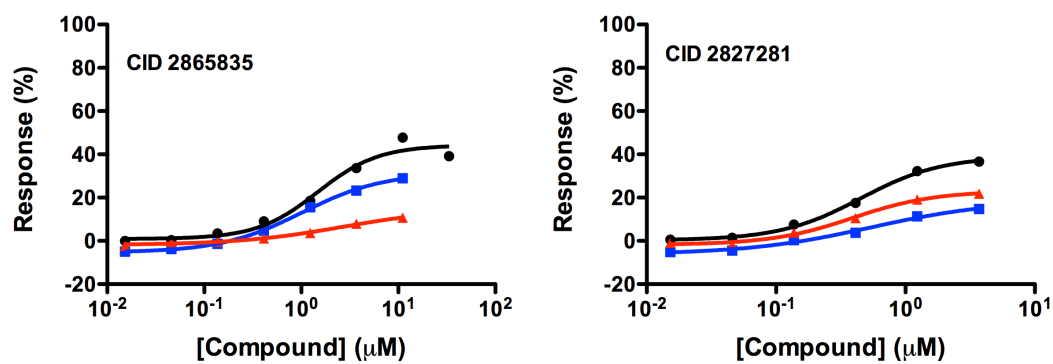
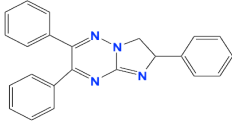
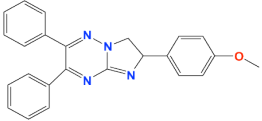
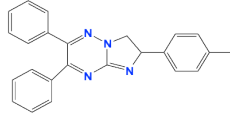
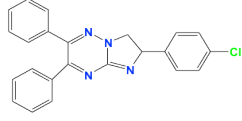
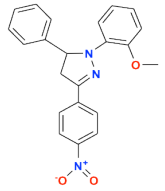
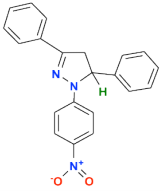
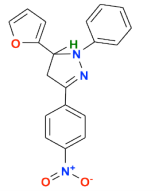
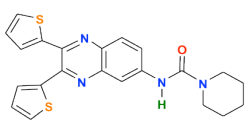
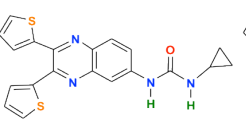
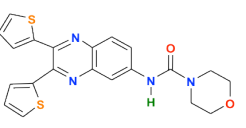
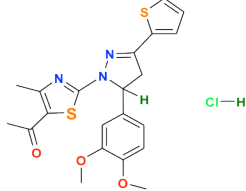


Figure 3.7 Dose response curves of compounds 2865835 and 2827281 with removed spurious values. Black circle is for BoNT/A LC. Blue square is for BoNT/F LC. Red triangle is for LF.

Specifically, all the compounds inhibited the activity of BoNT/A LC with the IC_{50} values $< 20 \mu M$, and some of them displayed selectivity across proteases (Table 3.2). For instance, in scaffold A, all of the compounds inhibited the activities of all three proteases. However, compound 5056211 provided an IC_{50} estimate $>20 \mu M$ in the BoNT/F LC assay. In scaffold B, CID 564008 showed strong inhibition against both BoNT/A & F, but very weak inhibition of LF. This suggests that this compound may selectively inhibit the activities of BoNT LC proteases. The discovery of such lead compounds through comparison of a parallel assays using related enzymes is likely to be an efficient method for discovery of highly specific protease inhibitors that can be extended to many other protease families.

Table 3.2 Summary of IC₅₀ values for 11 compounds against proteases in microsphere-based assay. They are diagramed into four scaffolds based on the structures.

CID (Scaffold A)	702952	5056211	1255814	3297919
Structure				
IC ₅₀ values (μM)				
BoNT/A LC	0.6	4.0	1.5	1.0
BoNT/F LC	5.3	>20	9.1	7.4
LF	1.6	3.3	2.0	1.6
CID (Scaffold B)	2865835	2827281	564008	
Structure				
IC ₅₀ values (μM)				
BoNT/A LC	0.9	0.3	0.4	
BoNT/F LC	>20	>20	0.5	
LF	>20	>20	>20	
CID (Scaffold C)	1329560	1299052	2214213	
Structure				
IC ₅₀ values (μM)				
BoNT/A LC	6.1	1.5	5.8	
BoNT/F LC	4.6	>20	9.6	
LF	6.7	1.6	7.6	
CID (Scaffold D)	2858748			
Structure				
IC ₅₀ values (μM)				
BoNT/ALC	7.5			
BoNT/F LC	>20			
LF	9.6			

3.3.5 Evaluation of Lead Compounds Against BoNT/A LC in Solution Assay

The IC₅₀ values for the 11 compounds were determined using a FRET peptide based solution assay. This was done to distinguish lead compounds that were only active in an assay using a full-length substrate vs those that would inhibit regardless of the presence of distal sites on the substrate. For this we focused on BoNT/A LC and used FRET peptide assays based on the SNAPtide fluorescent peptide developed by List Laboratories.¹³⁴ All 11 powder compounds have been tested here by 10-point titration assays (Figure 3.8). The results of IC₅₀ fits are in Table 3.3. Here, three compounds (CID 564008, CID 2214213 and CID 1299052) did not inhibit the activity of BoNT/A LC for the FRET peptide substrate, but inhibited the activity of BoNT/A LC for the full-length substrate in microsphere-based assays. This strongly suggested that these three compounds were inhibiting BoNT/A LC activity by changing the ability of the full-length substrate to bind to the protease. As tight binding is known to be mediated by the distal sites of SNAP-25, it is reasonable to hypothesize that these compounds are targeting these distal site interactions, but additional confirmatory work is necessary to fully support this conclusion.

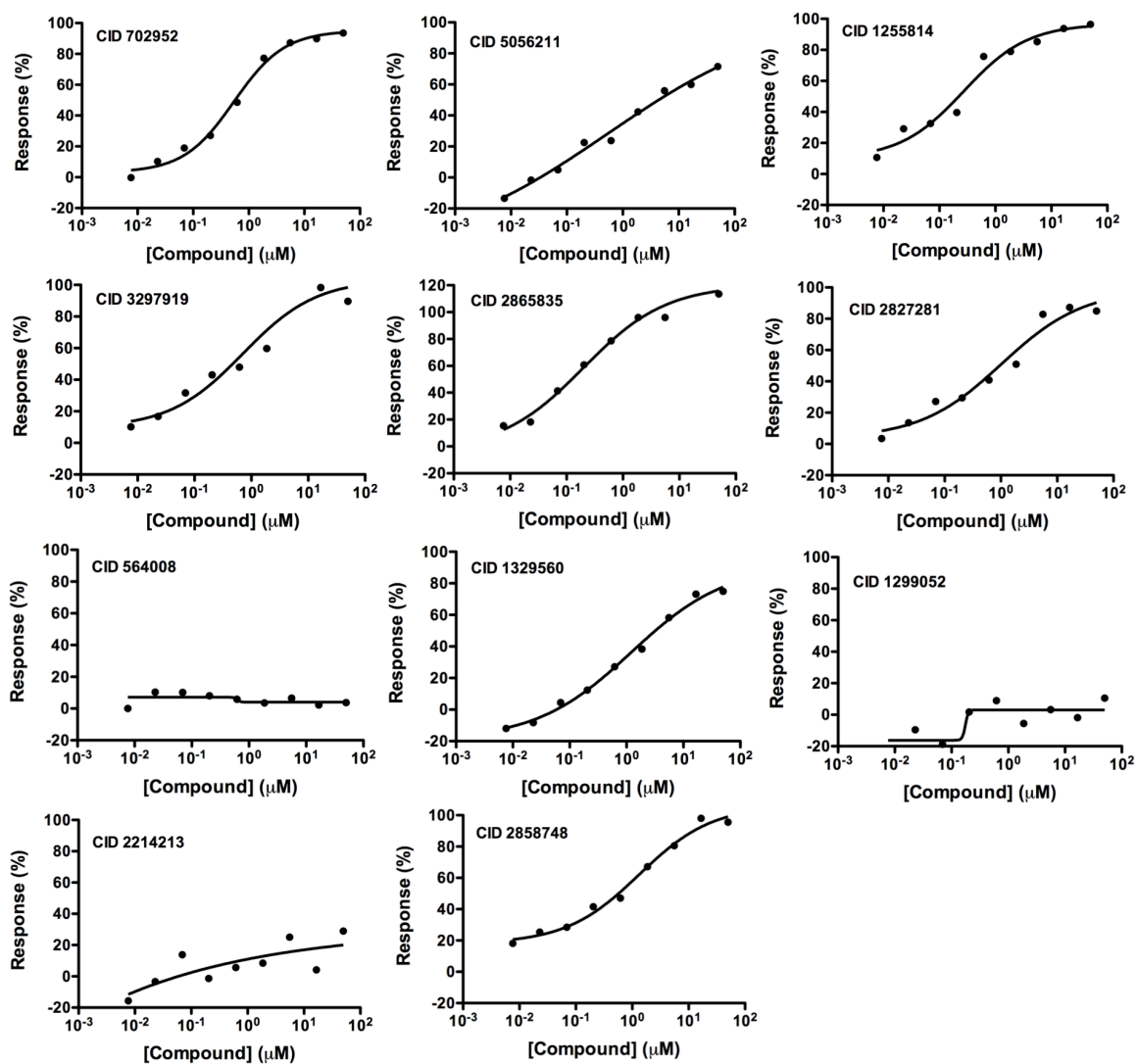


Figure 3.8 The dose responses curves of the compounds that inhibited the activity of BoNT/A LC in FRET peptide solution assay.

Table 3.3 Comparison of IC₅₀ values of 11 compounds for both microsphere-based and FRET peptide assays against BoNT/A LC.

CID	Inhibition (approximate IC ₅₀ , μ M)	
	Microsphere-based assay (Full-length substrate)	FRET peptide assay (Only cleavage sites)
702952	0.6	0.5
5056211	4.0	0.5
1255814	1.5	0.3
3297919	1.0	0.7
2865835	0.9	0.2
2827281	0.3	1.0
564008	0.4	NI
1329560	0.1	1.2
1299052	1.5	NI
2214213	5.8	NI
2858748	7.5	1.3
NI: No Inhibition		

One of the first confirmation steps to take is to evaluate whether the microsphere assay that has a tethered substrate is providing different results due to the surface attachment of the protease substrate. Though surface attachment enables simple use of full-length substrates, they also limit the concentration of substrate in the reaction and require enzyme saturating conditions (*i.e.* single turnover) to achieve maximal cleavage rates.^{69,}
¹³⁵ Therefore, a FRET assay that uses a full-length substrate was created as described in Chapter 4. Though this assay has many uses, in this Chapter we will only consider it for estimation of IC₅₀ values of lead inhibitory compounds.

In summary, the full-length FRET substrate (fIFRET) was constructed by incubating the biotinylated SNAP-25 GFP in the presence of a 3:1 molar excess of Cy3 labeled streptavidin (SA-Cy3). The binding of the SA-Cy3 to the SNAP-25 resulted in the quenching of GFP when the fIFRET was excited at 450 nm (to minimize direct excitation of Cy3). Upon the addition of protease, the SNAP-25 is cleaved, which separates the GFP from the SA-Cy3 and results in dequenching of GFP fluorescence, which is the indicator of protease activity.¹²⁴

In order to confirm the inhibitors, which were identified in both microsphere-based and FRET peptide assays, we carried out the FRET full-length solution assay to determine the IC₅₀ values of the eleven compounds that have structural-activity relationships. Here, all the compounds inhibited the activity of BoNT/A LC with the IC₅₀ values lower than 20 μ M using FRET full-length substrate. Additionally, three compounds including CID 564008, CID 2214213 and CID 1299052 were confirmed to inhibit BoNT/A LC activity (Figure 3.9). The IC₅₀ values of three inhibitors were 3.1 μ M, 0.4 μ M, and 0.6 μ M, respectively (Table 3.4). These results confirmed that these specific compounds might

block the binding of substrate and enzyme at distal elements that inhibited the cleavage activity of protease.

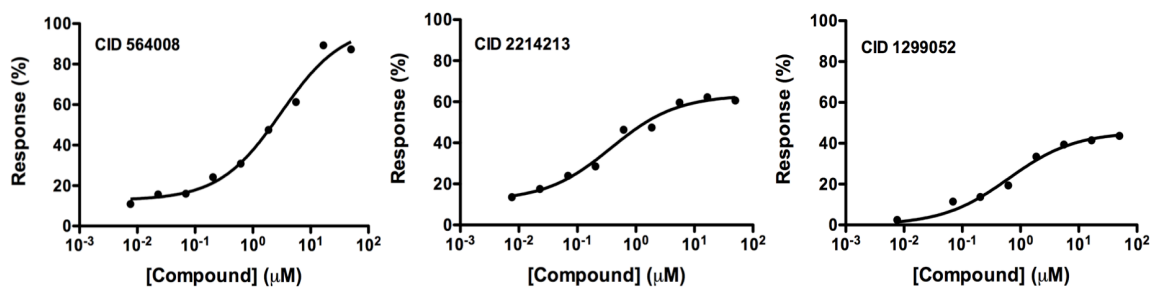
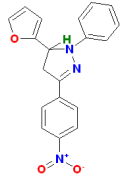
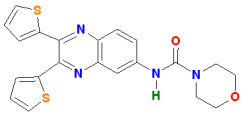
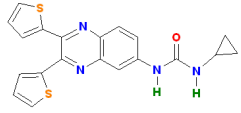


Figure 3.9 Dose response curves of three specific compounds that inhibited the activity of BoNT/A LC in FRET full-length assay.

Table 3.4. The IC₅₀ values of the three specific inhibitors by using different substrates and methods.

CID	Structure	IC ₅₀ (μM)		
		Microsphere (Full-length substrate)	FRET (Peptide substrate)	FRET (Full-length substrate)
564008		0.4	>20	3.1
2214213		5.8	>20	0.4
1299052		1.5	>20	0.6

3.4 Conclusion

In this study, we have designed a highly selective microsphere-based protease assay and small molecule inhibitor selection system, which could be critical for the efficacy of potential multiplex proteases and compounds assays. The improvement in high-throughput screening performance represents that this approach can be used to select more protease inhibitors efficiently. Our multiplexed microsphere protease assay combined with high throughput flow cytometry will be applicable to a broad range of proteases due to its ability to rapidly discover inhibitors from large chemical libraries. Here, we have identified several specific inhibitors for the proteases. This screen discovered a new inhibitory agent (riboflavin) that was specific for Lethal Factor. The major finding described here is the inhibitor (riboflavin) against LF, which is a conventional compound and people can get it from daily diet. In addition, we have identified several specific inhibitors with the IC_{50} values lower than 20 μ M for BoNT/A & F LCs and LF proteases. Some of these compounds displayed specific inhibition against only one kind of the proteases that they may not be the inhibitor against all the zinc-dependent metalloproteases. Additionally, a compound (CID 564008) specifically inhibited the activities of BoNT/A & F LCs. These compounds may represent the BoNTs inhibitors. These compounds (CID 564008, CID 2214213, and CID 1299052) were shown to be active at sites distal from the active site. Compared the results with those obtained from microsphere-based assay and FRET solution assay, the identification specific inhibitors indicated the great importance of distal events in the interaction between proteases and substrates. Blocking the binding of proteases and substrates at exosites would play an important role in the inhibition of protease activity. The

improvement in high-throughput screening performance represents that this approach can be used to select more protease inhibitors efficiently. Our multiplexed microsphere protease assay combined with high throughput flow cytometry will be applicable to a broad range of proteases due to its ability to rapidly discover inhibitors from large chemical libraries. The multiplexed microsphere-based protease assay for high-throughput screening has demonstrated a great ability to screen several proteases simultaneously that dramatically reduces screening labor and cost, immediately provides information on specificity of an inhibitor.

Chapter 4

Kinetic Analysis of Botulinum Neurotoxin Type A Light Chain Using FRET Full-length Substrate

4.1 Introduction

Assays of protease activity have been designed by combining substrates with appropriate reporters, such as fluorescence and bioluminescence.^{136,137} Therefore, Forster (or fluorescence) resonance energy transfer (FRET) has been widely used to assay the protease where two fluorophores (energy donor and acceptor) are typically attached to the ends of the substrate with a distance of less than 10 nm. FRET is a process in which energy is transferred nonradiatively from an excited state donor to a proximal ground state acceptor via resonant dipole-dipole interactions. When a protease substrate (peptide or full-length) brings donor and the acceptor into close proximity, the activity of protease gives rise to the change in FRET efficiency. The cleavage of the FRET substrate with a protease disrupts the energy transfer and the ratio of donor and acceptor fluorescence emission changes when both chromophores are fluorescent, or the fluorescent intensity increases when the acceptor is a quencher.

In this work, we developed a FRET assay that uses a full-length SNAP-25 substrate with a donor fluorophore (GFP) on one end of the full-length substrate and a paired acceptor (Cy3-streptavidin) on the other end, attached to the substrate biotinylation tag. This has the advantage that distal elements can be included in the substrate, the substrate can be used in saturating conditions required for Michaelis-Menten kinetics, and is based on the same substrate used in the microsphere assay.

4.2 Materials and Methods

4.2.1 Materials

Tween-20, dithiothreitol (DDT), isopropyl- β -D-thiogalactopyranoside (IPTG), Bovine Serum Albumin (BSA), Hepes Hemisodium Salt, Sodium Chloride, Phosphate-buffered Saline (PBS) and Biotin were bought from Sigma-Aldrich Corporation (St. Louis, MO). BoNT/A LC was bought from List Biological Laboratories (Campbell, CA). SoftLinkTM streptavidin resin was obtained from Promega Corporation (Madison, WI). Streptavidin-Cy3 conjugate was bought from Invitrogen.

4.2.2 GFP Quenching by Cy3-Streptavidin

The concentration of CyTM3-Streptavidin Conjugate (ZyMAXTM Grade) from Invitrogen was measured by A₅₅₂ and A₂₈₀ spectroscopic measurement (manufacturer protocol) using Nanodrop 2000C spectrophotometer. The general excitation wavelength of GFP is 488 nm, which could partially excite Cy3. Therefore we chose to use an excitation wavelength of 450 nm to avoid the excitation of Cy3 because this wavelength could only excite Cy3 with about 1%. To determine the biotinylated SNAP-25 GFP quenching by Cy3, 25 nM SNAP-25 GFP was incubated with increasing amounts of Cy3-streptavidin for 1 hour at room temperature in the protease buffer avoiding light, then the ratio of SNAP-25 GFP quenching by Cy3-streptavidin was optimized by exciting the sample at 450 nm in a PTI fluorimeter with slit lengths of 2 nm used with an emission scan between 488 nm to 650 nm.

4.2.3 FRET Solution Kinetic Assay

The real-time FRET based protease assays were employed to determine the kinetic constants of BoNT/A LC cleavage activity. The substrate concentrations were varied from 5 to 3000 nM with fixed 5 nM BoNT/A LC for the cleavage reaction. The biotinylated SNAP-25 GFP was incubated with CyTM3-Streptavidin conjugate at the molar ratio of 1:3. Then the sample was run for 1 minute in a PTI fluorimeter collecting 10 data point per second with slit sizes of 2 nm (the excitation wavelength was 450 nm and emission wavelength was 507 nm). Then, 5 nM BoNT/A LC was added at the 60 second time point and the reaction was monitored for additional 10 min. Samples were run in glass cuvettes with a stir bar providing continuous mixing. The concentration of cleaved SNAP-25 GFP was calculated as follows:

$$[C]_{cleaved} = \frac{F - F_{FRET}}{F_{GFP} - F_{FRET}} \times [C]_{GFP}$$

Where, $[C]_{cleaved}$ is the concentration of cleaved SNAP-25 GFP; F is the fluorescence intensity of each data point after adding 5 nM BoNT/A LC; F_{GFP} is the average fluorescence values of the free SNAP-25 GFP with the same concentration in the reaction; F_{FRET} is the average fluorescence values of FRET substrate without cleavage in the reaction; $[C]_{GFP}$ is initial concentration of SNAP-25 GFP for each reaction. The data in first 30 seconds after the cleavage were linearly fitted to determine initial rates of SNAP-25 cleavage as the initial velocity of the reaction. All these values were then plotted against different SNAP-25 GFP concentrations, and fitted to the Michaelis-Menten equation with the nonlinear fitting curve.

4.3 Results and Discussion

4.3.1 GFP Quenching by Cy3-Streptavidin

The full-length FRET substrate was constructed as shown in Figure 4.1A. The biotinylated SNAP-25 GFP was linked to Cy3 labeled streptavidin via the SNAP-25 biotinylation tag. Due to the spectral overlap of GFP and Cy3, when GFP was excited at 450 nm (to minimize direct excitation of Cy3), this system demonstrated a concentration dependent quenching of GFP fluorescence as increasing amounts of Cy3-streptavidin were added to the system due to FRET, which occurred between the two fluorophores as they were brought close together by the protease-sensitive linker (Figure 4.1B). This was considered as an indicator of protease activity because SNAP-25 proteolysis disrupted the energy transfer process by separating the donor and acceptor units. The emission spectra measurement indicated that the optimal molar ratio of SNAP-25 GFP and Cy3-streptavidin was obtained for the best FRET substrate.

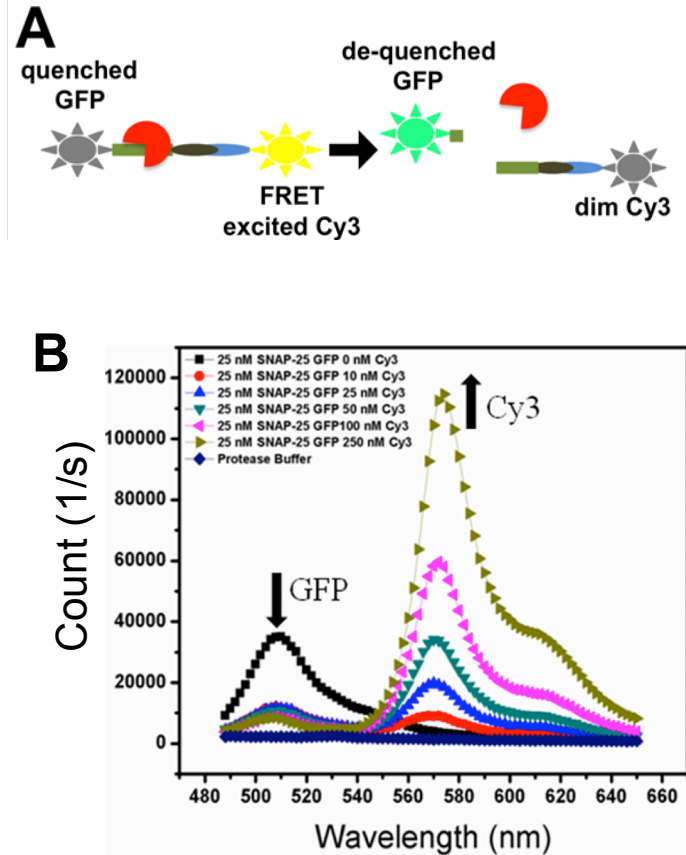


Figure 4.1 A. Schematic of full length FRET solution assay. B. Cy3 streptavidin titration onto 25 nM biotinylated SNAP-25 GFP. Excitation was done at 450 nm to avoid direct excitation of Cy3 and emission spectra from 488 nm to 650 nm were collected at one data point per nm.

4.3.2 BoNT/A LC Cleavage of A Full-length SNAP-25 Substrate in Solution

At present, the FRET assay has been widely used due to its inherent sensitivity to the molecular-scale rearrangement in donor-acceptor separation distance.¹³⁸ To study the cleavage of BoNT/A in a solution assay, a full-length FRET system was constructed by biotinylated SNAP-25 GFP conjugated with Cy3 labeled streptavidin. Subsequently, this FRET substrate was used to measure the enzymatic activity of BoNT/A LC. Proteolysis of SNAP-25 provided an increase in GFP fluorescence at 507 nm as the cleavage activity separated the two fluorophores. The first 60 seconds of fluorescence was recorded as background, the protease cleavage was initiated by the addition of BoNT/A LC. The cleavage rate increased in a concentration-dependent manner with the increasing of FRET-substrate concentration (Figure 4.2A). To determine the initial velocities at each substrate concentration, the increase in fluorescence as a function of time over the first 30 seconds was fitted to a line. The slopes of the lines provided the initial velocities, which were plotted as a function of increasing substrate concentration and fitted to a hyperbolic function to obtain the V_{\max} and K_m values of 4.37 ± 0.29 nM/s and 0.87 ± 0.14 μ M, respectively (Figure 4.2B). k_{cat} was calculated as 0.87 s^{-1} by dividing V_{\max} by the enzyme concentration (5 nM) used in the assay because of $V_{\max} = k_{\text{cat}}[E]_0$.¹³⁹ These values provide a specificity constant (k_{cat}/K_m) of $1 \times 10^6 \text{ M}^{-1}\text{s}^{-1}$.

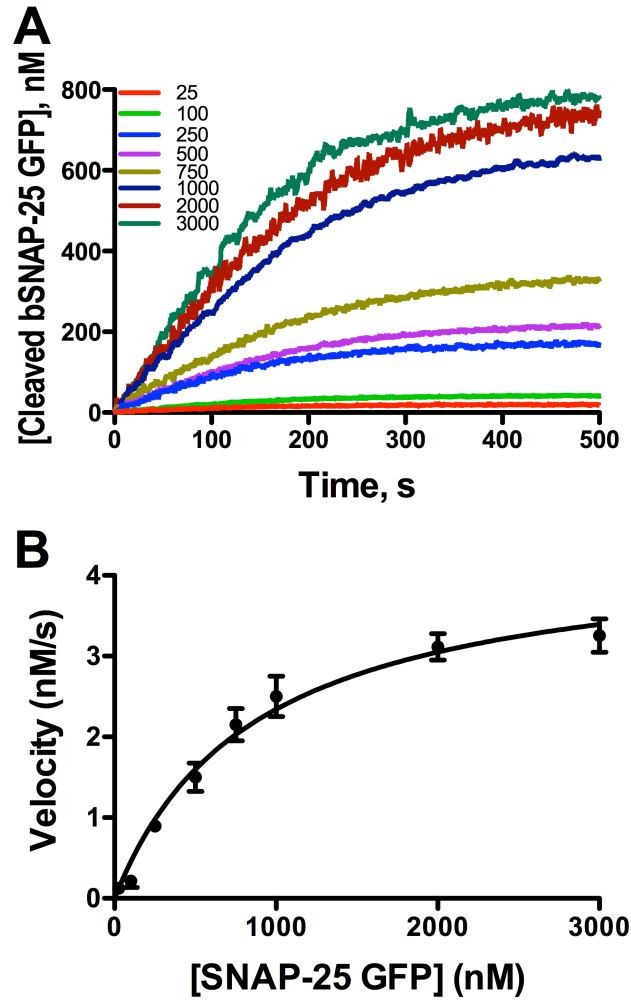


Figure 4.2 Cleavage analysis of BoNT/A LC based on FRET solution assay. A. Progress curves for the cleavage reactions using 5 nM BoNT/A LC and different starting concentrations of substrate, which are shown in the legend where the numbers indicate substrate concentration in nM. B. The concentration-dependent initial rates versus substrate (S) concentrations are fitted to a hyperbolic curve, $V_{\max}[S]/(K_m+[S])$, to obtain the kinetic constants V_{\max} and K_m .

Generally, the studies with BoNT/A LC and full-length substrates or at least 61-mer fragment of SNAP-25 exhibited the constant k_{cat}/K_m values between 10^4 and $10^6 \text{ M}^{-1}\text{s}^{-1}$, which were larger than the range of 10^2 to $10^3 \text{ M}^{-1}\text{s}^{-1}$ for BoNT/A LC and a 17-mer SNAP-25 fragment.¹⁴⁰ In addition, the values of K_m and k_{cat} associated with full-length SNAP-25 were less than those associated with the 17-mer of SNAP-25 fragment.¹⁴⁰ When compared to literature values of k_{cat} determined on full-length substrate (2.4 and 17 s^{-1}),^{141,142} the values in my work were smaller, but this was likely due to differences in buffers, enzyme preparations, and these assays were performed at room temperature rather than 37°C . It was also possible that the cleavage rate was reduced due to effects of the biotinylation and GFP domains found in our SNAP-25 GFP substrate. A fluorogenic assay using a 17-mer fragment of SNAP-25 resulted in values of K_m , k_{cat} and k_{cat}/K_m of $1.1 \pm 0.1 \text{ mM}$, $23 \pm 1 \text{ s}^{-1}$ and $21 \times 10^3 \text{ M}^{-1}\text{s}^{-1}$, respectively.¹⁴³ These results also suggested a probability that only a fraction of substrate-enzyme collisions were productive to form product and the cleavage reaction appeared to be the limiting step. The kinetic analysis of BoNT/A based on different substrates and methods have been widely studied because this toxin-substrate combination may represent an optimal condition for selecting a standard to evaluate the effectiveness of candidate inhibitors in *in vitro* assays.

4.3.3 Determination of The Cleavage Rate of A Small FRET Peptide

A 13-residue peptide based on the cleavage site of SNAPtide labeled on the N-terminus with FITC and the C-terminus with DABCYL¹⁴⁴ was used to measure cleavage rates. When the initial velocities of these cleavage assays were plotted as a function of

increasing FRET peptide concentration, they were clearly linear up to concentrations as high as 10 μM (Figure 4.3). The slope of this line (when $[\text{S}] \ll K_m$) is indicative of a specificity constant $k_{\text{cat}}/K_m = 1.12 \times 10^4 \text{ M}^{-1}\text{s}^{-1}$.^{145,146} The use of higher substrate concentrations in this assay was limited by the solubility of the FRET peptide, but even so this analysis allowed us to put limits on the possible values of k_{cat} and K_m for the FRET peptide substrate. As the concentration of BoNT/A LC used in this assay was 5 nM and the plot indicates V_{max} must be greater than $\sim 0.6 \text{ nM/s}$, this allowed us to estimate k_{cat} as $> 0.12 \text{ s}^{-1}$. However, I have also measured the cleavage rates of a FRET peptide (Figure 4.3) and the maximal rate determined ($> 0.12 \text{ s}^{-1}$), which was of the same relative order of magnitude as observed for our other assays. Additionally, as no saturation of rates occurred at concentrations as high as 10 μM , the K_m must be $> 10 \mu\text{M}$.

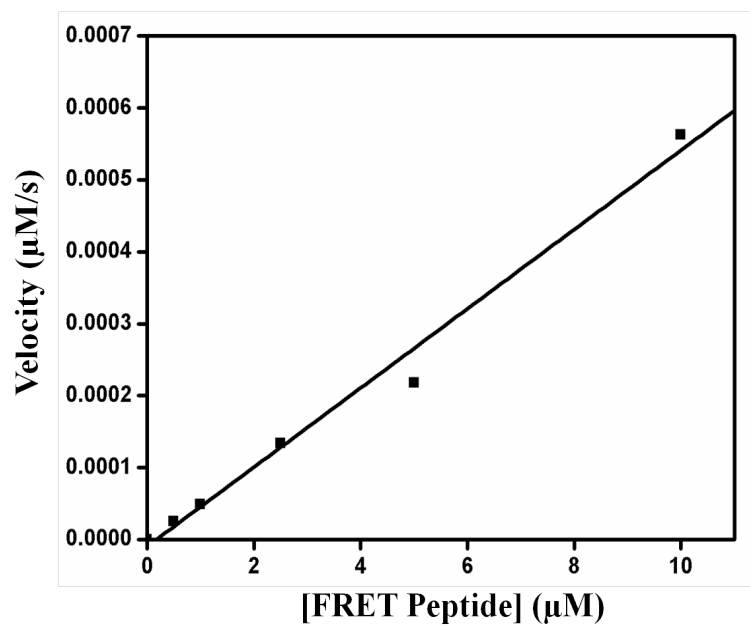


Figure 4.3 FRET peptide cleavage assay was shown as velocity versus peptide concentrations. The linear fitting curve was obtained to estimate k_{cat}/K_m ($= 1.12 \times 10^4 \text{ M}^{-1} \text{ s}^{-1}$) when $[S] \ll K_m$.

4.3.4 Inhibition Mechanism Determination of Specific Compounds Using Full-length Substrate in Solution

In order to determine the inhibition mechanisms of the three specific compounds, 5 μ M compounds were added into the samples before protease cleavage. All these compounds showed competitive inhibition with K_i values of 1.8 μ M, 3.6 μ M and 2.7 μ M for CID 564008, CID2214213 and CID 1299052, respectively (Figure 4.4 A, B and C). These results were consistent with the IC_{50} value determination based on both peptide and full-length substrates assays. The results also illustrated that these compounds may compete with enzyme binding to substrate at distal sites so that the blocked binding of enzyme and substrate inhibited the activity of protease cleavage. The identification of these compounds would provide a great platform to design more active structure-related compounds as potential inhibitors against BoNT/A LC. This discovery is also promising for clinical application of these compounds as beneficial medicines to treat many protease related diseases.

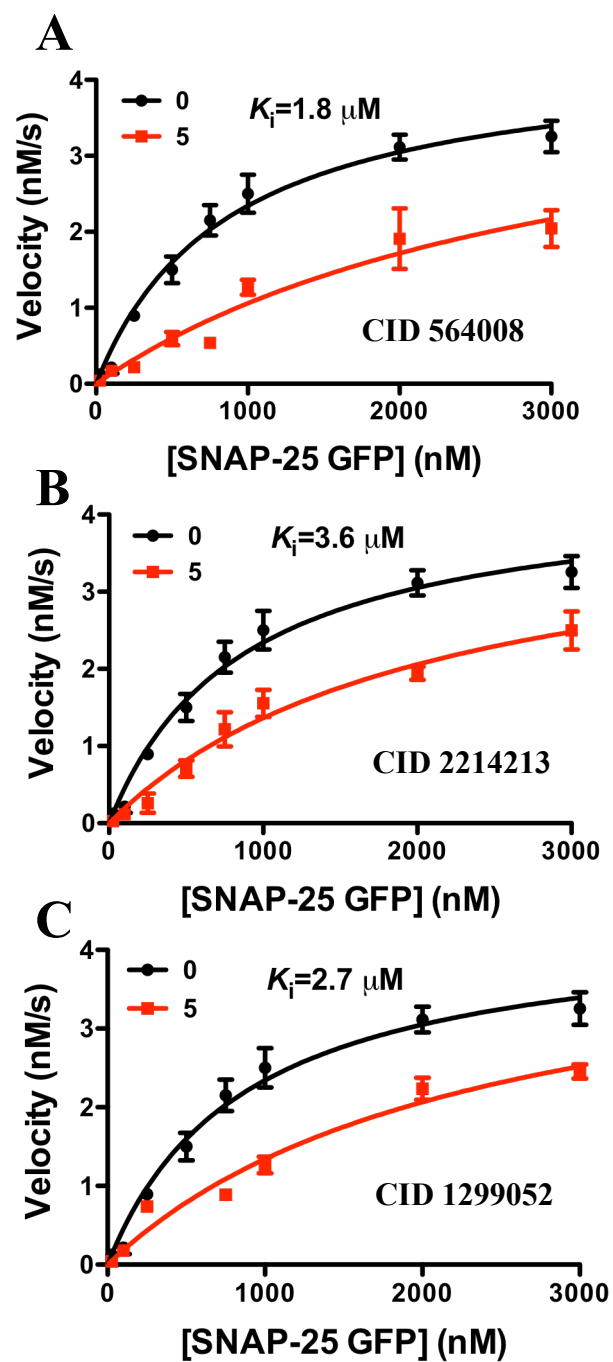


Figure 4.4 Inhibition determinations of three compounds. A. CID 564008 showed competitive inhibition with a K_i value of $1.8 \mu\text{M}$. B. CID 2214213 showed competitive inhibition with a K_i value of $3.6 \mu\text{M}$. C. CID 1299052 showed competitive inhibition with a K_i value of $2.7 \mu\text{M}$.

4.4 Conclusion

We have successfully developed the FRET solution assay with full-length substrate to determine the key kinetic constants of BoNT/A LC as well as the IC_{50} values of specific inhibitors. Due to the FRET pairs of GFP and Cy3, we carried out the FRET assays for BoNT/A LC to perform kinetic analysis and inhibitor identification. The identification of specific inhibitors would originate the design of some compounds that share similar structural characteristics with these inhibitors. The application of these compounds would provide a promising interest for clinical treatment of the diseases caused by BoNT/A toxin.

Chapter 5

Kinetic Study of Botulinum Neurotoxin Type A Light Chain on Microspheres by Flow Cytometry

5.1 Introduction

Multiplex microsphere assays have been developed for many enzymatic applications including the measurement of DNA polymerase activity, exonuclease activity, and protease activity.^{147,148,69} However, it is well recognized that, while microsphere and surface based assays in general have the advantage of making single turnover assays simple to perform, they do not permit substrate to be at saturating levels, which is required for the evaluation of Michaelis-Menten kinetics.¹⁴⁹ Nonetheless, to overcome this limitation several efforts have led to new kinetic models that may enable direct measurement of kinetic parameters, such as k_{cat} and K_m , when substrate is not saturated.^{150,151} Of specific interest here is an approach developed by Gutierrez et al, that treats heterogeneous assays as enzyme quasi-saturable systems (EQSS).¹³⁵ They have developed a quantitative model of general kinetic behavior in EQSS that enables determination of k_{cat} , K_m and K_i values. This model is mathematically consistent and has been used to quantify HIV protease activity on a flat surface.¹⁵² If this approach is valid it has significant value for the many surface based high-throughput screening (HTS) efforts for proteases and other enzymes.^{74,153}

The need for such models is particularly important for HTS for inhibitors of the botulinum neurotoxin type A light chain protease (BoNT/A LC).⁷² This protease is one part of BoNT, which is a bacterial endotoxin that exerts its paralytic effect by delivering

the LC protease into the cell. The specific location of cleavage is determined from which serotype the LC is derived from and BoNT/A LC cleaves synaptosomal associated protein of 25 kDa (SNAP-25) from the surface of the inner membrane of the neuron.⁷ The cleavage occurs in the C-terminus (Gln197-Arg198) of SNAP-25 and the specificity of this cleavage is driven in part by the binding of distal elements distal to the cleavage site.¹⁵⁴ BoNT/A LC is also part of BoTox, which is a carefully prepared and purified form of BoNT/A that is the best available therapeutic agent for a variety of human diseases due to a functional inhibition of cholinergic terminals.¹⁵⁵

To this end, a variety of microsphere based protease assays for high-throughput screening of protease activities have been developed.^{69,74} These assays, like other surface based protease assays, have the advantage that they can use large protein substrates containing distal binding elements. Inclusion of the distal site in HTS assays enables discovery of novel inhibitors that target this critical protein-protein interaction. Additionally, surface assays more closely mimic the natural surface based cleavage of SNAP-25 by BoNT/A LC. Microsphere based protease assays may offer an attractive version of these assays as they provide continuous time resolution and intrinsic resolution of free vs. bound fluorophores from the surface.¹⁰⁹ However, a complete demonstration of their ability to provide accurate kinetic analysis has not yet been demonstrated.

5.2 Materials and Methods

5.2.1 Materials

DNA oligonucleotide primers were synthesized by IDT (Coralville, IA) and Operon (Huntsville, AL). Terrific broth (TB) was purchased from Fisher scientific (Pittsburg, PA). Tris-base, Tween-20, Dithiothreitol (DTT), isopropyl- β -D-thiogalactopyranoside (IPTG), Bovine Serum Albumin (BSA), Hepes Hemisodium Salt, Sodium Chloride, Phosphate-buffered Saline (PBS), Carbenicillin, Chloramphenicol, and Biotin were bought from Sigma-Aldrich Corporation (St. Louis, MO). BoNT/A LC was bought from List Biological Laboratories (Campbell, CA). SoftLinkTM streptavidin resin was obtained from Promega Corporation (Madison, WI). Streptavidin-coated microspheres were obtained from Spherotech Corporation (Lake Forest, IL). Streptavidin-Cy3 conjugate was bought from Invitrogen (Grand Island, NY).

5.2.2 Expression and Purification of SNAP-25 GFP

Protein substrate synthesis with enhanced green fluorescent protein (EGFP) at the C-terminal and biotinylated tag at the N-terminal has been performed previously.⁶⁹ We have described the expression and purification of biotinylated tag and GFP domain BoNT/A LC substrate in our earlier work.⁷⁴ Briefly, a single colony with plasmid of interest was grown overnight in 3 mL Terrific broth (TB) media containing 50 μ g/mL carbenicillin, 34 μ g/mL chloramphenicol, then transferred to 250 mL TB 50 μ g/mL carbenicillin, 34 μ g/mL chloramphenicol, 40 μ M biotin and grown at 37°C until optical density at 600 nm (OD_{600}) reached 0.6-0.8. After, the cultures were induced with 100 μ M IPTC and grown

overnight at 30°C in a shaking incubator (250 rpm). The overexpressed SNAP-25 GFP protein with a biotinylated tag was purified by SoftLinkTM column with streptavidin-biotin system. The cultured cells were harvested by centrifugation at 3500 rpm on a Beckman Avanti J-301 centrifuge for 30 min at 4°C and washed by water twice to remove the biotin and were suspended in 40 mL lysis buffer (PBS+1 mM DTT). The resuspended cells were sonicated in an ice bath for 15 min and centrifuged at 14,800 rpm for another 30 min at 4°C. The clear supernatant was loaded onto a 5 mL SoftLinkTM avidin resin at a flow rate of 1 mL/min at 4°C. The PBS buffer with 5 mM biotin was used for eluting the protein from the column. Following, the eluted sample was dialyzed with protease buffer (50 mM HEPES, 100 mM NaCl, pH 7.4) for three times to remove the free biotin. The purified protein was confirmed with sodium dodecyl sulfate polyacrylamide gel electrophoresis (SDS-PAGE). The concentration was determined by using A₂₈₀ spectroscopic measurement and the calculated extinction coefficients.

5.2.3 Microsphere Based Protease Assays

To measure the minimal saturable concentration of biotinylated SNAP-25 GFP on 5 µm diameter streptavidin coated microspheres (SVP-50-5, Spherotech, Lake Forrest, IL), the substrate was titrated in 500 µL reaction volumes with 1.72×10^5 microspheres/mL per sample. After a one-hour incubation, all the microspheres were centrifuged at 14,800 rpm in an Eppendorf mini-spin plus centrifuge with a F45-12-11 rotor for 1 min and washed with protease buffer (50 mM HEPES, 100 mM NaCl, 1 mg/mL BSA, 0.025% Tween-20, pH 7.4) three times to remove the free substrate. Single point measurements were done

by flow cytometry on an Accuri C6 flow cytometer with the GFP fluorescent signal measured in the FL1 detection channel.

Then 25 nM SNAP-25 GFP was associated with the diameter of 5 μm streptavidin labeled microspheres in the protease buffer. Protease concentrations were 0, 2.5, 5, 10, 25, 50, 100, 200, 300 and 500 nM in total reaction volume of 500 μL , respectively. The substrate bound microspheres were prepared with an excess of 14 μL or 66 μL to be delivered at the delivery rate of the flow cytometer (14 $\mu\text{L}/\text{min}$ or 66 $\mu\text{L}/\text{min}$) over the 60 seconds required to establish a baseline. After 1 minute the tube was removed from the Accuri C6 flow cytometer (BD Biosciences, San Jose, CA) and BoNT/A LC dissolved in protease buffer was added to bring the final volume to 500 μL at the indicated concentrations. Upon protease addition the sample was mixed by vortexing for 5 seconds to start the cleavage reaction. All the samples were run continuously for 8 or 10 min. The 32 bit time resolution of the Accuri C6 ensured that we had 100 ms temporal resolution, which was more than sufficient for this assay.

5.2.4 Dead Time Measurement of Accuri C6 Flow Cytometer

For the analysis of the time delay between the addition of the protease and the appearance of beads exposed to protease in the flow cytometer, calibration beads with GFP fluorescence were added at the 60s time point when the blank beads without any fluorescence were running at fast, medium and slow flow rates of the Accuri. The fluorescence signals at each time point were collected and analyzed to obtain the dead time between blank beads and fluorescence beads.

5.3 Results and Discussion

5.3.1 Titration of Binding of SNAP-25 GFP to The Surface of Microspheres.

We constructed the protease substrate with biotinylation tag at N-terminal and GFP domain at C-terminal which was bound to streptavidin-coated microspheres. The specific binding between biotinylated SNAP-25 GFP and streptavidin-coated microspheres was performed based on the titration of biotinylated SNAP-25 GFP by increasing the substrate concentration (Figure 5.1). Microspheres were incubated at 25°C for 1 hour in the presence or absence of biotin. In the presence of biotin, there was almost no fluorescence signal due to biotin blocking the binding of SNAP-25 GFP to the streptavidin-coated microspheres (data not shown). The difference in fluorescence intensity between unblocked and blocked samples was calculated to determine the specific binding of biotinylated SNAP-25 GFP to microspheres. Fitting of binding data to a hyperbolic curve resulted in an estimated dissociation constant (K_D) of 7 nM for the biotin-streptavidin interaction. The curve of bound substrate concentration indicated that the concentration of substrate on the microsphere was low compared with traditional solution assay. At this point, the microsphere-based assay provides the advantage of saving substrate cost.

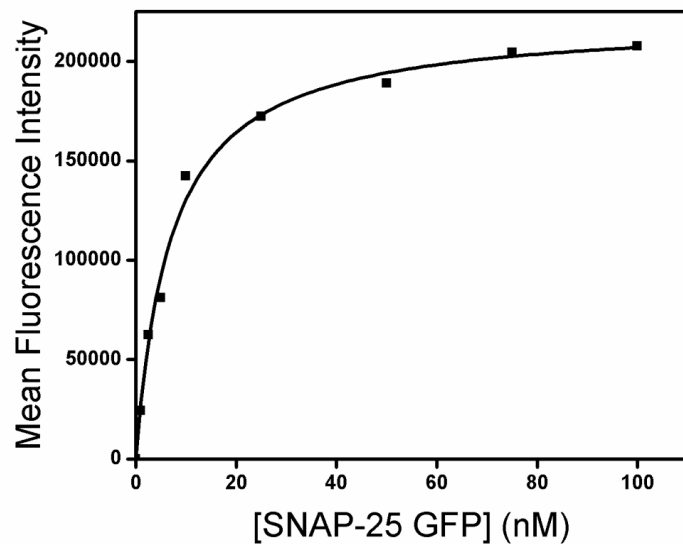


Figure 5.1 Equilibrium binding of SNAP-25 GFP on microspheres with a hyperbolic fitting curve. Streptavidin-coated microspheres were incubated with varying concentrations of SNAP-25 GFP and fluorescence on microspheres was measured by flow cytometry.

5.3.2 BoNT/A LC Cleavage of Full-length SNAP-25 Fusion Proteins from A Microsphere Surface

Our microsphere assay has been described in detail previously,⁷⁴ but in brief this assay uses titration of biotinylated SNAP-25 fusion protein concentration to determine the minimal saturating concentration for protease cleavage. The affinity of binding of biotinylated SNAP-25 GFP to streptavidin-coated microspheres is high with a dissociation constant (K_D) of 7 nM. This tight binding ensures that slow dissociation of the full-length substrate does not contribute to the observed cleavage rates (Figure 5.2). This was confirmed by showing constant fluorescence of the microsphere prior to our kinetic assay (Figure 5.2). Protease was added at known concentrations at 60 seconds, which resulted in a rapid loss of microsphere fluorescence. BoNT/A LC has been shown to be highly specific for our full-length SNAP-25 substrate in this assay.⁷⁴ Additionally, the intrinsic ability of a flow cytometer to resolve free vs. bound fluorescent molecules on particle surfaces eliminates the need for wash steps to measure the loss of microsphere fluorescence due to protease cleavage.¹⁵⁶ This property makes it simple to measure the both the time dependent fluorescence loss (Figure 5.2) and to determine the original fluorescence intensity of SNAP-25 GFP on the microspheres as well as the remaining fluorescence on microspheres after protease cleavage. Microsphere fluorescence intensity does not approach zero due to a small portion of the SNAP-25 GFP that may be non-specifically associated or adsorbed to the surface.⁷⁴

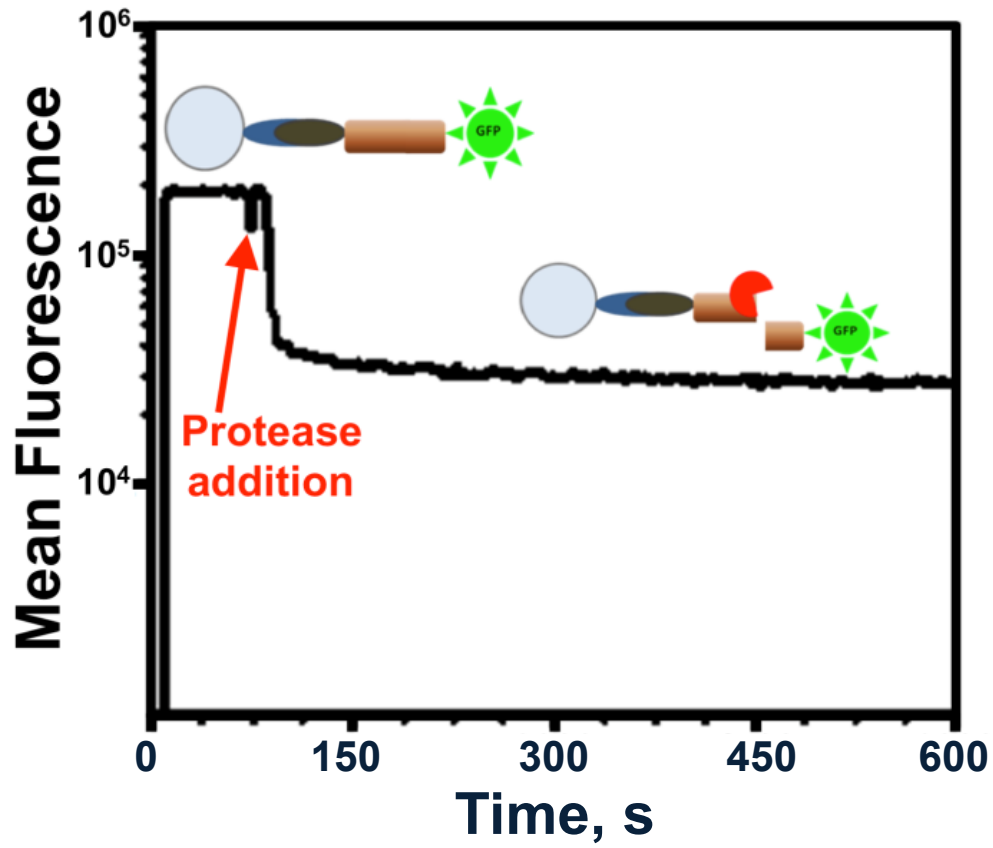


Figure 5.2 The fluorescence measurement of cleavage from microspheres vs. time. The full-length protease substrate was designed with the biotinylation tag at the N-terminal (brown oval) and the GFP domain at the C-terminal (green sun) separated by full-length SNAP-25 (brown cylinder) which is attached to streptavidin (blue crescent)-coated microspheres (gray circle). The fluorescence of GFP was measured before protease cleavage as baseline, then BoNT/A LC (red pie) was added at 60 s for cleavage, with the fluorescence change detected with increasing time.

5.3.3 Kinetics of BoNT/A LC Cleavage from The Microsphere Surface

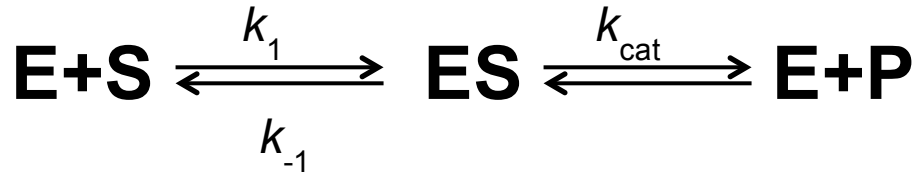
To determine the rate of cleavage vs. time, BoNT/A LC with various concentrations was incubated with SNAP-25 labeled microspheres (Figure 5.3A). The apparent rate of cleavage had clear concentration dependence (Figure 5.3B). In the simplest interpretation of such kinetics, it is viewed that the increasing concentrations of protease achieve rapid binding of the protease to the substrate and the forward cleavage reaction approaches that of the rate limiting step, which leads to an estimate of the rate limiting step of approximately 0.3 s^{-1} for the microsphere assay. This is a similar approach that was effective for nuclease cleavage of DNA from microspheres.¹⁴⁹ A more comprehensive view of this data can make use of the EQSS kinetic model, which is valid under the conditions shown in Equation 1.¹³⁵

$$\frac{f[S_0^{SP}]}{K_m + [E_0]} \ll 1 \quad (1)$$

Where f is the surface area per unit volume of the assay, $[S_0^{SP}]$ is the surface density of the substrate molecules, K_m is the Michaelis constant of the reaction, and $[E_0]$ is the total enzyme concentration.

Given that we have 10^6 microspheres/mL and that the microspheres are $5 \text{ }\mu\text{m}$ in diameter, the f value is roughly about 0.8 cm^{-1} . Considering the protein is 67 kDa , it would have a minimal radius of $\sim 2.5 \text{ nm}$ if packed as sphere. Maximal packing of spheres occurs in a regular hexagonal configuration, where each hexagon would have an area of $\sim 2.2 \times 10^{-13} \text{ cm}^2$ to fully contain a 2.5 nm radius protein leading to a maximal estimate of 4.6×10^{12} proteins per cm^2 for our substrate. Given the f value of 0.8 cm^{-1} then

$f[S_0]=3.7\times 10^{12}$ proteins/cm³ or 3.7×10^{15} proteins/L or 6 nM. Of course a reasonable assumption is that this level of packing is not achieved and that some lower fraction of surface coverage is achieved, which typically is about 10-25% of maximal packing. Given this a reasonable estimate of $f[S_0]$ is roughly 1 nM. Thus if the K_m of a reaction is 100 nM or greater, the conditions of Eq. 1 are easily satisfied for the microsphere-based assay. Using the microsphere system, any reaction that has a K_m greater than 100 nM satisfies the requirements of equation 1 and results in an EQSS system. For EQSS systems it is possible to make a pseudo steady state assumption that relates initial velocities to enzyme concentration. At this condition, the proposed reaction scheme is



Where, the total substrate concentration $[S]$ can be accounted for both free substrate $[S]_f$ and enzyme-substrate complex $[ES]$, which is defined as:

$$[S] = [S]_f + [ES], \quad (2)$$

Here, $[ES]$ depends on the rate of formation of the complex (k_1) and the rate of loss of the complex (k_{-1} and k_{cat}). Also, assuming that the amount of enzyme bound to substrate does not change the free enzyme concentration ($[E]=[E]_f$). The rate equations for these two processes are thus given by:

$$\frac{d[ES]}{dt} = k_1[E][S]_f, \quad (3)$$

$$\frac{-d[ES]}{dt} = (k_{-1} + k_{cat})[ES] \quad , (4)$$

Under steady state conditions there two rates must be equal, hence:

$$k_1[E][S]_f = (k_{-1} + k_{cat})[ES] \quad , (5)$$

This equation can be rearranged as:

$$[ES] = \frac{[E][S]_f}{(k_{-1} + k_{cat}) / k_1} \quad , (6)$$

Also, the term K_m is defined as:

$$K_m = \frac{k_{-1} + k_{cat}}{k_1} \quad , (7)$$

The equation (7) could be expressed as:

$$[ES] = \frac{[E][S]_f}{K_m} \quad , (8)$$

From equation (2), the $[S]_f$ can be replaced by $([S]-[ES])$. With this substitution, equation (8) can be recast as:

$$[ES] = \frac{[E][S]}{K_m + [E]} \quad , (9)$$

Also, the pseudo-first-order progress curve for an enzymatic reaction can be described by:

$$v = k_{cat}[ES] \quad , (10)$$

Combining equations (9) and (10), the velocity could be obtained as:

$$v = \frac{k_{cat}[E]}{K_m + [E]}[S], \quad (11)$$

This enables simple determination of both k_{cat} (k_2) and K_m from the fit of this equation to the data (Figure 5.3B). This approach provides an estimate of $0.52 \text{ s}^{-1} \pm 0.15 \text{ s}^{-1}$ for k_{cat} , $0.38 \pm 0.20 \text{ }\mu\text{M}$ for the K_m , and $1.4 \times 10^6 \text{ M}^{-1} \text{ s}^{-1}$ for the specificity constant (k_{cat}/K_m). While these rate measurements are of clear value, factors such as substrate surface density and transport effects near microsphere surfaces, such as slowed product release, could result in reduced accuracy for these values.^{135, 157}

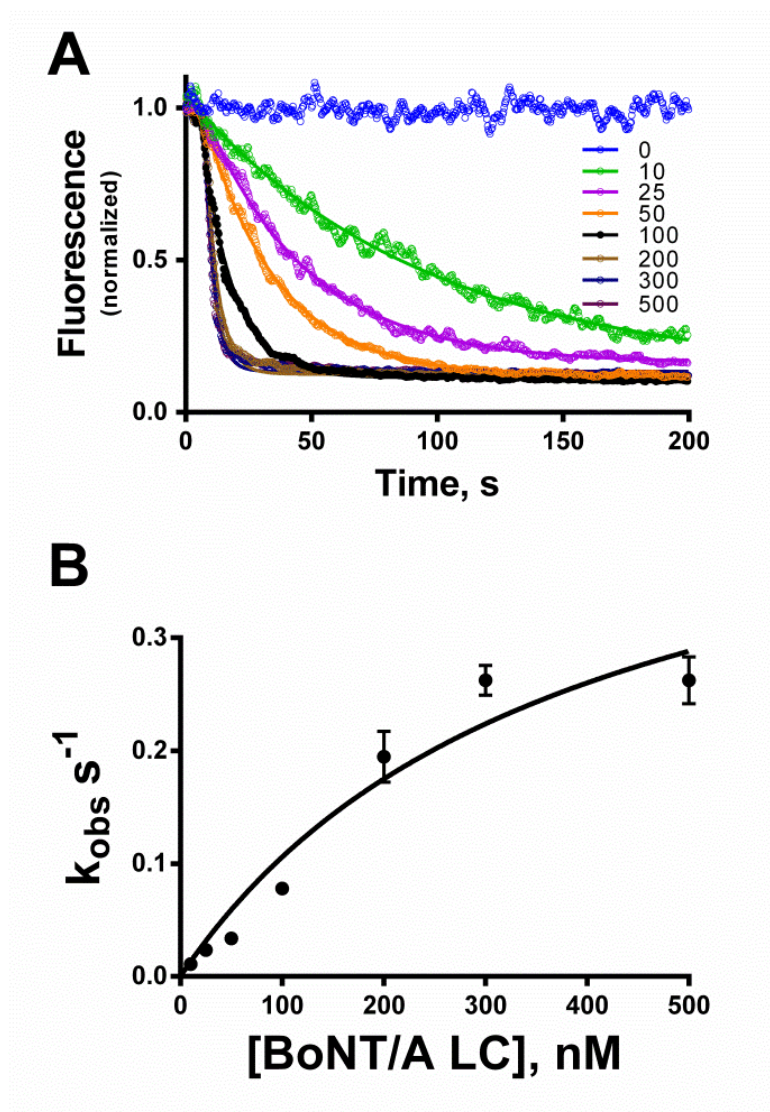


Figure 5.3 Kinetic analysis of BoNT/A LC based on microsphere. A. BoNT/A LC cleavage kinetics with increasing enzyme concentration, which are shown in the legend where the numbers indicate the concentration of BoNT/A LC in nM. The fitted lines are shown in matching colors on the plot. B. Plot of k_{obs} vs. BoNT/A LC concentrations, from which k_{cat} and K_m were calculated by hyperbolic fitting curve, $k_{cat}[E]/(K_m+[E])$. This fit provided an estimate of $0.52 \pm 0.15 \text{ s}^{-1}$ for k_{cat} and $0.38 \pm 0.20 \text{ }\mu\text{M}$ for K_m .

5.3.4 Dead Time Measurement of Accuri

In order to determine the time delay of Accuri C6 flow cytometer, I prepared blank beads and fluorescence beads labeled with SNAP-25 GFP. The fluorescent beads were added at 60-second after the blank beads to determine the time between bead addition and subsequent detection in the Accuri flow cytometer. All the calibrations were performed at different flow rates from slow speed (14 $\mu\text{L}/\text{min}$) to fast speed (66 $\mu\text{L}/\text{min}$) of the Accuri. The fluorescence signals at different time points were collected and analyzed to show that the dead times were about 9.6 s for the slow rate and 2.5 s for the fast rate, respectively (Figure 5.4). The prolonged dead time at the slow flow rate indicated that the calculated cleavage rates at higher protease concentrations were artificial results. In addition, the determination of the kinetic constants was not correct due to dead time limitations.

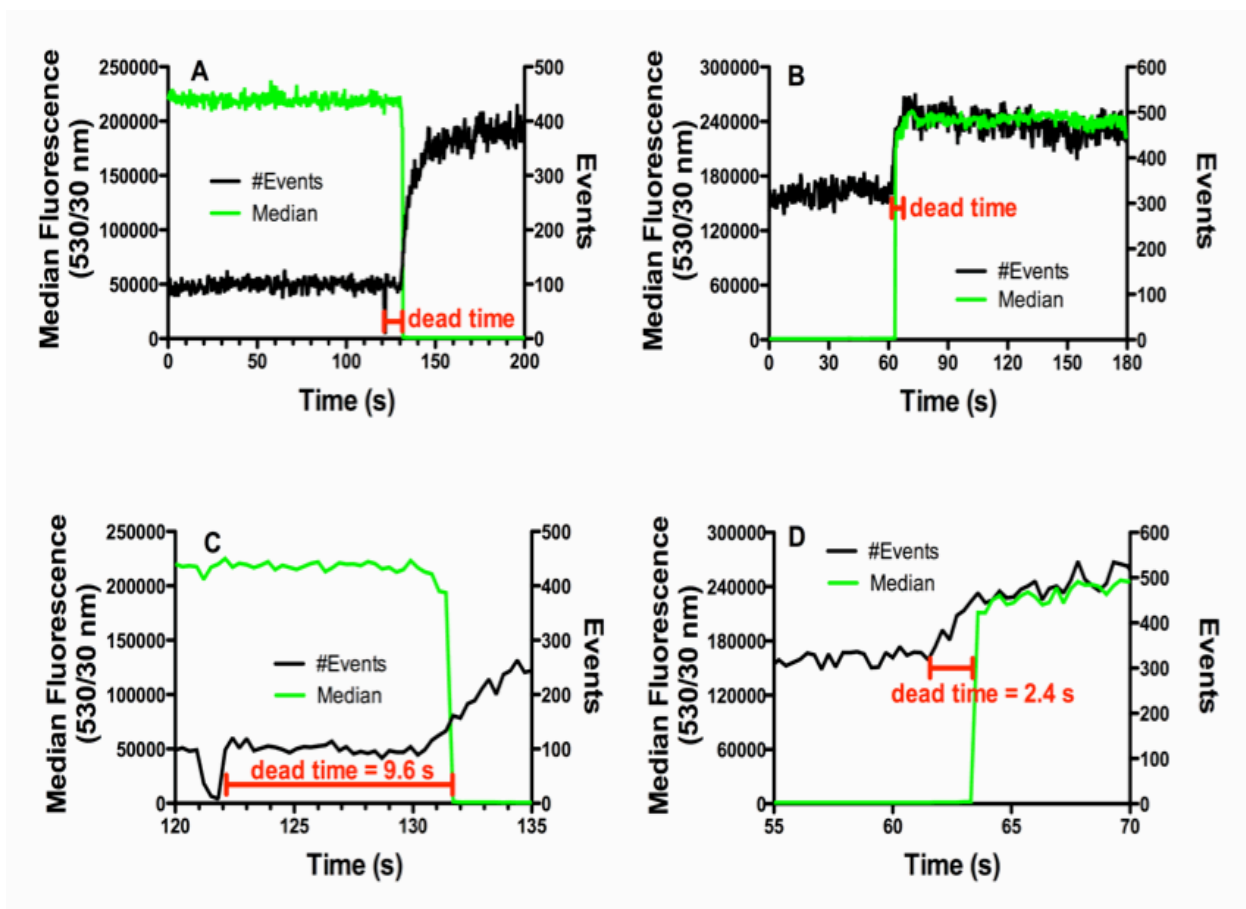


Figure 5.4 Dead time measurement of Accuri at slow and fast flow rates. A. The display of fluorescence and events at different time points at the slow flow rate. B. The display of fluorescence and events at the fast flow rate. C. The dead time determination of 9.6 s at slow flow rate. D. The dead time of 2.4 s at fast rate.

5.3.5 Protease Cleavage Measurement Using Accuri at Fast Flow Rate

Based on the determination of dead time of Accuri, I repeated the protease cleavage assays with different enzyme concentrations from 0 nM to 500 nM at the fast flow rate (66 $\mu\text{L}/\text{min}$) to obtain a better estimate of the true cleavage rates (Figure 5.5A). Due to the limitation of enzyme concentrations, I didn't obtain the saturated state to determine the kinetic constants including k_{cat} and K_{m} values, however, I still gained the $k_{\text{cat}}/K_{\text{m}}$ value of $9 \times 10^5 \text{ M}^{-1}\text{s}^{-1}$ with linear fitting the data points (Figure 5.5B). The smaller catalytic constant obtained here also indicated that we didn't determine the correct kinetic constants owing to the long dead time at slow flow rate. At this point, I have to increase the substrate concentration in order to carry out kinetic study of the protease on surface by flow cytometer since the low surface to volume ratio of microspheres limits the substrate concentration in nanomolar range. Therefore, it is very necessary to develop nanosphere-based protease assay for kinetic studies with increasing substrate concentrations. Basically, the nanospheres lead to the higher surface to volume ratio that results in higher substrate concentrations and may provide enough substrate for protease cleavage.

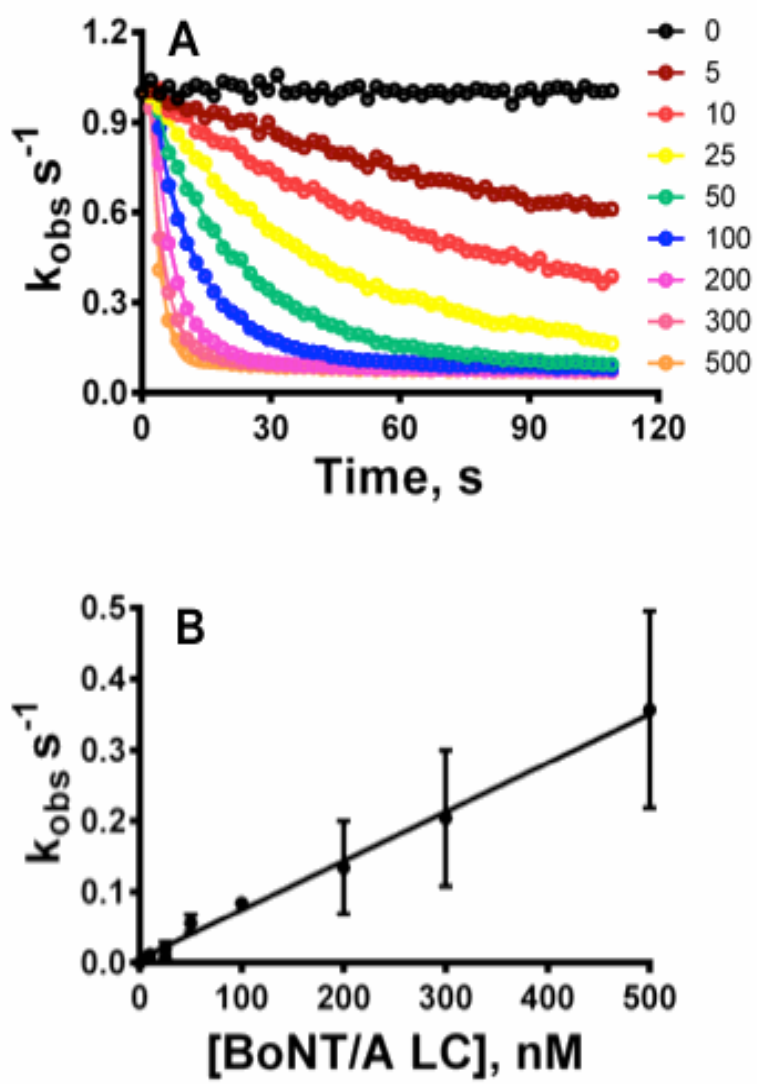


Figure 5.5 Protease cleavage assay at fast flow rate. A. The real cleavage measurement with increasing protease concentrations to 500 nM. B. The linear fitting of observed rates vs. protease concentrations.

5.4 Conclusion

We developed real-time measurements of BoNT/A LC by using the full-length fluorescent substrate on microspheres. Even though we didn't determine the main kinetic constants based on microspheres, it should be noted that this approach may or may not be generally applicable and that structural features of SNAP-25, such as the proximity of the N and C termini may make this a unique assay for the BoNT/A LC-SNAP25-GFP complex. The nanosphere-based protease cleavage assay will be employed to determine the key kinetic constants due to higher substrate concentrations. The successful use of surface-based protease assay along with their speed and simplicity indicate that these approaches will be highly attractive for HTS for inhibitors of proteases.

Chapter 6

Nanosphere-based Kinetic Analysis of Botulinum Neurotoxin Type A Light Chain

6.1 Introduction

Proteases are heavily involved in many normal biological processes as well as in diseases, including cancer, stroke and infection. As a result, protease activity is a widely studied topic and protease activity assays have significant medical relevance. Presently, there are a wide variety of protease assays. However, all current assays have one or more limitations that include use of small substrates, use of low substrate concentrations, and low multiplexing ability.

We have developed a multiplexed microsphere protease assay that can detect the activity of several metalloproteases simultaneously.⁶⁹ Multiplexed protease assays are attractive because many proteases exist as protein families operating in similar fashion across related disease, pathogens, and cellular processes.¹⁵⁸ For example, each of the seven types of Botulinum neurotoxin light chain proteases (A – G) recognizes different aspects of one protein of the SNARE complex.²⁰ We have demonstrated that multiplex assays can analyze many substrates and proteases simultaneously, making the discovery of lead compounds for a protease family faster and less labor intensive.^{69, 74} More importantly, the microsphere assay uses large protease substrates containing exosites that are required for full protease activity. This is an advantage of surface based protease assays, as typical FRET peptide assays cannot utilize large substrates and are not effective for studies of many protease substrate interactions. Furthermore, multiplexing using microsphere arrays makes it possible to screen multiple proteases, interactions of a

single protease with multiple substrates, or a combination of both.⁷⁴ However, protease assays must provide substrates at saturating concentrations to determine steady state kinetics routinely used to evaluate kinetics and lead compounds.

While planar and microsphere assays are amenable to multiplexing and incorporation of biomimetic membranes, practical considerations of surface area to reaction volume (SA/V) ratios limit substrate concentrations to the nM range. For a microsphere with radius 5 μm (surface area of roughly $3 \times 10^8 \text{ nm}^2$), a typical 60 kDa globular protein with a cross-sectional area of $\sim 20 \text{ nm}^2$, a typical microsphere maximally has $\sim 1 \times 10^6$ proteins attached to its surface. This microsphere has a volume of $5.2 \times 10^{-7} \mu\text{L}$, so for a practical analysis limit of 10% microsphere to reaction volume ratio, the maximum usable microsphere concentration is $\sim 190,000$ microspheres/ μL . This value and the number of surface proteins predict a maximum substrate concentration of about 300 nM for reactions occurring on this microsphere. Such conditions are not saturating for most proteases and prevent the determination of standard kinetic parameters (k_{cat} , K_{m} and K_{i}) for activity and inhibitor comparisons. If we neglect the effects of the analytical volume and use the same ratio of total particle volume to reaction volume, the use of nanospheres would make it possible to increase surface bound substrate to saturating concentrations ($\sim 60 \mu\text{M}$) for low affinity proteases. The increase in concentration is due to the simple inverse relationship between surface area to volume ratio of a sphere and the radius of a sphere ($\text{SA}/\text{V}=3/\text{radius}$). By decreasing the diameter of our spheres from 2.5-10 μm to 25-100 nm, while maintaining the same particle volume to reaction volume ratio, we increase the relative surface area and the effective substrate concentration in a reaction by 100 fold. The use of nanospheres makes it possible to increase surface bound substrate to

saturating concentration for low affinity proteases. The development of a nanosphere-based protease assay enables the use of full-length protease substrates, multiplexed assays, and, most importantly, provides high substrate concentrations in a surface assay format.

To create the nanosphere assay, which is based on our microsphere protease assay platform, I hypothesize that the use of nanospheres bearing surface bound substrates will retain the advantages of microsphere assays yet provide high surface area to volume ratio that will enable substrate concentrations in the μM range. To demonstrate this approach I implemented our nanosphere protease assay using the toxin protease models to first demonstrate the concept and then with BoNT/A LC through 380 nm streptavidin-coated nanospheres. Cleavage from the surface of the nanosphere was detected via observing nanosphere fluorescence changes on a flow cytometer.

6.2 Materials and Methods

6.2.1 Materials

BoNT/A LC was bought from List Biological Laboratories (Campbell, CA). 380 nm Streptavidin-coated nanospheres were obtained from Spherotech Corporation (Lake Forest, IL). Streptavidin-Cy3 conjugate was bought from Invitrogen (Grand Island, NY). Bovine Serum Albumin (BSA), Hepes Hemisodium Salt, Sodium Chloride, Phosphate-buffered Saline (PBS) and Biotin were bought from Sigma-Aldrich Corporation (St. Louis, MO).

6.2.2 Prepare Fluorescent Fusion Protease Substrates

We developed fusion protein substrates specific for BoNT/A LC, which was SNAP-25 GFP containing a biotinylation tag at N-terminal and a GFP domain at C-terminal. The detailed construction was described in Chapter 4. The substrates would be cleaved by proteases both in solution and on nanospheres. These nanospheres are commercially available and offer an effective method to explore the utility of nanosphere based protease assays.

6.2.3 Determine Events Rate by BD FORTESSA Flow Cytometry

The nanospheres with the concentration of 3.3×10^{11} nanospheres/mL were diluted into varied concentrations: 10^{10} , 10^9 , 10^8 , 10^7 and 10^6 per mL. Each sample was tested by FORTESSA flow cytometer triggering on the fluorescence of nanospheres in the PE-Cy5 detection channel (667 nm). The event rates were determined by dividing the number of events with 40 seconds at different particle concentrations.

6.2.4 Titration of Protease Substrate on Nanospheres

To measure the minimal saturable concentration of biotinylated SNAP-25 GFP on 380 nm streptavidin coated nanospheres, the substrate at appropriate concentrations was titrated in 500 μ L reaction volumes with 1×10^8 nanospheres/mL per sample. To determine the specific binding between substrate and nanospheres, the unblocked sample was carried out with nanospheres and substrate for one-hour incubation at room temperature. In addition, the blocked sample was carried out that the nanospheres were

incubated in the presence of 80 mM biotin for 30 min and protein substrate was added for additional one-hour incubation at room temperature. After incubation, all the nanospheres were centrifuged at 14,800 rpm in an Eppendorf mini-spin plus centrifuge with a F45-12-11 rotor for 1 min and washed with protease buffer (50 mM HEPES, 100 mM NaCl, 1 mg/mL BSA, 0.025% Tween-20, pH 7.4) three times to remove the free substrate. Single point measurements were done by flow cytometry on a BD FORTRESSA flow cytometer with the GFP fluorescent signal measured in the FITC (520 nm) detection channel.

6.2.5 Nanosphere-based Protease Cleavage Assay

500 nM SNAP-25 GFP was associated with 380 nm streptavidin labeled nanospheres in protease buffer. Protease concentrations were 0,5,10, 20, and 40 nM and the total reaction volume was 500 μ L for each sample, respectively. The substrate bound microspheres were prepared with an excess of 12 μ L volume to be delivered at the delivery rate of 12 μ L/min on the flow cytometry over the 60 seconds required to establish a baseline. After one minute the tube was removed from the BD FORTRESSA flow cytometer (BD Biosciences, San Jose, CA) and BoNT/A LC in the protease buffer was added to bring the final volume to 500 μ L at the indicated concentrations. Upon protease addition the sample was mixed to start the cleavage reaction. All the samples were run continuously for 8 or 10 min. All the mean FITC fluorescence values were converted into normalized fluorescence values by dividing the data point after adding BoNT/A LC by the average fluorescence values of the first 60 seconds.

6.2.6 Size Measurement of Nanospheres

In order to determine the size of nanospheres, we measured the sizes of the nanospheres based on different concentration as described in event rate determination. The measurement was carried out using dynamic light scattering method.

6.3 Results and Discussion

6.3.1 Predicted and Measured Event Rates

Using BD FORTRESSA flow cytometer, we assumed the interrogation volume of this machine with a diameter of 5 μm and height of 10 μm , and predicted the event rates at slow flow rate (12 $\mu\text{L}/\text{min}$) against various particle concentrations (Figure 6.1 Red line). In addition, we determined the real event rates by triggering on the fluorescence of the nanospheres. The observed rates were plotted against particle concentrations (Figure 6.1 Blue line). The results showed that the observed event rates were about 10^3 fold less than predicted rates, which meant not only single nanosphere but also doublets or aggregates may go through the laser beam. Both linear fitting curves displayed the similar slopes that also indicated that we successfully triggered on the fluorescence from nanospheres by flow cytometry. At this point, we would like to perform the substrate titration on nanospheres in order to obtain minimal saturation concentration for the protease cleavage assay to determine the kinetic constants.

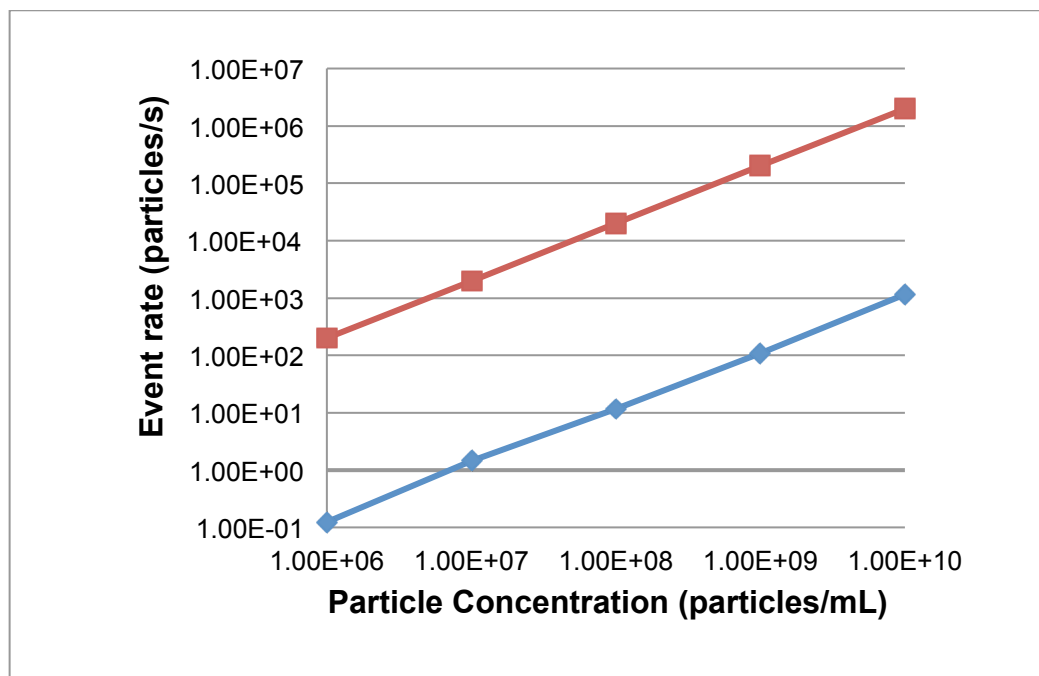


Figure 6.1 Predicted and observed event rates are shown as red squares and blue diamonds, respectively.

6.3.2 Titration of SNAP-25 GFP on 380 nm Nanospheres

The specific binding between biotinylated SNAP-25 GFP and streptavidin-coated nanospheres was performed based on the titration of biotinylated SNAP-25 GFP by increasing the substrate concentration (Figure 6.2). The results of block titration showed slightly increased fluorescence signal due to the biotin bound to streptavidin-coated nanospheres. The difference of fluorescence values between unblock and block samples was calculated to determine the specific binding of biotinylated SNAP-25 GFP to nanospheres. The curve of bound substrate concentration illustrated that the concentration of substrate on the nanospheres was increased to the micromolar range compared with the microsphere-based titration (Chapter 5). Here, we didn't obtain the saturated state owing to the limitation of substrate concentrations. However, the titrated results showed that the biotinylation-tag SNAP-25 GFP was successfully bound to the nanospheres and the fluorescence on the nanospheres was detected by flow cytometry.

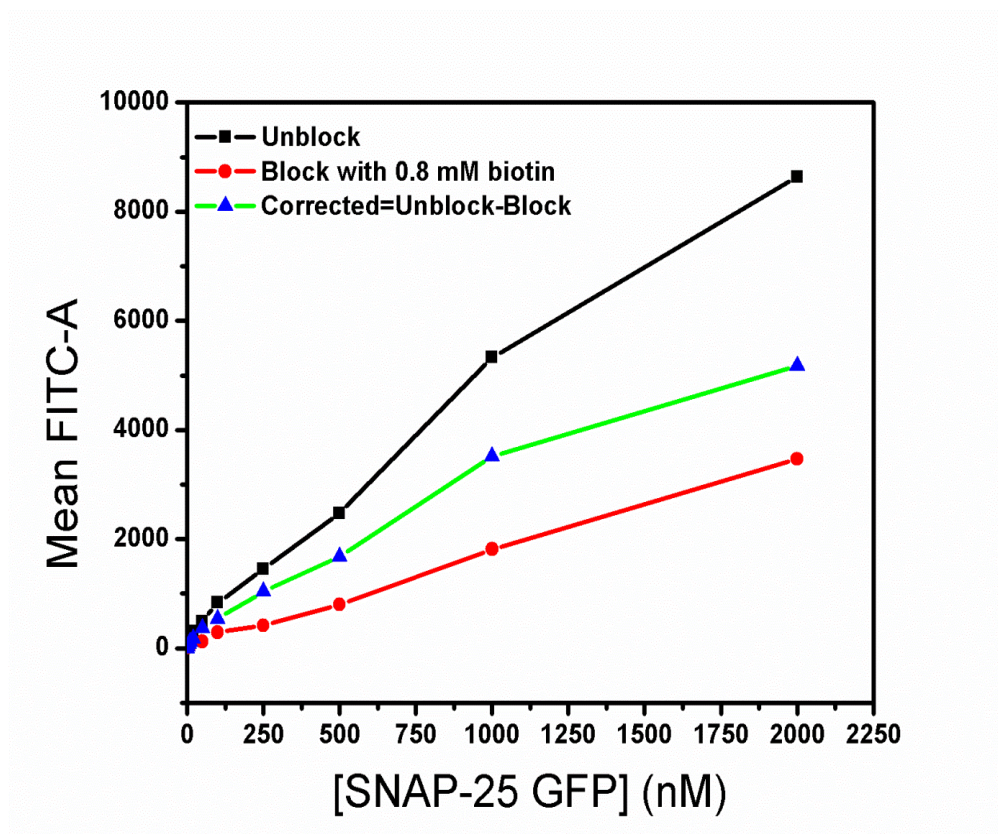


Figure 6.2 Titration of SNAP-25 GFP on nanospheres. The streptavidin-coated nanospheres were incubated with varied concentrations of SNAP-25 GFP and fluorescence on nanospheres was measured by flow cytometry.

6.3.3 Protease Cleavage Assay on Nanospheres

In this case, we detected nanosphere presence via intrinsic nanosphere fluorescence to trigger collection. Protease activity was detected as loss of GFP fluorescence from the nanosphere. To make this assay possible, we needed to ensure that I only had about 10% occupancy on average within the detection volume of the FORTESSA, which essentially a 10 μm high by 5 μm diameter cylinder (defined by the laser spot size and the sample stream diameter). This volume ($\sim 2 \times 10^{-10}$ mL) requires me to use no more than about 2×10^9 nanospheres/mL.

The cleavage activity of BoNT/A LC was measured based on the fluorescence change on nanospheres. With the addition of the protease, the loss of fluorescence on the nanospheres was detected by flow cytometry. The cleavage of BoNT/A LC against SNAP-25 GFP occurred very quickly in first 200 seconds and achieved a steady state with extended time. The kinetics of protease cleavage were then shown as normalized fluorescence vs time with a series of BoNT/A LC concentrations (Figure 6.3A). At low concentrations of protease, the cleavage traces of BoNT/A LC against substrate were slow with increasing time. Then the obvious cleavage was detected with higher concentrations of BoNT/A LC. In nanosphere-based assay, the SNAP-25 GFP concentration was much less than the K_m , the loss of substrate was still considered as a function of time under first-order reaction. Assuming that nanosphere fluorescence is proportional to concentrations, the observed rates of cleavage were obtained from exponential fitting curves and plotted against the concentrations of BoNT/A LC (Figure 6.3B). These results showed that the cleavage rates depended on the concentrations of BoNT/A LC and approached a saturating rate at higher concentrations. Therefore, the

faster rates with higher BoNT/A LC concentrations were obtained because the enzyme adsorbed to substrate bound nanospheres at high concentrations retained a significant fraction of their solution activity.¹⁵⁹

While we have performed my current assays in real time using 10^8 nanospheres/mL that only provides nM concentrations, future assays could be performed at high nanosphere concentrations as high as 10^{13} nanospheres/mL. These assays could not be performed real time, we will perform the protease reaction by quenching cleavage of the metalloprotease via chelator addition, and then dilute to analyze on the flow cytometer. This will allow me to perform reactions with surface bound substrate at the concentration of 2 μ M, which would not be possible using microspheres. We will use this nanosphere-based assay to determine the K_m and k_{cat} for each of our proteases. We will also use these parameters as a guideline to develop end point assays for high throughput screening.

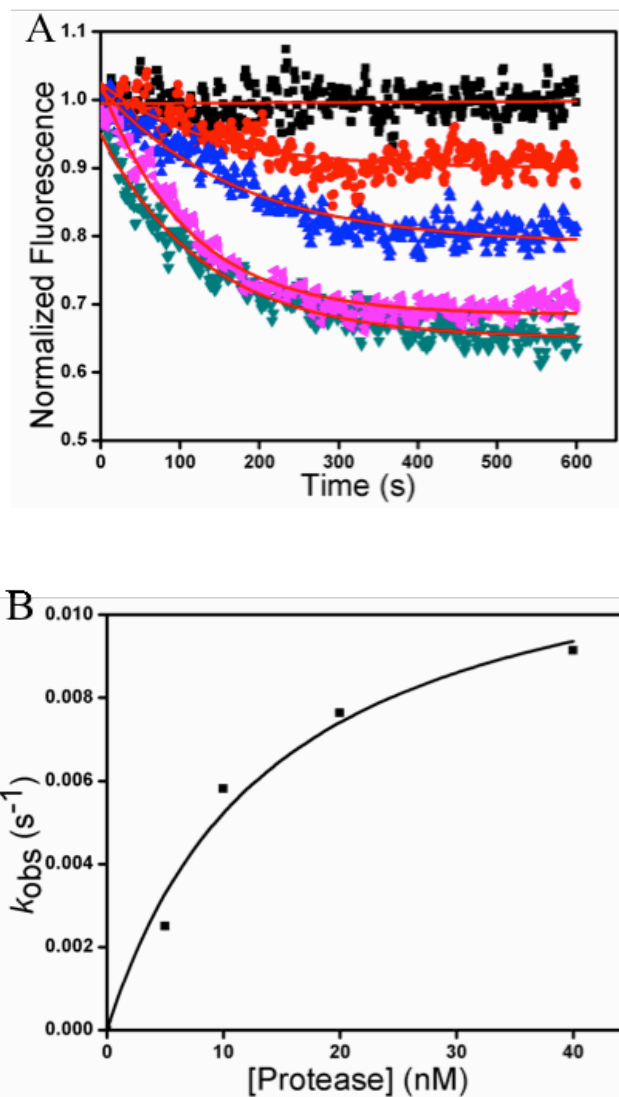


Figure 6.3 Protease cleavage of SNAP-25 on nanospheres. A. BoNT/A LC cleaved SNAP-25 with increasing protease concentrations. BoNT/A LC concentrations were 0, 5, 10, 20 and 40 nM. B. Plot of observed rates against BoNT/A LC concentrations.

6.3.4 Size Measurement of Nanospheres

To measure the size of our nanospheres, dynamic light scattering has been used to determine the size distribution of the particles. The nanospheres with concentrations of 10^{10} , 10^9 , 10^8 , 10^7 and 10^6 particles/mL were tested here. The optimal concentration of 10^8 particles/mL showed the best radius results of the nanospheres in Figure 6.4. From the result, the main radius is around 178 nm representing a diameter of 356 nm nanospheres that is very close to the size from the technical instruction of the nanospheres we have purchased. In addition, there are three other radii including 3 nm, 2263 nm and 147823 nm. The 3 nm radius is probably the noise of the instrument, but the 2263 and 147823 nm radii may represent the presence of aggregates. This result also confirmed that the observed event rates we obtained previously were much slower than predicted rates triggering on fluorescence by flow cytometry because of low sensitivity of the instrument or aggregating of nanospheres.

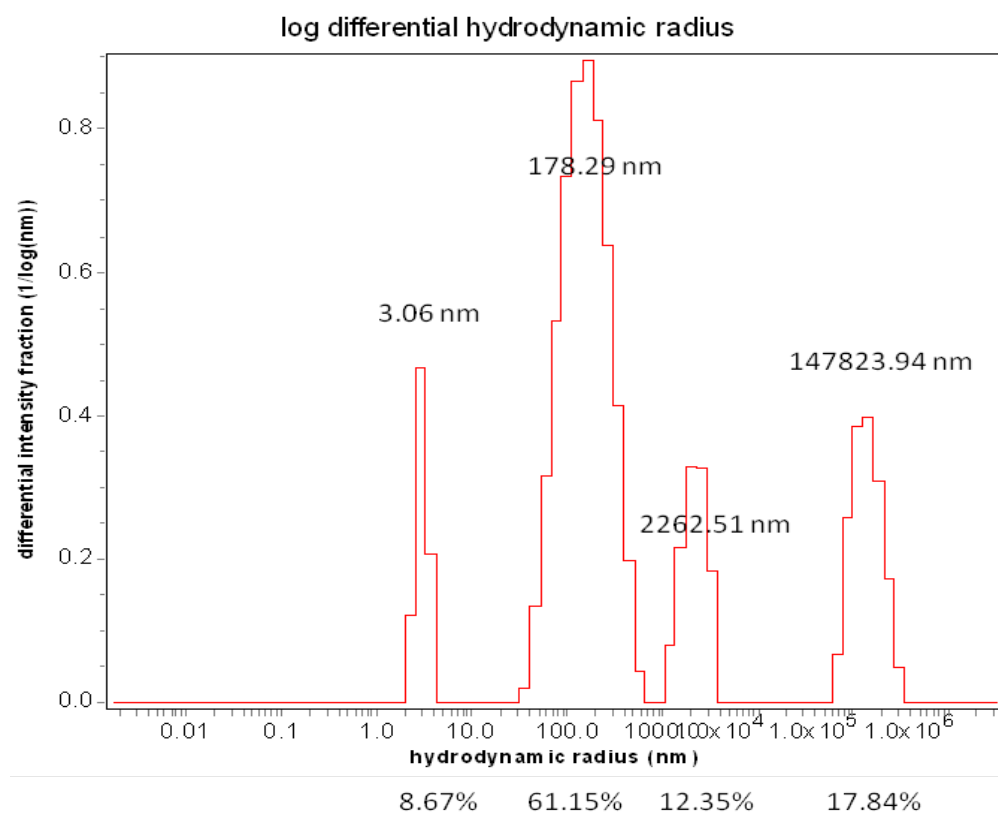


Figure 6.4 Dynamic light scattering measurements of nanospheres to obtain the size.

6.4 Conclusion

In this chapter, we have developed the nanosphere-based protease assay that provides high surface area to volume ratio enabling substrate concentrations in the μM range for kinetic studies. We have performed the protease cleavage assay on nanospheres with increased substrate concentration. In addition, the exact kinetic model should be considered here to determine the key kinetic constants of BoNT/A LC on nanospheres. These kinetic pathways will be combined with mutagenesis studies and any discovered small molecule inhibitors to explore how proteases and their substrates interact.

Chapter 7

Conclusions and Future Directions

7.1 Conclusions

7.1.1 Parallel Protease Assay Using Suspension Microsphere Arrays for High-throughput Screening

In this work, we have successfully developed microsphere-based protease assay using 384 and 1536-well plate high-throughput screening to identify potential inhibitors for *Bacillus anthracis* lethal factor (LF) and Botulinum neurotoxin type A & F light chains (BoNT/A & F LCs) via flow cytometry. We have demonstrated the construction of full-length protease substrates with a biotinylation tag and N-terminal and a GFP domain at C-terminal. We have performed the multiplexed protease assay by running several proteases simultaneously in the same reaction volume since each protease can specifically recognize and cleave their own substrates. The identification of inhibitors by high-throughput screening has been described in Chapter 3 from Prestwick chemical library and NIH chemical library.

7.1.2 Selection of Potential Inhibitors for Bacterial Metalloproteases

In my research, we have identified several specific inhibitors for lethal factor, BoNT/A LC. In Chapter 3, riboflavin has been distinguished from 1128 compounds as a specific inhibitor for lethal factor with the IC₅₀ values around 15 μ M in both microsphere-based and FRET peptide solution assays. Later, we have found several inhibitors against LF,

BoNT/A & F LCs from 350,000 chemical library using 1536-well plates. These compounds showed great inhibition with the IC_{50} values lower than 20 μ M for the proteases. The multiplexed microsphere-based protease assay for high-throughput screening have demonstrated a great ability to screen several protease simultaneously that dramatically reduces screening labor and cost, immediately provides information on specificity of an inhibitor and displays an promising approach for study of many protein members from a family of related proteases simultaneously.

7.1.3 FRET Solution Assays for Protease Kinetic Analysis

In my work, we have developed FRET solution assays containing both peptide and full-length substrates. We have bought commercially available FRET peptides including MAPKKide and SNAPtide for LF and BoNT/A LC to determine the IC_{50} values of potential inhibitors identified in microsphere-based assay. Due to the limited substrate dissolved in solution, we didn't obtain the important kinetic constants like k_{cat} , K_m or K_i values. In addition, we designed a full-length FRET substrate that contained a FRET pair of GFP and Cy3 linked by a biotinylation-tag full-length protease substrate conjugated to Cy3 labeled streptavidin. We have employed these substrates to evaluate the inhibitors and demonstrate the kinetic studies for BoNT/A LC. Both substrates have been used to confirm and estimate the inhibitors for determination of specific inhibition. Compared the results with those obtained from microsphere-based assay, the identification of specific inhibitors indicates the great importance of distal events in the interaction between proteases and substrates. Blocking the binding of proteases and substrates at exosites has

been proved to inhibit the activity of a protease. We have determined the key kinetic constants of BoNT/A LC including k_{cat} , K_m and k_{cat}/K_m values using full-length substrates. We have also determined the inhibition mechanisms of some specific compounds against BoNT/A LC. All of them are competitive inhibitors the K_i values lower than 5 μM . These kinetic constants would provide more information of BoNT/A LC and its inhibitors.

7.2 Future Directions

7.2.1 Nanosphere-based Protease Assay

While planar and microsphere assays are amenable to multiplexing and incorporation of biomimetic membranes, practical considerations of surface area to reaction volume (SA/V) ratios limit substrate concentrations to the nM range. The use of nanospheres would make it possible to increase surface bound substrate to saturating concentrations ($\sim 60 \mu\text{M}$) for low affinity proteases. The increase in concentration is due to the simple inverse relationship between surface area to volume ratio of a sphere and the radius of a sphere ($\text{SA}/\text{V}=3/\text{radius}$). By decreasing the diameter of our spheres from 2.5-10 μm to 25-100 nm, while maintaining the same particle volume to reaction volume ratio, we can increase the relative surface area and the effective substrate concentration in a reaction by 100 fold. We estimate that each nanosphere will bear between 50 and 200 molecules of most substrates, which will allow concentrations in the μM range when 1×10^{13} nanospheres per mL are used. These nanospheres are commercially available and offer an effective method to explore the utility of nanosphere-based protease assays. The use of nanospheres will make it possible to increase surface bound substrate to saturating

concentration for screening of low affinity proteases. The development of a nanosphere-based protease assay will enable the use of full-length protease substrates, multiplexed assays, and, most importantly, provide high substrate concentrations in a surface assay format. We will optimize and configure the assay for screening format in 384-well plates for demonstration screening of the Prestwick library (1280 off-patent chemical compounds). This effort will consist of optimizing endpoint protease assays in small volumes and then analyzing on the HyperCyt[®] flow cytometer.

7.2.2 Future Drug Targets: Matrix Metalloproteases

Of specific interest here is that overexpression of matrix metalloproteases (MMPs) is suggested to lead to tissue degradation and pathological disorders such as arthritis and metastatic cancer.^{160,161} The consequences of deregulation of MMP activity can include cancer-associated processes like tumorigenesis and tumor neovascularisation, invasion and metastasis, as well as apoptosis, intestinal defense activation and pathologies of the nervous systems.¹⁶² We will implement our nanosphere-based protease assay using our toxin protease models to first demonstrate the concept and then with MMPs that have reduced specificity and affinity for their substrates, which necessitates the use of higher substrate concentrations to detect protease activity. As MMPs play important roles in many forms of cancer, the discovery of specific MMP inhibitors is very clinically relevant. We will design fusion protein substrates for several MMPs (MMP-2, 3, & 9) and attach them to the surface of commercial nanospheres. We will design the constructions of MMP substrates: cystatin C for MMP2, connective tissue growth factor

(CTGF) for MMP3 and amyloid beta A4 protein for MMP9.¹⁶³ Gene sequences of all the substrates can be synthesized by Blue Heron Biotech Company (<https://www.blueheronbio.com>). Cleavage from the surface of the nanosphere will be detected via observing fluorescence changes from nanospheres on a flow cytometer. Once developed, we will optimize the assay for use in high throughput flow cytometry screening and demonstrate its effectiveness by screening the Prestwick library of chemical compounds for potential MMP inhibitors. Identifying more specific inhibitors will be important as, unfortunately, existing MMP inhibitors have not performed very well in clinical trials, so selection of potential MMP inhibitors and development of novel applications of these inhibitors will be potentially very useful for treatment of MMP related diseases such as cancer metastasis.

7.2.3 High-throughput Screening and Kinetic Studies of MMPs

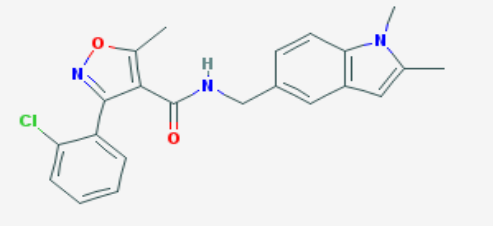
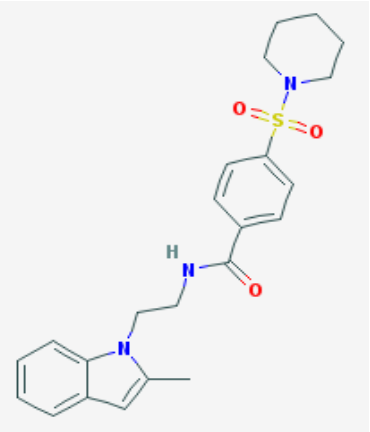
We will optimize and configure the assay for screening format in 384-well plates for demonstration screening of the Prestwick library (1280 off-patent chemical compounds). This effort will consist of optimizing endpoint protease assays (MMPs are Zn-dependent metalloproteases, EDTA is used to stop the reaction at a given time) in small volumes and then analyzing on the HyperCyt[®] flow cytometer. This demonstration screen will be used as preliminary data for subsequent funding via funding mechanisms available to collaborators of the UNM Center for Molecular Discovery. We will also use the nanosphere-based assays to determine inhibition modes and kinetic parameters (K_i). These kinetic pathways will be combined with mutagenesis studies and any discovered small molecule inhibitors to explore how proteases and their substrates interact.

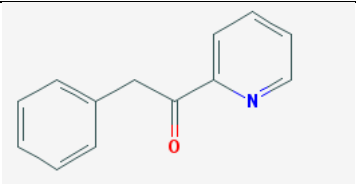
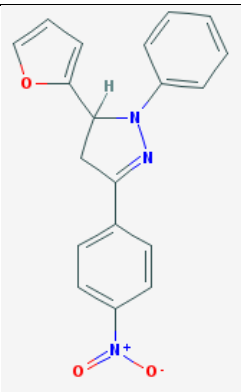
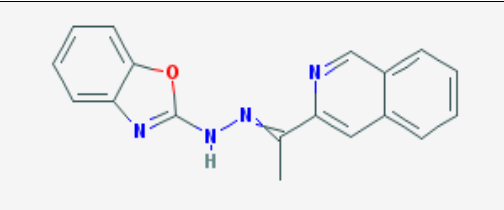
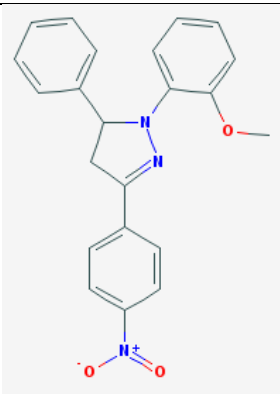
List of Appendices

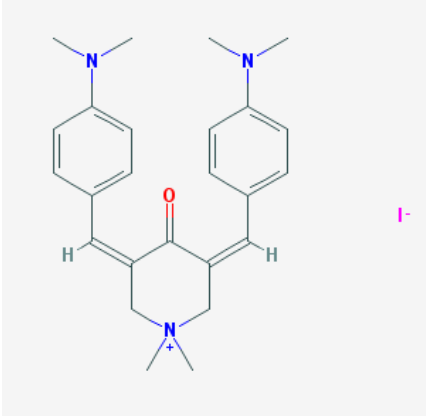
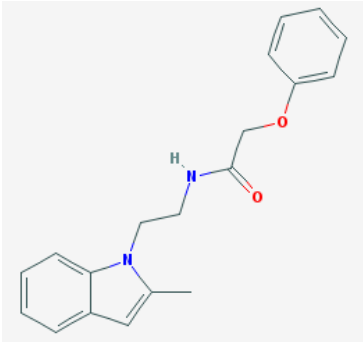
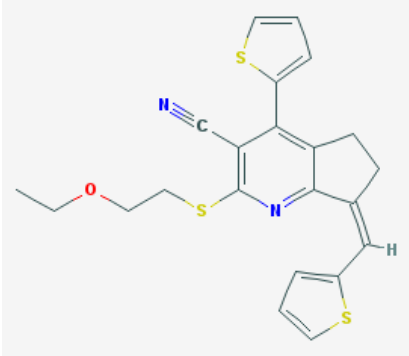
Appendix 1. DNA Sequence of VMAP-2 with Restriction Sites (*SacI* and *BamHI*)

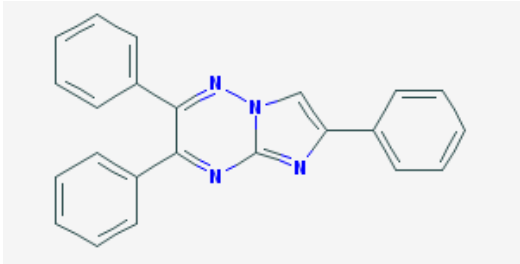
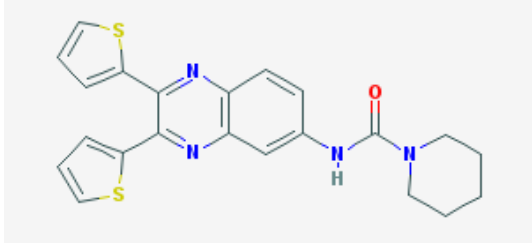
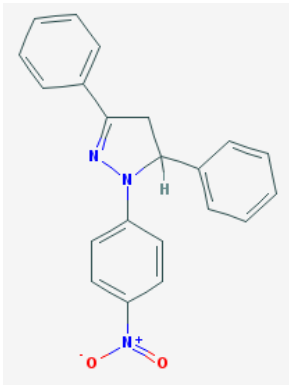
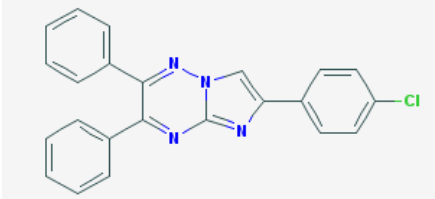
GAGCTCATGTCTGCTACCGCTGCCACGGCCCCCCTGCTGCCCCGGCTGGGG
 AGGGTGGTCCCCCTGCACCCCCTCCAAACCTCACCAGTAACAGGAGACTGCA
 GCAGACCCAGGCCCAGGTGGATGAGGTGGTGGACATCATGAGGGTGAACGT
 GGACAAGGTCCTGGAGCGAGACCAGAAGCTGTCTCGGAGCTGGACGACCGTGC
 AGATGCACTCCAGGCGGGGGCCTCCCAAGTTTGAAACAAGCGCAGCCAAGCTC
 AAGCGCAAATACTGGTGGAAAAACC TCAAGATGATGTCTA**GGATCC**

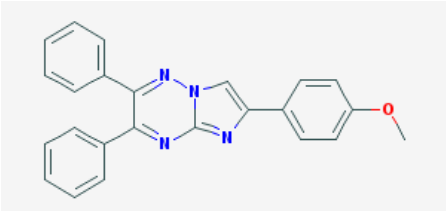
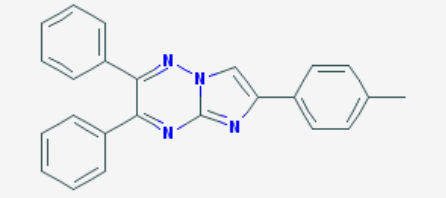
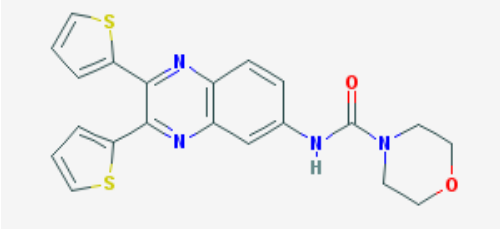
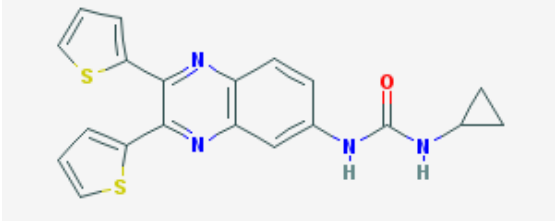
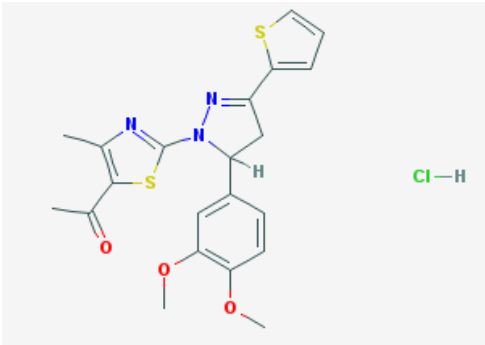
Appendix 2. Identified Inhibitors for Botulinum Neurotoxin Type A Light Chain in Microsphere-based High-throughput Screening

Compound	Structure	IC ₅₀ value
CID 4464849		4.2
CID 4293343		1.0

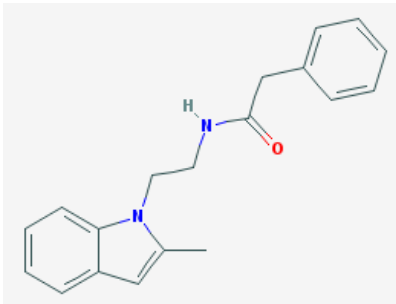
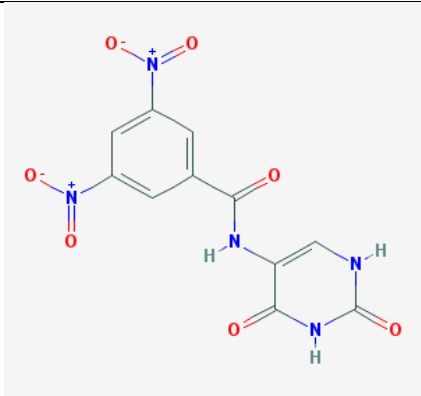
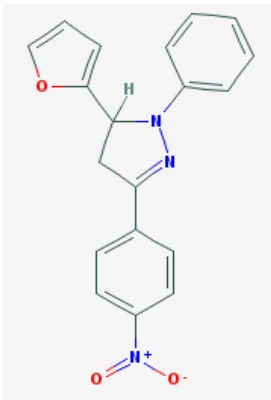
CID 256073		8.6
CID 564008		2.0
CID 392789		5.1
CID 2865835		1.0

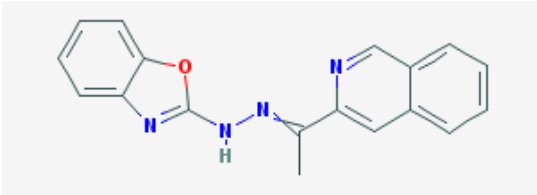
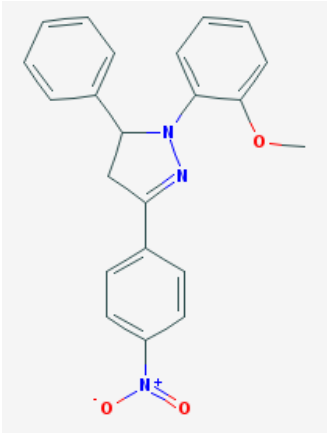
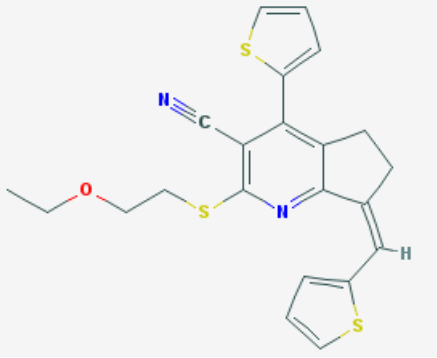
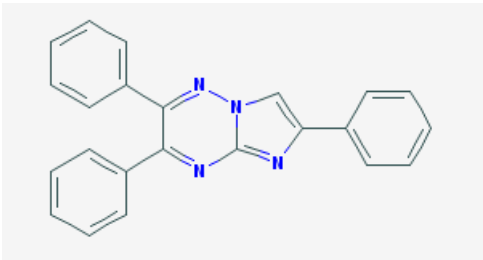
<p>CID 45281164</p>		<p>1.6</p>
<p>CID 4129168</p>		<p>4.9</p>
<p>CID 12006136</p>		<p>17.8</p>

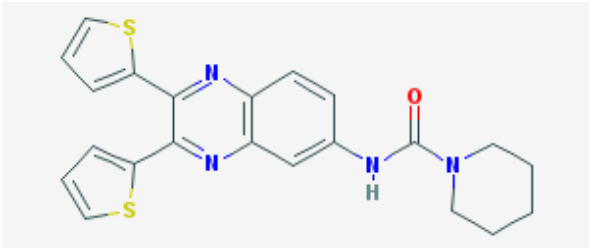
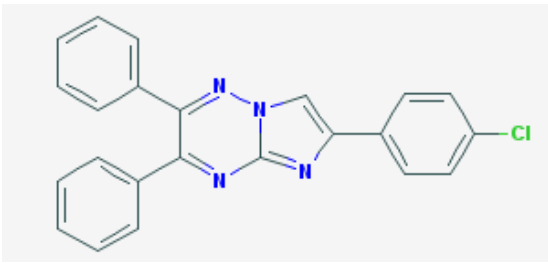
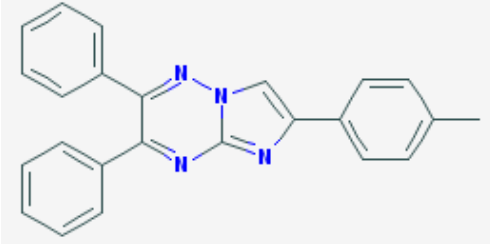
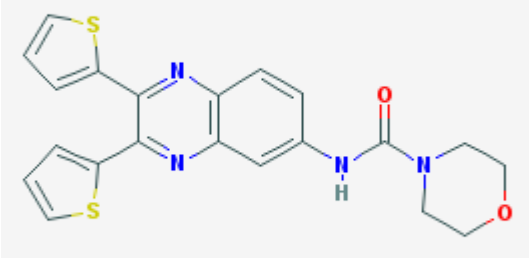
<p>CID 702952</p>		<p>0.6</p>
<p>CID 1329560</p>		<p>6.1</p>
<p>CID 2827281</p>		<p>0.3</p>
<p>CID 3297919</p>		<p>1</p>

CID 5056211		4
CID 1255814		1.5
CID 2214213		5.8
CID 1299052		1.5
CID 2858748		7.5

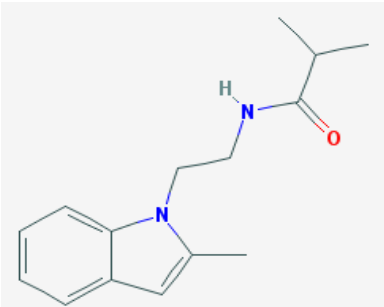
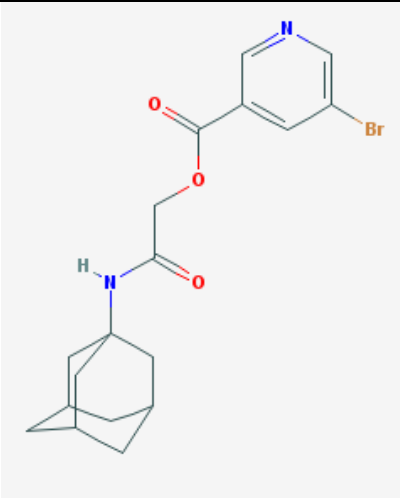
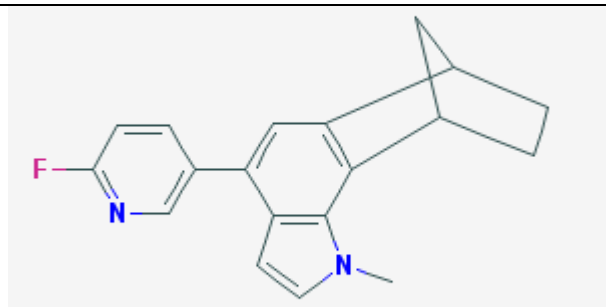
**Appendix 3. Identified Inhibitors for Botulinum Neurotoxin Type F Light Chain in
Microsphere-based High-throughput Screening**

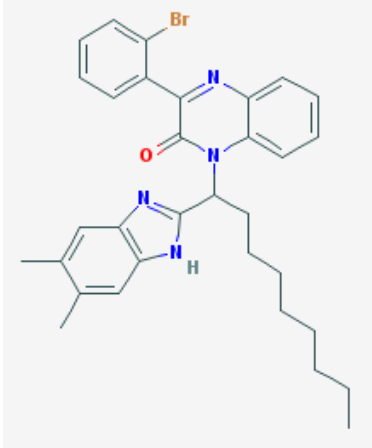
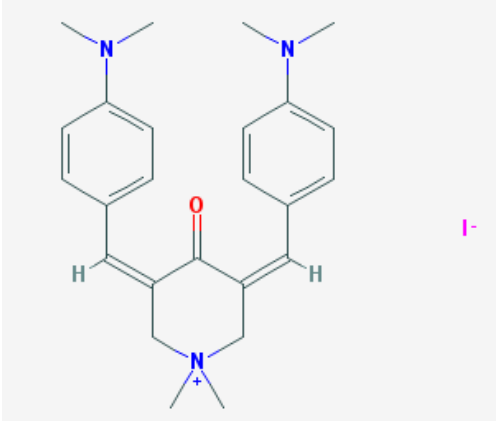
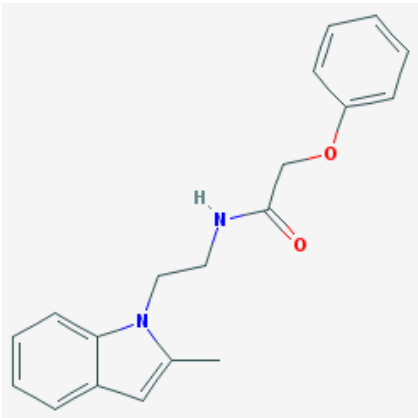
Compounds	Structure	IC ₅₀ value
CID 3626685		2.9
CID 3095057		2.7
CID 564008		2.3

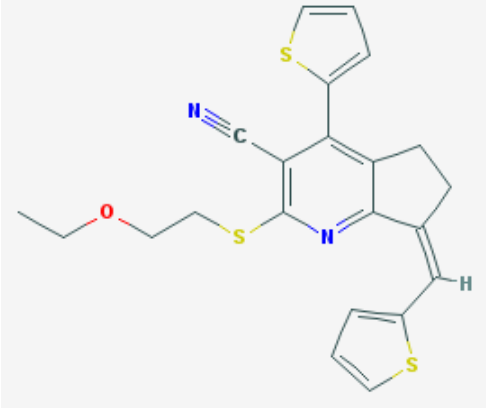
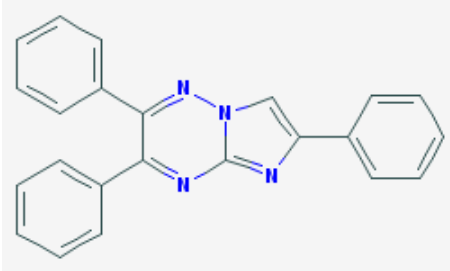
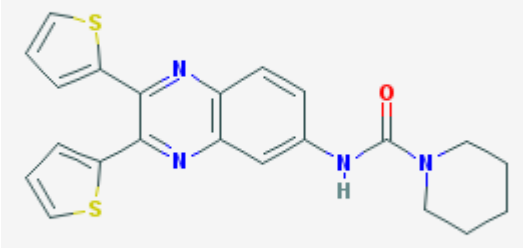
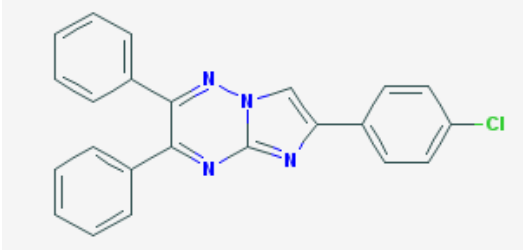
<p>CID 392789</p>		<p>9.4</p>
<p>CID 2865835</p>		<p>0.4</p>
<p>CID 12006136</p>		<p>8.0</p>
<p>CID 702952</p>		<p>5.3</p>

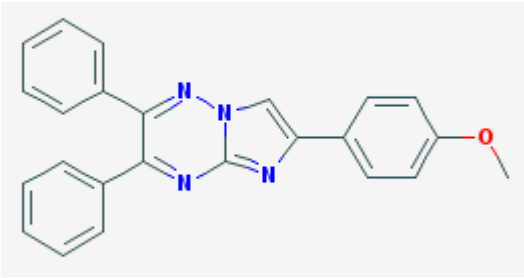
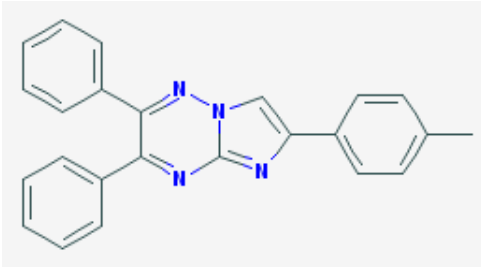
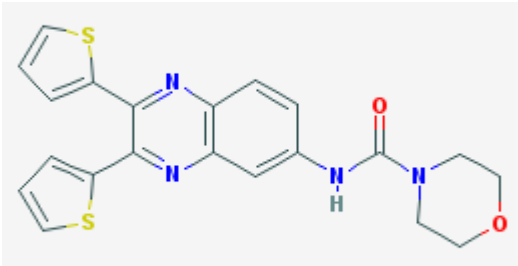
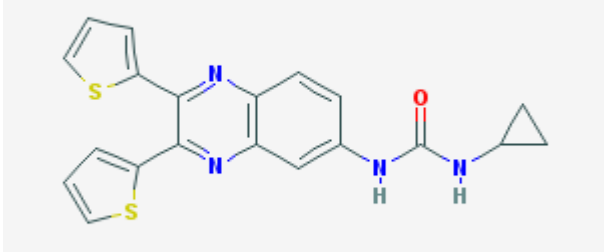
<p>CID 1329560</p>		<p>4.6</p>
<p>CID 3297919</p>		<p>7.4</p>
<p>CID 1255814</p>		<p>9.1</p>
<p>CID 2214213</p>		<p>9.6</p>

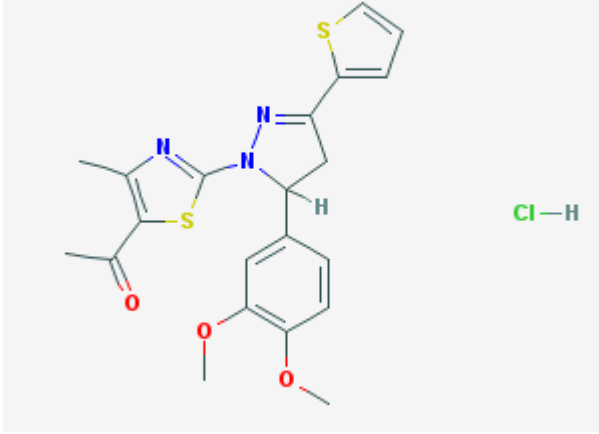
**Appendix 4. Identified Inhibitors for *Bacillus Anthracis* Lethal Factor in
Microsphere-based High-throughput Screening**

Compound	Structure	IC ₅₀ value
CID 3335282		19.5
CID 4472168		11.5
CID 51360688		10.6

<p>CID 51361178</p>		<p>17.9</p>
<p>CID 45281164</p>		<p>0.6</p>
<p>CID 4129168</p>		<p>1.4</p>

<p>CID 12006136</p>		<p>16.7</p>
<p>CID 702952</p>		<p>1.6</p>
<p>CID 1329560</p>		<p>6.7</p>
<p>CID 3297919</p>		<p>1.6</p>

<p>CID 5056211</p>		<p>3.3</p>
<p>CID 1255814</p>		<p>2</p>
<p>CID 2214213</p>		<p>7.6</p>
<p>CID 1299052</p>		<p>1.6</p>

<p>CID 2858748</p>	 <p>Chemical structure of CID 2858748, showing a complex molecule with a thiazole ring, a pyrrole ring, and a substituted benzene ring, with a thienyl group attached to the pyrrole ring. The structure is shown in a 3D perspective view.</p>	<p>9.6</p>
---------------------------	---	-------------------

References

1. Johnson, S. L.; Pellecchia, M., Structure- and fragment-based approaches to protease inhibition. *Curr Top Med Chem* **2006**, 6 (4), 317-329.
2. Barrett, A. J.; Rawlings, N. D.; Woessner, J. F., *Handbook of proteolytic enzymes*. Academic Press: San Diego, 1998; p xxix, 1666 p.
3. Travis, J.; Potempa, J., Bacterial proteinases as targets for the development of second-generation antibiotics. *Bba-Protein Struct M* **2000**, 1477 (1-2), 35-50.
4. Coleman, J. E., Zinc enzymes. *Curr Opin Chem Biol* **1998**, 2 (2), 222-234.
5. Shinoda, S.; Miyoshi, S.; Wakae, H.; Rahman, M.; Tomochika, K., Bacterial proteases as pathogenic factors, with special emphasis on *Vibrio* proteases. *J Toxicol-Toxin Rev* **1996**, 15 (4), 327-339.
6. Vollmer, P.; Waley, I.; RoseJohn, S.; Bhakdi, S., Novel pathogenic mechanism of microbial metalloproteinases: Liberation of membrane-anchored molecules in biologically active form exemplified by studies with the human interleukin-6 receptor. *Infect Immun* **1996**, 64 (9), 3646-3651.
7. Schiavo, G.; Matteoli, M.; Montecucco, C., Neurotoxins affecting neuroexocytosis. *Physiol Rev* **2000**, 80 (2), 717-766.
8. Humeau, Y.; Doussau, F.; Grant, N. J.; Poulain, B., How botulinum and tetanus neurotoxins block neurotransmitter release. *Biochimie* **2000**, 82 (5), 427-446.
9. Hase, C. C.; Finkelstein, R. A., Bacterial extracellular zinc-containing metalloproteases. *Microbiol Rev* **1993**, 57 (4), 823-837.
10. Miyoshi, S.; Shinoda, S., Microbial metalloproteases and pathogenesis. *Microbes Infect* **2000**, 2 (1), 91-98.
11. Oguma, K.; Fujinaga, Y.; Inoue, K., Structure and function of clostridium-botulinum Toxins. *Microbiol Immunol* **1995**, 39 (3), 161-168.
12. Moncrief, J. S.; Obiso, R.; Barroso, L. A.; Kling, J. J.; Wright, R. L.; Vantassell, R. L.; Lyerly, D. M.; Wilkins, T. D., The enterotoxin of *bacteroides-fragilis* is a metalloprotease. *Infect Immun* **1995**, 63 (1), 175-181.
13. Klimpel, K. R.; Arora, N.; Leppla, S. H., Anthrax toxin lethal factor contains a zinc metalloprotease consensus sequence which is required for lethal toxin activity. *Mol Microbiol* **1994**, 13 (6), 1093-1100.

14. de Bernard, M.; Rossetto, O.; Montecucco, C., Bacterial toxins: Intracellular trafficking and target identification. *Method Microbiol* **2002**, *31*, 297-317.
15. Rotz, L. D.; Khan, A. S.; Lillibridge, S. R.; Ostroff, S. M.; Hughes, J. M., Public health assessment of potential biological terrorism agents. *Emerg Infect Dis* **2002**, *8* (2), 225-230.
16. Simpson, L. L., *Botulinum neurotoxin and tetanus toxin*. Academic Press: San Diego, 1989; p xiii, 422 p.
17. Sugiyama, H., Clostridium-botulinum neurotoxin. *Microbiol Rev* **1980**, *44* (3), 419-448.
18. Gill, D. M., Bacterial toxins - a table of lethal amounts. *Microbiol Rev* **1982**, *46* (1), 86-94.
19. Sharma, S. K.; Ferreira, J. L.; Eblen, B. S.; Whiting, R. C., Detection of type A, B, E, and F Clostridium botulinum neurotoxins in foods by using an amplified enzyme-linked immunosorbent assay with digoxigenin-labeled antibodies. *Appl Environ Microb* **2006**, *72* (2), 1231-1238.
20. Montal, M., Botulinum neurotoxin: A marvel of protein design. *Annu Rev Biochem* **2010**, *79*, 591-617.
21. Schiavo, G.; Rossetto, O.; Santucci, A.; Dasgupta, B. R.; Montecucco, C., Botulinum neurotoxins are zinc proteins. *J Biol Chem* **1992**, *267* (33), 23479-23483.
22. Bittner, M. A.; Dasgupta, B. R.; Holz, R. W., Isolated light-chains of botulinum neurotoxins inhibit exocytosis - studies in digitonin-permeabilized chromaffin cells. *J Biol Chem* **1989**, *264* (18), 10354-10360.
23. Bi, G. Q.; Alderton, J. M.; Steinhardt, R. A., Calcium-regulated exocytosis is required for cell membrane resealing. *J Cell Biol* **1995**, *131* (6), 1747-1758.
24. Arnon, S. S., Botulinum toxin as a biological weapon: Medical and public health management (vol 285, pg 1059, 2001). *Jama-J Am Med Assoc* **2001**, *285* (16), 2081-2081.
25. Jahn, R.; Lang, T.; Sudhof, T. C., Membrane fusion. *Cell* **2003**, *112* (4), 519-533.
26. Jahn, R.; Scheller, R. H., SNAREs - engines for membrane fusion. *Nat Rev Mol Cell Bio* **2006**, *7* (9), 631-643.
27. Schiavo, G.; Stenbeck, G.; Rothman, J. E.; Sollner, T. H., Binding of the synaptic vesicle v-SNARE, synaptotagmin, to the plasma membrane t-SNARE, SNAP-25, can

explain docked vesicles at neurotoxin-treated synapses. *P Natl Acad Sci USA* **1997**, 94 (3), 997-1001.

28. Zhang, X. D.; Kim-Miller, M. J.; Fukuda, M.; Kowalchuk, J. A.; Martin, T. F. J., Ca²⁺-dependent synaptotagmin binding to SNAP-25 is essential for Ca²⁺-triggered exocytosis. *Neuron* **2002**, 34 (4), 599-611.

29. Blaustein, R. O.; Germann, W. J.; Finkelstein, A.; Dasgupta, B. R., The N-terminal half of the heavy-chain of botulinum type A neurotoxin forms channels in planar phospholipid-bilayers. *Febs Lett* **1987**, 226 (1), 115-120.

30. Turton, K.; Chaddock, J. A.; Acharya, K. R., Botulinum and tetanus neurotoxins: structure, function and therapeutic utility. *Trends Biochem Sci* **2002**, 27 (11), 552-558.

31. Washbourne, P.; Pellizzari, R.; Baldini, G.; Wilson, M. C.; Montecucco, C., Botulinum neurotoxin types A and E require the SNARE motif in SNAP-25 for proteolysis. *Febs Lett* **1997**, 418 (1-2), 1-5.

32. Rossetto, O.; Schiavo, G.; Montecucco, C.; Poulain, B.; Deloye, F.; Lozzi, L.; Shone, C. C., Snare motif and neurotoxins. *Nature* **1994**, 372 (6505), 415-416.

33. Cornille, F.; Martin, L.; Lenoir, C.; Cussac, D.; Roques, B. P.; FournieZaluski, M. C., Cooperative exosite-dependent cleavage of synaptobrevin by tetanus toxin light chain. *J Biol Chem* **1997**, 272 (6), 3459-3464.

34. Vaidyanathan, V. V.; Yoshino, K.; Jahnz, M.; Dorries, C.; Bade, S.; Nauenburg, S.; Niemann, H.; Binz, T., Proteolysis of SNAP-25 isoforms by botulinum neurotoxin types A, C, and E: Domains and amino acid residues controlling the formation of enzyme-substrate complexes and cleavage. *J Neurochem* **1999**, 72 (1), 327-337.

35. Breidenbach, M. A.; Brunger, A. T., Substrate recognition strategy for botulinum neurotoxin serotype A. *Nature* **2004**, 432 (7019), 925-929.

36. Chen, S.; Kim, J. J. P.; Barbieri, J. T., Mechanism of substrate recognition by botulinum neurotoxin serotype A. *J Biol Chem* **2007**, 282 (13), 9621-9627.

37. Pellizzari, R.; Mason, S.; Shone, C. C.; Montecucco, C., The interaction of synaptic vesicle-associated membrane protein synaptobrevin with botulinum neurotoxins D and F. *Febs Lett* **1997**, 409 (3), 339-342.

38. Montecucco, C.; Schiavo, G., Structure and function of tetanus and botulinum neurotoxins. *Q Rev Biophys* **1995**, 28 (4), 423-472.

39. Bennett, M. K.; Scheller, R. H., A molecular description of synaptic vesicle membrane trafficking. *Annual Review of Biochemistry* **1994**, *63*, 63-100.
40. Chilcote, T. J.; Galli, T.; Mundigl, O.; Edelmann, L.; Mcpherson, P. S.; Takei, K.; Decamilli, P., Cellubrevin and synaptobrevins - similar subcellular-localization and biochemical-properties in Pc12 cells. *J Cell Biol* **1995**, *129* (1), 219-231.
41. Rossetto, O.; Gorza, L.; Schiavo, G.; Schiavo, N.; Scheller, R. H.; Montecucco, C., VAMP synaptobrevin isoforms 1 and 2 are widely and differentially expressed in nonneuronal tissues. *J Cell Biol* **1996**, *132* (1-2), 167-179.
42. Trimble, W. S.; Gray, T. S.; Elferink, L. A.; Wilson, M. C.; Scheller, R. H., Distinct patterns of expression of two VAMP genes within the rat brain. *The Journal of neuroscience : the official journal of the Society for Neuroscience* **1990**, *10* (4), 1380-7.
43. McMahon, H. T.; Ushkaryov, Y. A.; Edelmann, L.; Link, E.; Binz, T.; Niemann, H.; Jahn, R.; Sudhof, T. C., Cellubrevin is a ubiquitous tetanus-toxin substrate homologous to a putative synaptic vesicle fusion protein. *Nature* **1993**, *364* (6435), 346-349.
44. Li, J. Y.; Edelmann, L.; Jahn, R.; Dahlstrom, A., Axonal transport and distribution of synaptobrevin I and II in the rat peripheral nervous system. *The Journal of neuroscience : the official journal of the Society for Neuroscience* **1996**, *16* (1), 137-47.
45. Mock, M.; Fouet, A., Anthrax. *Annu Rev Microbiol* **2001**, *55*, 647-671.
46. Mock, M.; Mignot, T., Anthrax toxins and the host: a story of intimacy. *Cell Microbiol* **2003**, *5* (1), 15-23.
47. Liu, S. H.; Schubert, R. L.; Bugge, T. H.; Leppla, S. H., Anthrax toxin: structures,, functions and tumour targeting. *Expert Opin Biol Th* **2003**, *3* (5), 843-853.
48. Smith, H.; Keppie, J.; Stanley, J. L.; Harrissmith, P. W., The chemical basis of the virulence of bacillus-anthraxis .4. secondary shock as the major factor in death of guinea-pigs from anthrax. *Brit J Exp Pathol* **1955**, *36* (3), 323-335.
49. Stanley, J. L.; Smith, H., Purification of factor I and recognition of a third factor of anthrax toxin. *J Gen Microbiol* **1961**, *26* (1), 49-&.
50. Fish, D. C.; Klein, F.; Lincoln, R. E.; Walker, J. S.; Dobbs, J. P., Pathophysiological changes in the rat associated with anthrax toxin. *J Infect Dis* **1968**, *118* (1), 114-24.

51. Klein, F.; Haines, B. W.; Jones, W. I.; Lincoln, R. E.; Hodges, D. R.; Mahlandt, B. G., Anthrax toxin - causative agent in death of rhesus monkeys. *Science* **1962**, *138* (3547), 1331-&.
52. Scobie, H. M.; Rainey, G. J. A.; Bradley, K. A.; Young, J. A. T., Human capillary morphogenesis protein 2 functions as an anthrax toxin receptor. *P Natl Acad Sci USA* **2003**, *100* (9), 5170-5174.
53. Bradley, K. A.; Mogridge, J.; Mourez, M.; Collier, R. J.; Young, J. A. T., Identification of the cellular receptor for anthrax toxin. *Nature* **2001**, *414* (6860), 225-229.
54. Sanchez, A. M.; Bradley, K. A., Anthrax toxin: can a little be a good thing? *Trends Microbiol* **2004**, *12* (4), 143-145.
55. Duesbery, N. S.; Webb, C. P.; Leppla, S. H.; Gordon, V. M.; Klimpel, K. R.; Copeland, T. D.; Ahn, N. G.; Oskarsson, M. K.; Fukasawa, K.; Paull, K. D.; Vande Woude, G. F., Proteolytic inactivation of MAP-kinase-kinase by anthrax lethal factor. *Science* **1998**, *280* (5364), 734-737.
56. Pellizzari, R.; Guidi-Rontani, C.; Vitale, G.; Mock, M.; Montecucco, C., Anthrax lethal factor cleaves MKK3 in macrophages and inhibits the LPS/IFN gamma-induced release of NO and TNF alpha. *Febs Lett* **1999**, *462* (1-2), 199-204.
57. Guichard, A.; Nizet, V.; Bier, E., New insights into the biological effects of anthrax toxins: linking cellular to organismal responses. *Microbes Infect* **2012**, *14* (2), 97-118.
58. Collier, R. J.; Young, J. A. T., Anthrax toxin. *Annu Rev Cell Dev Bi* **2003**, *19*, 45-70.
59. Bromberg-White, J.; Lee, C. S.; Duesbery, N., Consequences and utility of the zinc-dependent metalloprotease activity of anthrax lethal toxin. *Toxins* **2010**, *2* (5), 1038-1053.
60. Johnson, L. L.; Dyer, R.; Hupe, D. J., Matrix metalloproteinases. *Curr Opin Chem Biol* **1998**, *2* (4), 466-471.
61. Rossetto, O.; Megighian, A.; Scorzeto, M.; Montecucco, C., Botulinum neurotoxins. *Toxicon* **2013**, *67*, 31-36.
62. Agrawal, A.; Pulendran, B., Anthrax lethal toxin: a weapon of multisystem destruction. *Cell Mol Life Sci* **2004**, *61* (22), 2859-2865.

63. Hugli, T. E., Protease inhibitors: Novel therapeutic application and development. *Trends Biotechnol* **1996**, *14* (11), 409-412.
64. Tanaka, R. D.; Clark, J. M.; Warne, R. L.; Abraham, W. M.; Moore, W. R., Mast-cell tryptase - a new target for therapeutic intervention in asthma. *Int Arch Allergy Imm* **1995**, *107* (1-3), 408-409.
65. Vassar, R.; Bennett, B. D.; Babu-Khan, S.; Kahn, S.; Mendiaz, E. A.; Denis, P.; Teplow, D. B.; Ross, S.; Amarante, P.; Loeloff, R.; Luo, Y.; Fisher, S.; Fuller, L.; Edenson, S.; Lile, J.; Jarosinski, M. A.; Biere, A. L.; Curran, E.; Burgess, T.; Louis, J. C.; Collins, F.; Treanor, J.; Rogers, G.; Citron, M., Beta-secretase cleavage of Alzheimer's amyloid precursor protein by the transmembrane aspartic protease BACE. *Science* **1999**, *286* (5440), 735-741.
66. West, M. L.; Fairlie, D. P., Targeting HIV-1 protease - a test of drug-design methodologies. *Trends Pharmacol Sci* **1995**, *16* (2), 67-75.
67. Leung, D.; Abbenante, G.; Fairlie, D. P., Protease inhibitors: Current status and future prospects. *J Med Chem* **2000**, *43* (3), 305-341.
68. Fernandez, D.; Pallares, I.; Vendrell, J.; Aviles, F. X., Progress in metallocarboxypeptidases and their small molecular weight inhibitors. *Biochimie* **2010**, *92* (11), 1484-1500.
69. Saunders, M. J.; Kim, H.; Woods, T. A.; Nolan, J. P.; Sklar, L. A.; Edwards, B. S.; Graves, S. W., Microsphere-based protease assays and screening application for lethal ZXF factor and factor Xa. *Cytom Part A* **2006**, *69A* (5), 342-352.
70. Dickerson, T. J.; Janda, K. D., The use of small molecules to investigate molecular mechanisms and therapeutic targets for treatment of botulinum neurotoxin a intoxication. *Acs Chem Biol* **2006**, *1* (6), 359-369.
71. Schmidt, J. J.; Stafford, R. G., A high-affinity competitive inhibitor of type A botulinum neurotoxin protease activity. *Febs Lett* **2002**, *532* (3), 423-426.
72. Sukonpan, C.; Oost, T.; Goodnough, M.; Tepp, W.; Johnson, E. A.; Rich, D. H., Synthesis of substrates and inhibitors of botulinum neurotoxin type A metalloprotease. *J Pept Res* **2004**, *63* (2), 181-193.

73. Yiadom, K. P. A. B.; Muhie, S.; Yang, D. C. H., Peptide inhibitors of botulinum neurotoxin by mRNA display. *Biochemical and biophysical research communications* **2005**, 335 (4), 1247-1253.
74. Saunders, M. J.; Graves, S. W.; Sklar, L. A.; Oprea, T. I.; Edwards, B. S., High-throughput multiplex flow cytometry screening for botulinum neurotoxin type A light chain protease inhibitors. *Assay Drug Dev Techn* **2010**, 8 (1), 37-46.
75. Burnett, J. C.; Schmidt, J. J.; Stafford, R. G.; Panchal, R. G.; Nguyen, T. L.; Hermone, A. R.; Vennerstrom, J. L.; McGrath, C. F.; Lane, D. J.; Sausville, E. A.; Zaharevitz, D. W.; Gussio, R.; Bavari, S., Novel small molecule inhibitors of botulinum neurotoxin A metalloprotease activity. *Biochem Bioph Res Co* **2003**, 310 (1), 84-93.
76. Boldt, G. E.; Kennedy, J. P.; Hixon, M. S.; McAllister, L. A.; Barbieri, J. T.; Tzipori, S.; Janda, K. D., Synthesis, characterization and development of a high-throughput methodology for the discovery of botulinum neurotoxin A inhibitors. *J Comb Chem* **2006**, 8 (4), 513-521.
77. Boldt, G. E.; Kennedy, J. P.; Janda, K. D., Identification of a potent botulinum neurotoxin a protease inhibitor using in situ lead identification chemistry. *Org Lett* **2006**, 8 (8), 1729-1732.
78. Hines, H. B.; Kim, A. D.; Stafford, R. G.; Badie, S. S.; Brueggeman, E. E.; Newman, D. J.; Schmidt, J. J., Use of a recombinant fluorescent substrate with cleavage sites for all botulinum neurotoxins in high-throughput screening of natural product extracts for inhibitors of serotypes A, B, and E. *Appl Environ Microb* **2008**, 74 (3), 653-659.
79. Zuniga, J. E.; Schmidt, J. J.; Fenn, T.; Burnett, J. C.; Arac, D.; Gussio, R.; Stafford, R. G.; Badie, S. S.; Bavari, S.; Brunger, A. T., A potent peptidomimetic inhibitor of botulinum neurotoxin serotype A has a very different conformation than SNAP-25 substrate. *Structure* **2008**, 16 (10), 1588-1597.
80. Schmidt, J. J.; Stafford, R. G., Fluorogenic substrates for the protease activities of botulinum neurotoxins, serotypes A, B, and F. *Appl Environ Microb* **2003**, 69 (1), 297-303.

81. Schmidt, J. J.; Stafford, R. G.; Bostian, K. A., Type A botulinum neurotoxin proteolytic activity: development of competitive inhibitors and implications for substrate specificity at the S-1 ' binding subsite. *Febs Lett* **1998**, *435* (1), 61-64.
82. Schmidt, J. J.; Stafford, R. G., Botulinum neurotoxin serotype F: Identification of substrate recognition requirements and development of inhibitors with low nanomolar affinity. *Biochemistry-Us* **2005**, *44* (10), 4067-4073.
83. Bakry, N.; Kamata, Y.; Simpson, L. L., Lectins from *Triticum-Vulgaris* and *Limax-Flavus* Are Universal Antagonists of Botulinum Neurotoxin and Tetanus Toxin. *J Pharmacol Exp Ther* **1991**, *258* (3), 830-836.
84. Fuchs, O.; Babusiak, M.; Vyoral, D.; Petrak, J., Role of zinc in eukaryotic cells, zinc transporters and zinc-containing proteins. Review article. *Sbornik lekarsky* **2003**, *104* (2), 157-70.
85. Tonello, F.; Seveso, M.; Marin, O.; Mock, M.; Montecucco, C., Pharmacology - Screening inhibitors of anthrax lethal factor. *Nature* **2002**, *418* (6896), 386-386.
86. Gaddis, B. D.; Perez, C. M. R.; Chmielewski, J., Inhibitors of anthrax lethal factor based upon N-oleoyldopamine. *Bioorg Med Chem Lett* **2008**, *18* (7), 2467-2470.
87. Karginov, V. A.; Nestorovich, E. M.; Schmidtman, F.; Robinson, T. M.; Yohannes, A.; Fahmi, N. E.; Bezrukov, S. M.; Hecht, S. M., Inhibition of S-aureus alpha-hemolysin and B-anthraxis lethal toxin by beta-cyclodextrin derivatives. *Bioorgan Med Chem* **2007**, *15* (16), 5424-5431.
88. Hanna, M. L.; Tarasow, T. M.; Perkins, J., Mechanistic differences between in vitro assays for hydrazone-based small molecule inhibitors of anthrax lethal factor. *Bioorg Chem* **2007**, *35* (1), 50-58.
89. Jiao, G. S.; Simo, O.; Nagata, M.; O'Malley, S.; Hemscheidt, T.; Cregar, L.; Millis, S. Z.; Goldman, M. E.; Tang, C., Selectively guanidinylated derivatives of neamine. Syntheses and inhibition of anthrax lethal factor protease. *Bioorg Med Chem Lett* **2006**, *16* (19), 5183-5189.
90. Bannwarth, L.; Goldberg, A. B.; Chen, C.; Turk, B. E., Identification of exosite-targeting inhibitors of anthrax lethal factor by high-throughput screening. *Chem Biol* **2012**, *19* (7), 875-882.

91. Kim, J.; Park, H. C.; Gedi, V.; Park, H. Y.; Roberts, A. G.; Atkins, W. M.; Yoon, M. Y., Yeast-hybrid based high-throughput assay for identification of anthrax lethal factor inhibitors. *Biochem Bioph Res Co* **2011**, *404* (1), 517-522.
92. Johnson, S. L.; Chen, L. H.; Pellecchia, M., A high-throughput screening approach to anthrax lethal factor inhibition. *Bioorg Chem* **2007**, *35* (4), 306-312.
93. Min, D. H.; Tang, W. J.; Mrksich, M., Chemical screening by mass spectrometry to identify inhibitors of anthrax lethal factor. *Nat Biotechnol* **2004**, *22* (6), 717-723.
94. Overall, C. M.; Kleifeld, O., Tumour microenvironment - Opinion - Validating matrix metalloproteinases as drug targets and anti-targets for cancer therapy. *Nat Rev Cancer* **2006**, *6* (3), 227-239.
95. Concha, N. O.; Abdel-Meguid, S. S., Controlling apoptosis by inhibition of caspases. *Curr Med Chem* **2002**, *9* (6), 713-726.
96. Schwienhorst, A., Direct thrombin inhibitors - a survey of recent developments. *Cell Mol Life Sci* **2006**, *63* (23), 2773-2791.
97. White, C. M., Thrombin-directed inhibitors: Pharmacology and clinical use. *Am Heart J* **2005**, *149* (1), S54-S60.
98. Bjurlin, M. A.; Bloomer, S.; Nelson, C. J., Characterization of proteolytic activity of proteases. *Biotechnol Lett* **2002**, *24* (3), 191-195.
99. Zhao, Z. J.; Raftery, M. J.; Niu, X. M.; Daja, M. M.; Russell, P. J., Application of in-gel protease assay in a biological sample: Characterization and identification of urokinase-type plasminogen activator (uPA) in secreted proteins from a prostate cancer cell line PC-3. *Electrophoresis* **2004**, *25* (7-8), 1142-1148.
100. Laack, E.; Kohler, A.; Kugler, C.; Dierlamm, T.; Knuffmann, C.; Vohwinkel, G.; Niestroy, A.; Dahlmann, N.; Peters, A.; Berger, J.; Fiedler, W.; Hossfeld, D. K., Pretreatment serum levels of matrix metalloproteinase-9 and vascular endothelial growth factor in non-small-cell lung cancer. *Ann Oncol* **2002**, *13* (10), 1550-1557.
101. Ohuchi, E.; Azumano, I.; Yoshida, S.; Iwata, K.; Okada, Y., A one-step sandwich enzyme immunoassay for human matrix metalloproteinase 7 (matrilysin) using monoclonal antibodies. *Clin Chim Acta* **1996**, *244* (2), 181-198.

102. Shi, L. F.; De Paoli, V.; Rosenzweig, N.; Rosenzweig, Z., Synthesis and application of quantum dots FRET-based protease sensors. *J Am Chem Soc* **2006**, *128* (32), 10378-10379.
103. Medintz, I. L.; Clapp, A. R.; Brunel, F. M.; Tiefenbrunn, T.; Uyeda, H. T.; Chang, E. L.; Deschamps, J. R.; Dawson, P. E.; Mattoussi, H., Proteolytic activity monitored by fluorescence resonance energy transfer through quantum-dot-peptide conjugates. *Nat Mater* **2006**, *5* (7), 581-589.
104. Chang, E.; Miller, J. S.; Sun, J. T.; Yu, W. W.; Colvin, V. L.; Drezek, R.; West, J. L., Protease-activated quantum dot probes. *Biochem Bioph Res Co* **2005**, *334* (4), 1317-1321.
105. Stockholm, D.; Bartoli, M.; Sillon, G.; Bourg, N.; Davoust, J.; Richard, I., Imaging calpain protease activity by multiphoton FRET in living mice. *J Mol Biol* **2005**, *346* (1), 215-222.
106. Bruchez, M.; Moronne, M.; Gin, P.; Weiss, S.; Alivisatos, A. P., Semiconductor nanocrystals as fluorescent biological labels. *Science* **1998**, *281* (5385), 2013-2016.
107. Willard, D. M.; Mutschler, T.; Yu, M.; Jung, J.; Van Orden, A., Directing energy flow through quantum dots: towards nanoscale sensing. *Anal Bioanal Chem* **2006**, *384* (3), 564-571.
108. Edwards, B. S.; Young, S. M.; Saunders, M. J.; Bologa, C.; Oprea, T. I.; Ye, R. D.; Prossnitz, E. R.; Graves, S. W.; Sklar, L. A., High-throughput flow cytometry for drug discovery. *Expert Opin Drug Dis* **2007**, *2* (5), 685-696.
109. Sklar, L. A.; Carter, M. B.; Edwards, B. S., Flow cytometry for drug discovery, receptor pharmacology and high-throughput screening. *Curr Opin Pharmacol* **2007**, *7* (5), 527-534.
110. Nolan, J. P.; Sklar, L. A., Suspension array technology: evolution of the flat-array paradigm. *Trends Biotechnol* **2002**, *20* (1), 9-12.
111. Josko, D., Botulin toxin: a weapon in terrorism. *Clin Lab Sci* **2004**, *17* (1), 30-4.
112. Rossetto, O.; de Bernard, M.; Pellizzari, R.; Vitale, G.; Caccin, P.; Schiavo, G.; Montecucco, C., Bacterial toxins with intracellular protease activity. *Clin Chim Acta* **2000**, *291* (2), 189-199.

113. Arnon, S. S.; Schechter, R.; Inglesby, T. V.; Henderson, D. A.; Bartlett, J. G.; Ascher, M. S.; Eitzen, E.; Fine, A. D.; Hauer, J.; Layton, M.; Lillibridge, S.; Osterholm, M. T.; O'Toole, T.; Parker, G.; Perl, T. M.; Russell, P. K.; Swerdlow, D. L.; Tonat, K.; Biodefense, W. G. C., Botulinum toxin as a biological weapon - Medical and public health management. *Jama-J Am Med Assoc* **2001**, 285 (8), 1059-1070.
114. Tighe, A. P.; Schiavo, G., Botulinum neurotoxins: Mechanism of action. *Toxicon* **2013**, 67, 87-93.
115. Marvaud, J. C.; Raffestin, S.; Popoff, M. R., Botulism - Agent means of action of botulinum neurotoxins forms of acquisition, treatment and prevention. *Cr Biol* **2002**, 325 (8), 863-878.
116. Simpson, L. L., Identification of the major steps in botulinum toxin action. *Annu Rev Pharmacol* **2004**, 44, 167-193.
117. Sollner, T.; Whitehart, S. W.; Brunner, M.; Erdjumentbromage, H.; Geromanos, S.; Tempst, P.; Rothman, J. E., SNAP receptors implicated in vesicle targeting and fusion. *Nature* **1993**, 362 (6418), 318-324.
118. Pellizzari, R.; Rossetto, O.; Schiavo, G.; Montecucco, C., Tetanus and botulinum neurotoxins: mechanism of action and therapeutic uses. *Philos T Roy Soc B* **1999**, 354 (1381), 259-268.
119. Foran, P.; Lawrence, G. W.; Shone, C. C.; Foster, K. A.; Dolly, J. O., Botulinum neurotoxin C1 cleaves both syntaxin and SNAP-25 in intact and permeabilized chromaffin cells: Correlation with its blockade of catecholamine release. *Biochemistry-U S* **1996**, 35 (8), 2630-2636.
120. Supuran, C. T.; Scozzafava, A.; Clare, B. W., Bacterial protease inhibitors. *Med Res Rev* **2002**, 22 (4), 329-372.
121. Hammond, S. E.; Hanna, P. C., Lethal factor active-site mutations affect catalytic activity in vitro. *Infect Immun* **1998**, 66 (5), 2374-2378.
122. Roques, B. P., Novel approaches to targeting neuropeptide systems. *Trends Pharmacol Sci* **2000**, 21 (12), 475-483.
123. Schmidt, J. J.; Stafford, R. G.; Millard, C. B., High-throughput assays for botulinum neurotoxin proteolytic activity: Serotypes A, B, D, and F. *Analytical biochemistry* **2001**, 296 (1), 130-137.

124. Nagai, T.; Miyawaki, A., A high-throughput method for development of FRET-based indicators for proteolysis. *Biochemical and biophysical research communications* **2004**, *319* (1), 72-77.
125. Phillips, R. W.; Abbott, D., High-throughput enzyme-linked immunoabsorbant assay (ELISA) electrochemiluminescent detection of botulinum toxins in foods for food safety and defence purposes. *Food Addit Contam A* **2008**, *25* (9), 1084-1088.
126. Gutierrez, O. A.; Salas, E.; Hernandez, Y.; Lissi, E. A.; Castrillo, G.; Reyes, O.; Garay, H.; Aguilar, A.; Garcia, B.; Otero, A.; Chavez, M. A.; Duarte, C. A., An immunoenzymatic solid-phase assay for quantitative determination of HIV-1 protease activity. *Analytical biochemistry* **2002**, *307* (1), 18-24.
127. Breuer, S.; Sepulveda, H.; Chen, Y.; Trotter, J.; Torbett, B. E., A Cleavage enzyme-cytometric bead array provides biochemical profiling of resistance mutations in HIV-1 gag and protease. *Biochemistry-Us* **2011**, *50* (20), 4371-4381.
128. Edwards, B. S.; Zhu, J. S.; Chen, J.; Carter, M. B.; Thal, D. M.; Tesmer, J. J. G.; Graves, S. W.; Sklar, L. A., Cluster cytometry for high-capacity bioanalysis. *Cytom Part A* **2012**, *81A* (5), 419-429.
129. Saunders, M. J.; Edwards, B. S.; Zhu, J.; Sklar, L. A.; Graves, S. W., Microsphere-based flow cytometry protease assays for use in protease activity detection and high-throughput screening. *Current protocols in cytometry / editorial board, J. Paul Robinson, managing editor ... [et al.]* **2010**, *Chapter 13*, Unit 13 12 1-17.
130. Gill, S. C.; von Hippel, P. H., Calculation of protein extinction coefficients from amino acid sequence data. *Analytical biochemistry* **1989**, *182* (2), 319-26.
131. Ramirez, S.; Aiken, C. T.; Andrzejewski, B.; Sklar, L. A.; Edwards, B. S., High-throughput flow cytometry: Validation in microvolume bioassays. *Cytom Part A* **2003**, *53A* (1), 55-65.
132. Breidenbach, M. A.; Brunger, A. T., New insights into clostridial neurotoxin-SNARE interactions. *Trends Mol Med* **2005**, *11* (8), 377-381.
133. Mack, M.; Grill, S., Riboflavin analogs and inhibitors of riboflavin biosynthesis. *Appl Microbiol Biot* **2006**, *71* (3), 265-275.

134. Baldwin, M. R.; Bradshaw, M.; Johnson, E. A.; Barbieri, J. T., The C-terminus of botulinum neurotoxin type A light chain contributes to solubility, catalysis, and stability. *Protein expression and purification* **2004**, 37 (1), 187-195.
135. Gutierrez, O. A.; Chavez, M.; Lissi, E., A theoretical approach to some analytical properties of heterogeneous enzymatic assays. *Anal Chem* **2004**, 76 (9), 2664-2668.
136. Nagai, T.; Miyawaki, A., A high-throughput method for development of FRET-based indicators for proteolysis. *Biochem Bioph Res Co* **2004**, 319 (1), 72-77.
137. Mahajan, N. P.; Harrison-Shostak, D. C.; Michaux, J.; Herman, B., Novel mutant green fluorescent protein protease substrates reveal the activation of specific caspases during apoptosis. *Chem Biol* **1999**, 6 (6), 401-409.
138. Rodems, S. M.; Hamman, B. D.; Lin, C.; Zhao, J.; Shah, S.; Heidary, D.; Makings, L.; Stack, J. H.; Pollok, B. A., A FRET-based assay platform for ultra-high density drug screening of protein kinases and phosphatases. *Assay Drug Dev Techn* **2002**, 1 (1), 9-19.
139. Copeland, R. A.; Marcinkeviciene, J.; Haque, T. S.; Kopcho, L. M.; Jiang, W. J.; Wang, K.; Ecret, L. D.; Sizemore, C.; Amsler, K. A.; Foster, L.; Tadesse, S.; Combs, A. P.; Stern, A. M.; Trainor, G. L.; Slee, A.; Rogers, M. J.; Hobbs, F., Helicobacter pylori-selective antibacterials based on inhibition of pyrimidine biosynthesis. *J Biol Chem* **2000**, 275 (43), 33373-33378.
140. Lebeda, F. J.; Cer, R. Z.; Mudunuri, U.; Stephens, R.; Singh, B. R.; Adler, M., The zinc-dependent protease activity of the botulinum neurotoxins. *Toxins (Basel)* **2010**, 2 (5), 978-97.
141. Li, L.; Binz, T.; Niemann, H.; Singh, B. R., Probing the mechanistic role of glutamate residue in the zinc-binding motif of type A botulinum neurotoxin light chain. *Biochemistry-Us* **2000**, 39 (9), 2399-2405.
142. Binz, T.; Bade, S.; Rummel, A.; Kollewe, A.; Alves, J., Arg(362) and Tyr(365) of the botulinum neurotoxin type a light chain are involved in transition state stabilization. *Biochemistry-Us* **2002**, 41 (6), 1717-1723.
143. Schmidt, J. J.; Stafford, R. G., Fluorogenic substrates for the protease activities of botulinum neurotoxins, serotypes A, B, and F. *Appl Environ Microbiol* **2003**, 69 (1), 297-303.

144. Baldwin, M. R.; Bradshaw, M.; Johnson, E. A.; Barbieri, J. T., The C-terminus of botulinum neurotoxin type A light chain contributes to solubility, catalysis, and stability. *Protein Expres Purif* **2004**, *37* (1), 187-195.
145. Chapman, K. T.; Kopka, I. E.; Durette, P. L.; Esser, C. K.; Lanza, T. J.; Izquierdomartin, M.; Niedzwiecki, L.; Chang, B.; Harrison, R. K.; Kuo, D. W.; Lin, T. Y.; Stein, R. L.; Hagmann, W. K., Inhibition of matrix metalloproteinases by N-carboxyalkyl peptides. *J Med Chem* **1993**, *36* (26), 4293-4301.
146. Wahl, R. C., The calculation of initial velocity from product progress curves when $[S] \ll K_M$. *Anal Biochem* **1994**, *219* (2), 383-384.
147. Liang, F.; Lai, R.; Arora, N.; Zhang, K. L.; Yeh, C. C.; Barnett, G. R.; Voigt, P.; Corrie, S. R.; Barnard, R. T., Multiplex-microsphere-quantitative polymerase chain reaction: Nucleic acid amplification and detection on microspheres. *Anal Biochem* **2013**, *432* (1), 23-30.
148. Chen, J. W.; Iannone, M. A.; Li, M. S.; Taylor, J. D.; Rivers, P.; Nelsen, A. J.; Slentz-Kesler, K. A.; Roses, A.; Weiner, M. P., A microsphere-based assay for multiplexed single nucleotide polymorphism analysis using single base chain extension. *Genome Res* **2000**, *10* (4), 549-557.
149. Nolan, J. P.; Shen, B. H.; Park, M. S.; Sklar, L. A., Kinetic analysis of human flap endonuclease-1 by flow cytometry. *Biochemistry-U S A* **1996**, *35* (36), 11668-11676.
150. Trigiane, G.; Gast, A. P.; Robertson, C. R., Pseudo first-order cleavage of an immobilized substrate by an enzyme undergoing two-dimensional surface diffusion. *J Colloid Interf Sci* **1999**, *213* (1), 81-86.
151. Lee, H. J.; Wark, A. W.; Goodrich, T. T.; Fang, S. P.; Corn, R. M., Surface enzyme kinetics for biopolymer microarrays: a combination of Langmuir and Michaelis-Menten concepts. *Langmuir* **2005**, *21* (9), 4050-4057.
152. Gutierrez, O. A.; Salas, E.; Hernandez, Y.; Lissi, E. A.; Castrillo, G.; Reyes, O.; Garay, H.; Aguilar, A.; Garcia, B.; Otero, A.; Chavez, M. A.; Duarte, C. A., An immunoenzymatic solid-phase assay for quantitative determination of HIV-1 protease activity. *Anal Biochem* **2002**, *307* (1), 18-24.

153. Schmidt, J. J.; Stafford, R. G.; Millard, C. B., High-throughput assays for botulinum neurotoxin proteolytic activity: Serotypes A, B, D, and F. *Anal Biochem* **2001**, *296* (1), 130-137.
154. Schiavo, G.; Rossetto, O.; Catsicas, S.; Delaureto, P. P.; Dasgupta, B. R.; Benfenati, F.; Montecucco, C., Identification of the nerve-terminal targets of botulinum neurotoxin serotype-A, serotype-D, and Serotype-E. *J Biol Chem* **1993**, *268* (32), 23784-23787.
155. Montecucco, C.; Schiavo, G.; Tugnoli, V.; deGrandis, D., Botulinum neurotoxins: Mechanism of action and therapeutic applications. *Mol Med Today* **1996**, *2* (10), 418-424.
156. StPierre, Y.; Desrosiers, M.; Tremblay, P.; Esteve, P. O.; Opdenakker, G., Flow cytometric analysis of gelatinase B (MMP-9) activity using immobilized fluorescent substrate on microspheres. *Cytometry* **1996**, *25* (4), 374-380.
157. Goldstein, B.; Coombs, D.; He, X. Y.; Pineda, A. R.; Wofsy, C., The influence of transport on the kinetics of binding to surface receptors: application to cells and BIAcore. *J Mol Recognit* **1999**, *12* (5), 293-299.
158. Drag, M.; Salvesen, G. S., Emerging principles in protease-based drug discovery. *Nat Rev Drug Discov* **2010**, *9* (9), 690-701.
159. Sandwick, R. K.; Schray, K. J., Conformational states of enzymes bound to surfaces. *J Colloid Interf Sci* **1988**, *121* (1), 1-12.
160. Chang, C.; Werb, Z., The many faces of metalloproteases: cell growth, invasion, angiogenesis and metastasis. *Trends Cell Biol* **2001**, *11* (11), S37-S43.
161. Ishiguro, N.; Ito, T.; Oguchi, T.; Kojima, T.; Iwata, H.; Ionescu, M.; Poole, A. R., Relationships of matrix metalloproteinases and their inhibitors to cartilage proteoglycan and collagen turnover and inflammation as revealed by analyses of synovial fluids from patients with rheumatoid arthritis. *Arthritis Rheum* **2001**, *44* (11), 2503-2511.
162. Overall, C. M.; Lopez-Otin, C., Strategies for MMP inhibition in cancer: Innovations for the post-trial era. *Nat Rev Cancer* **2002**, *2* (9), 657-672.
163. Morrison, C. J.; Butler, G. S.; Rodriguez, D.; Overall, C. M., Matrix metalloproteinase proteomics: substrates, targets, and therapy. *Curr Opin Cell Biol* **2009**, *21* (5), 645-653.